SERDP

FINAL REPORT

Development of Novel Functionalized Polymeric Thin Films for Equilibrium Passive Sampling of PFAS in Surface and Groundwater

Upal Ghosh
Songjing Yan
University of Maryland Baltimore County

Gregory Foster
Batool Murtadha
Matthew Badia
George Mason University

April 2022

SERDP Project ER20-1336

REPORT DOCUMENTATION PAGE

Form Approved
OMB No. 0704-0188

1. REPORT DATE *(DD-MM-YYYY)*	2. REPORT TYPE	3. DATES COVERED *(From - To)*
30/09/2022	FINAL REPORT	11/21/2019 - 11/20/2022

4. TITLE AND SUBTITLE
Development of novel functionalized polymeric thin films for equilibrium passive sampling of PFAS compounds in surface and groundwater

5a. CONTRACT NUMBER
W912HQ20P0007

5b. GRANT NUMBER

5c. PROGRAM ELEMENT NUMBER

6. AUTHOR(S)
Upal Ghosh, Songjing Yan
Gregory Foster, Batool Murtadha, Matthew Badia

5d. PROJECT NUMBER
ER20-C2-1336

5e. TASK NUMBER

5f. WORK UNIT NUMBER

7. PERFORMING ORGANIZATION NAME(S) AND ADDRESS(ES)

University of Maryland
Baltimore County
1000 Hilltop Circle
Baltimore, MD 21250

George Mason University
4400 University Dr,
Fairfax, VA 22030

8. PERFORMING ORGANIZATION REPORT NUMBER
ER20-1336

9. SPONSORING / MONITORING AGENCY NAME(S) AND ADDRESS(ES)

Strategic Environmental Research and Development Program
4800 Mark Center Drive, Suite 16F16
Alexandria, VA 22350-3605

10. SPONSOR/MONITOR'S ACRONYM(S)
SERDP

11. SPONSOR/MONITOR'S REPORT NUMBER(S) ER20-1336

12. DISTRIBUTION / AVAILABILITY STATEMENT

DISTRIBUTION STATEMENT A. Approved for public release: distribution unlimited.

13. SUPPLEMENTARY NOTES

14. ABSTRACT

The overarching goal of this 1-year SERDP SEED project was to develop and test a range of functionalized polymeric membranes for use in equilibrium passive sampling of PFAS compounds. The following objectives were addressed in this project: 1) develop novel polymeric thin films for equilibrium passive sampling that will be either solid or liquid sorbents embedded in a thin polymer sheet; 2) perform equilibrium partitioning studies with PFAS compounds covering a range of properties and interpret isotherm data based on sorption models; 3) test equilibrium reversibility for the top two choices of polymers and assess the use of performance reference compounds to quantify the extent of equilibrium; 4) evaluate the mechanism of the sorption process. We demonstrate that several composite polymers can be synthesized that remain stable in the water environment and provide adequate sorption of PFAS from aqueous solution at equilibrium. Initial results presented in this report show great promise for pursuing the concept of equilibrium passive sampling for PFAS in water.

15. SUBJECT TERMS
PFAS, fluorinated compounds, passive sampling

16. SECURITY CLASSIFICATION OF:			17. LIMITATION OF ABSTRACT	18. NUMBER OF PAGES	19a. NAME OF RESPONSIBLE PERSON
a. REPORT	b. ABSTRACT	c. THIS PAGE			Upal Ghosh
U	U	U	UU	137	19b. TELEPHONE NUMBER *(include area code)* 420-455-8665

Table of Contents

1.0 Executive summary

The demand for an accurate assessment of risk to humans and ecosystems from the presence of PFAS compounds has attracted lot of attention. Polymeric equilibrium passive samplers can be tailored to measure time-integrated freely dissolved concentrations of a range of pollutants including per- and polyfluoroalkyl substances (PFAS). While much progress has been made in passive sampling for hydrophobic organic compounds (HOCs) and metals, passive sampling is still in the early stages of development for PFAS compounds.

The overarching goal of this 1-year SERDP SEED project was to develop and test a range of functionalized polymeric thin films and polymer-inclusion membranes for use in equilibrium passive sampling of PFAS compounds. To achieve this goal, the following objectives were addressed in this project: 1) develop novel polymeric thin films for equilibrium passive sampling that will be either solid or liquid sorbents embedded in a thin polymer sheet; 2) perform equilibrium partitioning studies with PFAS compounds covering a range of properties and interpret isotherm data based on sorption models; 3) test equilibrium reversibility for the top two choices of polymers and assess the use of performance reference compounds to quantify the extent of equilibrium; 4) evaluate the mechanism of the sorption process.

We began the development of PFAS samplers by evaluating potential materials. We explored four broad classes of polymers: Polydimethylsiloxane (PDMS), agarose (AG), cellulose acetate (CA) and cellulose triacetate (CTA) that were cast as the thin base film in the functionalized passive sampler construction in this project. We used a range of sorbent amendments to allow equilibrium sorption of a wide range of PFAS compounds: activated carbon, commercially available materials Oasis HLB and Oasis WAX, and human serum albumin. These sorbents have shown affinities to a wide range of PFAS compounds in previous research. The solid sorbents were embedded in a thin polymer sheet. A range of polymer and polymer composites were prepared to test sorption capacity and linearity. Polymers were chosen for pore size, the sorbent capacity of PFAS, and the ability to potentially include sorbents. A wide variety of polymers were synthesized and tested. Our goal was to synthesize passive sampling materials having a range of properties, including:

- Ability to synthesize consistent thin films that are structurally stable in water deployments.

- Partition coefficients close to the measured partitioning for PFAS in natural sediments ($10^{1.5}$ to $10^{3.5}$).
- Sorption isotherms that can be described across the concentration range of interest, from the ng/L range commonly found in natural uncontaminated waters to the ug/L concentrations found at contaminated sites.
- Capable of accumulating detectable and reproducible masses of PFAS in thin layer deployments at field-relevant concentrations.
- A reasonably rapid equilibrium from water.

In this research, we demonstrate for the first time that several composite polymers can be synthesized that remain stable in the water environment and provide adequate sorption of PFAS from aqueous solution at equilibrium. Thus, conceptually, we can develop an equilibrium passive sampler for PFAS in water that is able to respond to the dissolved concentration of PFAS. The casting approach allows adjustment of size and sorbent ratios to meet target PFAS concentrations. A material with a log K_d of 3 for PFAS, exposed to an aqueous PFAS concentration of 5 ng/L (a moderate-to-low value for contaminated sediment pore water), would be capable of accumulating 500 pg of PFAS (a readily detectable amount) in a 100 mg mass of the polymer. For most materials under consideration, the size is roughly less than 2”x1”. Several advanced materials have achieved this degree of sorption within 7 days of deployment in a single point isotherm study for various PFAS compounds. This constitutes a promising proof of concept for an equilibrium-based, polymeric passive sampling system for PFAS in sediment pore water.

Isotherm studies across a concentration range demonstrated that the Langmuir model provided the best fit for the full range of concentrations evaluated, however, the linear model may adequately describe the partitioning behavior of most compounds at the low concentration range. This work lays the foundation of equilibrium passive sampling technology and provides the capability of ag+AC, CA+WAX, CA+HSA passive samplers to be used to measure the freely dissolved concentration of PFAS compounds.

For all target PFAS compounds, the uptake is rapid and 7 days appears to be sufficient for loading from the aqueous medium. The single time point desorption kinetics matched reasonably well with the adsorption kinetics, which provides promising early indication that the desorption kinetics can be used to predict the adsorption kinetics for an analogous compound. Therefore, we

may be able to use stable isotope labeled PFAS compounds as PRCs, and further determine the fraction to steady state.

We believe that the initial results presented in this report show great promise for pursuing the concept of equilibrium passive sampling for PFAS compounds. Further work is needed to operationalize the passive sampling system explicitly designed to quantify the time-weighted average bioavailable PFAS concentration in a reproducible fashion. Subsequent research will need to address questions regarding applicability to complex water chemistries, the ability to predict bioaccumulation, applicability in the field, and interpretations of field deployments

1.1 List of acronyms

AC: activated carbon

AFFFs: Aqueous Film Forming Foams

Ag: agarose

CA: cellulose acetate

C_{free}: freely dissolved concentration

$C_{s,max}$: maximum adsorption capacity

$C_{s:}$ adsorbed concentrations in the sorbent

CTA: cellulose tricetate

C_w: chemical concentration in water

DBL: diffusive boundary layer

DGT: diffusive gradients in a thin-film

DL: detection limits

DOC: dissolved organic carbon

DoD: Depart of Defense

ELAP: Environmental Laboratory Accreditation Program

FOSA: perfluorooctane sulfonamide

FtS 8:2: sodium 1H,1H,2H,2H-perfluoro1-decanesulfonate

GAC: granular activated carbon

GMU: George Mason University

HLB: hydrophilic-lipophilic balanced copolymer

HOC: hydrophobic organic compound

HSA: human serum albumin

IS: internal standards

K: partition coefficient

K_d: solidsediment- or soil-water partitioning coefficient

K_p: partition constant

K_{ps}: passive sampler-water partitioning coefficient

LC--MS: Liquid Chromatography/Mass Spectrometry

MRM: Multiple Reaction Monitoring

NMeFOSSA: n-methyl perfluorooctanesulfonamidoacetic acid

PAC: powdered activated carbon

PDMS: polydimethylsiloxane

PE: polyethylene

PFAS: per- and polyfluoroalkyl substances

PFBA: perfluorobutanoic acid

PFBS: perfluorobutane sulfonate

PFOA: perfluorooctanoic acid

PFOS: perfluorooctane sulfonate

PFTreA: perfluorotetradecanoic acid

PIM: polymer inclusion membrane

POCIS: polar organic chemical integrative sampler

POM: polyoxymethylene

PP: polypropylene

PRC: performance reference compound

PS: passive sampler

QA: quality assurance

S_e: amounts of target compounds sorbed at equilibrium

SOP: standard operating procedures

SPE: solid phase extraction

SS: surrogate standards

S_t: amounts of target compounds sorbed at time t

t: time

WAX: weak anion exchange

μ: sorption rate coefficient

1.2 List of Figures

1.3 List of Tables

2.0 Objectives

While much progress has been made in the field of passive sampling for hydrophobic organic compounds (HOCs) and metals, the field of passive sampling is still in the early stages of development for PFAS compounds. The work described here seeks to develop an innovative, previously untested equilibrium passive sampler for PFAS compounds. Recognizing the large range of chemical properties involved including polarity and molecular weight, we explored tailoring the polymeric sampler to target a suite of PFAS compounds. As opposed to kinetic samplers like the Polar Organic Chemical Integrative Sampler (POCIS) that has been investigated recently for sampling PFAS compounds, we targeted the development of an equilibrium passive sampler that attains equilibrium during a typical deployment period to quantify the time-weighted average PFAS concentration in a reproducible fashion. Our work follows from research we are currently doing to develop an equilibrium passive sampling approach for mercury and methylmercury in environmental waters. Recognizing that our approach is novel, untested, and potentially involves some risk, we submitted a Limited Scope Proposal for 1-year duration. We use the 1-year study as a proof-of-concept before proposing to address the subsequent questions regarding applicability to complex water chemistries, the ability to predict bioaccumulation, applicability in the field, and interpretations of field deployments.

The key objectives of this 1-year research project, therefore, were to:

1) Develop a range of functionalized polymeric thin films for use in equilibrium passive sampling of representative PFAS compounds. These polymers were formulated to include a range of sorbents and materials used in the formulation of polymer inclusion membranes (PIM) for the separation of both polar and nonpolar chemicals. These passive sampler sorption moieties target a range of compound properties and should be able to attain equilibrium during a typical deployment period.

2) Experimentally measure polymer/water partition constants for the selected PFAS compounds and develop isotherm models. A critical component of our approach is the development of an equilibrium passive sampler. Thus, accurate measurement of partitioning characteristics is critical for the technology.

3) Test reversibility of the equilibrium that reflects changing concentration in the external water phase. We believe that for the functionalized polymers to perform as a true equilibrium sampler providing integrative measurements, the concept of equilibrium reversibility needs to be demonstrated. Therefore, we measured the kinetics of sorption and desorption of two PFAS compounds to confirm the mechanistic underpinning of a reversible equilibrium and provide the proof-of-concept of using performance reference compounds (PRCs) for checking and correcting for non-equilibrium where necessary.

4) Evaluate the mechanism of accumulation in the polymer. We performed sorption experiments with different thickness polymers to confirm that the sorption mechanism entails diffusion within the polymer and sorption into target domains in contrast to surface adsorption on the film.

3.0 Background

3.1 Importance of dissolved water measurements for PFAS compounds

The concentration of a pollutant in its freely dissolved aqueous phase provides a measure of its chemical activity and can be readily related to toxicity and bioaccumulation (Mayer et al., 2014; Peijnenburg et al., 2014). This has been demonstrated for nonpolar organic compounds (USEPA 2017) and also for ionizable compounds and metals (USEPA 2007). Where feasible, direct measurement of the compounds in the filtered water phase accurately assesses the dissolved concentrations. However, extensive volume water sampling is often not feasible or efficient for sparingly soluble compounds or those present at trace amounts. For example, in the sediment environment, extraction of sediment porewater may yield small volumes in most practical applications. In addition, when compounds strongly associate with particles or ligands like dissolved organic carbon (DOC), the separation of dispersed phases poses a significant challenge for accurate measurements. As a result, dissolved concentrations of these compounds are typically only a fraction of the total concentration in water, and water represents only one of the multiple exposure pathways.

Nevertheless, freely dissolved concentration (C_{free}) measurements are still useful because the compounds are often in thermodynamic equilibrium among water, sediment, animal, and sampler compartments (Ghosh et al., 2014). This chemical activity-based approach permits the use of equilibrium partitioning coefficients (K_p) to calculate unknown concentrations or to predict the outcome of a perturbation such as the addition of an engineered sediment amendment or an ongoing contaminant input. In most fate modeling approaches involving HOCs, C_{free} is the most commonly defined and important master variable.

Several DoD sites are addressing new regulations that bring greater scrutiny to the impacts of the use of PFAS containing Aqueous Film Forming Foams (AFFFs). In addition, new legislation is considering declaring PFAS as hazardous chemicals that the USEPA may regulate under the Superfund Program. These major regulatory changes have created the need for an accurate assessment of the risk to humans and ecosystems from the presence of PFAS compounds. While the risk assessment paradigm for PFAS compounds is still under scientific and regulatory development (Conder et al., 2008), the one we would like to follow here is analogous to the

existing paradigm for both polar and nonpolar pollutants in the aquatic environment, with C_{free} as a critical component.

3.2 Passive sampling technology

Polymeric equilibrium passive samplers have been extensively investigated as a tool to measure C_{free} of target compounds in air or aquatic environment. The basic approach of passive sampling is to use sorbents to concentrate the contaminants of interest from a target environment, then process and extract the chemical accumulated sorbents (Huckins et al., 1990). Sorbent polymers like polyethylene (PE), polyoxymethylene (POM), and polydimethylsiloxane (PDMS) are commonly used passive sampler materials for hydrophobic organic compounds due to their high sorbent water partition coefficients (US EPA/SERDP/ESTCP. 2017).

Passive sampling technologies were developed as a reliable and easily implemented approach with minimal disturbance to monitor contaminants in sediments and water. Compared to conventional techniques, passive sampling technologies can obtain dissolved water concentrations directly from the environment (i.e. *in situ*) and provide low detection limits. Because of the passive sampler sorbent's high affinity, only a small amount of sorbent is needed to measure the target compounds to a detectable level, as opposed to large volumes of water needed to achieve the same detection limits for traditional methods (Greenwood et al., 2009).

Much progress has been made in the field of passive sampling for hydrophobic organic compounds (HOCs) (Ghosh et al., 2014; US EPA/SERDP/ESTCP. 2017), metals (Peijnenburg et al., 2014), and methylmercury (Sanders et al., 2020). The two major strategies for passive sampling of contaminants are equilibrium samplers and diffusion based samplers, such as DGT or Chemcatchers®. Equilibrium samplers are often used for HOCs, for which the freely dissolved concentration in water or sediment pore water is widely used as good surrogates for bioaccumulation measurements and availability to organisms (Lu et al., 2011; Beckingham et al., 2013; Ng et al., 2014; Fadaei et al., 2015; Yan et al., 2020). Equilibrium samplers use thin polymers sheets with partition coefficients for HOCs similar to their binding constants to sediment organic matter. They effectively concentrate dissolved-phase HOCs onto the polymers sheets, which can be extracted for analysis. Because of the polymer's relatively small mass to surface area ratio exposed to sediment, the samplers do not deplete pore water pools or create concentration gradients that could lead to significant HOC depletion from the adjacent

sediments. If diffusive boundary layer (DBL) issues are overcome and the samplers come to equilibrium, the equation for predicting aqueous HOC concentrations is simple:

$$C_{free} = \frac{C_{sorbent}}{K_{sorbent-water}}$$

Here, C is the concentration of the HOC of interest freely dissolved in water or in sorbent, and K is the partition coefficient between water and the polymer sorbent. Performance reference compounds are used to check for equilibrium and correct for non-equilibrium when needed (Ghosh et al., 2014).

3.3 Challenges for PFAS passive sampling measurement

While equilibrium passive samplers are increasingly well established for neutral organics, the field of passive sampling is still in the early stages of development for PFAS compounds. The best studied is the POCIS device, which has a sorbent material (receiving phase) enclosed between two polyethersulfone or other diffusion-limiting membranes (Cerveny et al., 2016; Li et al., 2016; Persson, 2015; Kaserzon et al., 2019) and polyurethane foam passive sampling disks (Ahrens et al., 2013). Challis et al. (2018) developed diffusive gradients in thin-films (DGT) passive sampler for PFAS with a 0.5-1.5 mm thickness. Recent work by Wang et al. (2017) explored the use of immobilized ionic liquids in silica gel to develop a POCIS passive sampler for PFAS. In all of these devices, accumulation in the sorbent over some time is used to calculate the external concentration driving force integrated throughout the deployment. These are kinetic devices used to estimate the water or air concentration based on the measured rate of uptake using empirically-derived mass transfer coefficients. The mass transfer through the diffusion-limiting membrane is calibrated. However, any field condition that can impact kinetics, such as the external boundary layer in the air/water side, will bias the result (Kaserzon et al., 2013). An alternate and more robust paradigm in passive sampling is using an equilibrium sampler that is expected to come close, if not entirely, to equilibrium. In the equilibrium approach, external factors such as hydrodynamic conditions and fouling have much less impact on the measurements and can be easily corrected. Performance reference compounds are used to confirm or correct an equilibrium where necessary. We pursued this latter approach to measure PFAS compounds in water. To our knowledge, equilibrium passive sampling has not been successfully demonstrated for PFAS compounds before.

The primary bottleneck for using this approach for PFAS compounds is the lack of knowledge of suitable sorbents that provide adequate sorption with predictable equilibrium distribution between the solid phase and water. Sorbents chosen for PFAS compounds must take into account the large range of chemical properties of PFAS compounds. In ongoing research, we have developed passive samplers for methylmercury (Sanders et al., 2020) by exploring the use of a range of sorbents including activated carbon embedded in thin polymeric sheets. The motivation of embedding fine sorbent particles in a thin polymer sheet lies in the enhancement of mass transfer and progress towards achieving equilibrium partitioning with water. Sampler equilibration time in water and sediments/soils was approximately 1 to 2 weeks. In soil and sediment slurries and stagnant microcosms, samplers made good predictions of directly measured aqueous concentrations of methylmercury. This work opens the way for a novel approach to equilibrium passive sampling of polar molecules.

The present project aimed to develop such a sampler to enable reproducible measurements of dissolved PFAS compounds and improve risk assessment and management for PFAS-contaminated sites by accurately measuring C_{free}. The sampler can also enable time integrated measurements in sediments, surface water, and groundwater, and allow efficient determination of C_{free} necessary for phase partitioning calculations and estimation of biouptake and toxicity. Finally, a successful PFAS equilibrium passive sampler can be integrated with the current practice of passive equilibrium sampling for organic compounds, not just in the device and deployment aspects, but also in the data interpretation and use in risk assessment. The overarching goal is to move away from direct water sampling, or a kinetic sampler like the POCIS to an equilibrium passive sampler similar to the current state of the art for hydrophobic organic compounds. We developed and tested a range of functionalized polymeric thin films for use in equilibrium passive sampling of representative PFAS compounds in this present work.

3.4 Literature cited

Ahrens, L., Harner, T., Shoeib, M., Koblizkova, M., Reiner, E.J. Characterization of two passive air samplers for per- and polyfluoroalkyl substances. *Environmental Science & Technology*. 47, 2013, 14024-140-33.

Beckingham B, Ghosh U. Polyoxymethylene passive samplers to monitor changes in bioavailability and diffusive flux of PCBs after activated carbon amendment to sediment in the field. *Chemosphere*. 2013, 91:1401-1407.

Challis, J.K. (2018). Development and evaluation of passive sampling devices to characterize the sources, occurrence, and fate of polar organic contaminants in aquatic systems. PhD thesis, University of Manitoba.

Cerveny, D., Grabic, R., Fedorova, G., Grabicova, K., Turek, J., Kodes, V., Golovko, O., Zlabek, V., Randak, T. Perfluoroalkyl substances in aquatic environment – comparison of fish and passive sampling approaches. *Environmental Research.* 2016, 144, 92-98.

Conder, J.M., R.A. Hoke, W. de Wolf, M.H. Russell, and R.C. Buck. Are PFCAs bioaccumulative? A critical review and comparison with regulatory criteria and persistent lipophilic compounds. *Environmental Science & Technology.* 2008, 42:995-1003.

Fadaei, H.; Watson, A.; Place, A.; Connolly, J.; Ghosh, U. Effect of PCB Bioavailability Changes in Sediments on Bioaccumulation in Fish. *Environmental Science & Technology*. 2015, 49 (20), 12405-12413.

Ghosh U, Driscoll SK, Burgess RM, Jonker MTO, Reible D, Gobas F, Choi Y, Apitz SE, Maruya KA, Gala WR, Mortimer M, Beegan C. Passive sampling methods for contaminated sediments: practical guidance for selection, calibration, and implementation. *Integr Environ Assess Manag*. 2014; DOI: 10.1002/ieam.1507.

Greenwood, R., Mills, G.A., Vrana, B., 2009. Potential applications of passive sampling for monitoring nonpolar industrial pollutants in the aqueous environment in support of REACH. *Journal of chromatography*. A 1216, 631-639.

Huckins, J.N., Gibson, V., Lebo, J., Manuweera, G., Gale, R., 1990. Insitu Semipermeable Polymeric Samplers for Monitoring Hydrophobic Contaminants in Water. *Abstr Pap Am Chem S* 200, 29-Envr.

Kaserzon, S.L. Vermeirssen, E.L.M., Hawker, D.W., Kennedy, K., Bentley, C., Thompson, J., Booij, K., Mueller, J.F. Passive sampling of perfluorinated chemicals in water: Flow rate effects on chemical uptake. *Environmental Pollution*. 177, 2013, 58-63.

Kaserzon, S. L., Vijayasarathy, S., Bräunig, J., Mueller, L., Hawker, D. W., Thomas, K. V., & Mueller, J. F. (2019). Calibration and validation of a novel passive sampling device for the time integrative monitoring of per- and polyfluoroalkyl substances (PFASs) and precursors in contaminated groundwater. *Journal of Hazardous Materials*, 366, 423–431.

Li, Y., Yang, C., Bao, Y., Ma, X., Lu, G., & Li, Y. (2016). Aquatic passive sampling of perfluorinated chemicals with polar organic chemical integrative sampler and environmental factors affecting sampling rate. *Environmental Science and Pollution Research*, 23, 16096–16103.

Lu, X.; Skwarski, A.; Drake, B.; Reible, D. Predicting Bioavailability of PAHs and PCBs with Porewater Concentrations Measured By Solid-Phase Microextraction Fibers. *Environmental Toxicology and Chemistry* 2011, 30 (5), 1109-1116.

Mayer, P., Witt, G., You, J., Escher, B.I., Parkerton, T.F., Adams, R.G., Cargill, J.G., Gan, J., Gouin, T., Gschwend, P.M., Hawthorne, S.B., Helm, P., 2014. Passive sampling methods for contaminated sediments: scientific rationale supporting use of freely dissolved concentrations. *Integrated Environmental Assessment and Management.* 10, 197 209.

Ng, CA; Hungerbuhler, K. Bioaccumulation of Perfluorinated Alkyl Acids: Observations and Models. *Environmental Science & Technology*. 46, 4637-4648. 2014.

Persson, C. (2015) Calibration and application of passive sampling in drinking water for perfluoroalkyl substances. Masters thesis, Department of Earth Sciences, Uppsala University.

Peijnenburg, WJGM, Teasdale, P.R., Reible, D., Mondon, J., Bennet, W.W., Campbell, P.G.C. Passive sampling methids for contaminated sediments: State of the science for metals. *Integrated Environmental Assessment and Management*. 10, 2014, 179–196.

Sanders, J. P.; McBurney, A.; Gilmour, C. C.; Schwartz, G. E.; Washburn, S.; Kane Driscoll, S. B.; Brown, S. S.; Ghosh, U. Development of a Novel Equilibrium Passive Sampling Device for Methylmercury in Sediment and Soil Porewaters. *Environ. Toxicol. Chem.* 2020, 39 (2), 323–334 DOI: 10.1002/etc.4631.

USEPA 2007. Framework for Metals Risk Assessment. Office of the Science Advisor. Risk Assessment Forum. US Environmental Protection Agency, Washington, DC 20460. EPA 120/R-07/001 March, 2007.

USEPA 2017. Developing Sediment Remediation Goals at Superfund Sites Based on Pore Water for the Protection of Benthic Organisms from Direct Toxicity to Nonionic Organic Contaminants. EPA/600/R 15/289 | October 2017.

US EPA/SERDP/ESTCP. 2017. Laboratory, Field, and Analytical Procedures for Using Passive Sampling in the Evaluation of Contaminated Sediments: User's Manual. EPA/600/R- 16/357. Office of Research and Development, Washington, DC 20460.

Wang, L., Gong, X., Wang, R., Gan, Z., Lu, Y., Sun, H. Application of an immobilized ionic liquid for the passive sampling of perfluorinated substances in water. *Journal of Chromatography* A. 1515, 2017, 45-53.

Yan, S.; Rakowska, M.; Shen, X.; Himmer, T.; Irvine, C.; Zajac-Fay, R.; Eby, J.; Janda, D.; Ohannessian, S.; Reible, D. Bioavailability Assessment in Activated Carbon Treated Coastal Sediment with in Situ and Ex Situ Porewater Measurements. *Water Research.* 2020, 185, 116259.

4.0 Organization of the report

This research project entailed four key research objectives as described below. Objectives 1 and 2 are described separately in chapters 5 and 6, respectively. Objective #3 and #4 explore the transport kinetics of PFAS in the passive samplers, and are discussed together in chapter 7. The specific methods, results, and discussion associated with each of the objectives have been written separately allowing focused discussion of each objective. The results presented here are in the process of being prepared for peer-reviewed publications.

Chapter 5: (Objective 1) Development of novel polymeric thin films for equilibrium passive sampling.

Chapter 6: (Objective 2) Equilibrium partitioning studies with a selected group of PFAS compounds covering a range of properties.

Chapter 7: (Objective 3) Testing of reversible equilibrium with matching kinetics of sorption and desorption, and (Objective 4) Mechanism of accumulation in polymer.

5.0 Research Objective #1: Development of novel polymeric thin films for equilibrium passive sampling

5.1 Introduction

There is a need for a simple, passive sampling system explicitly designed to quantify the time-weighted average bioavailable PFAS concentration in a reproducible fashion. While we still must define, at least empirically, the PFAS complexes and phases that are available to organisms, we believe that one of the essential aspects of PFAS passive sampler development will be the measurement of freely dissolved PFAS in water and sediment porewater. Some polymers, including polyethylene (PE), polyoxymethylene (POM), and polydimethylsiloxane (PDMS), are widely used for passive sampling of hydrophobic organic contaminants. However, these standard polymers are not sufficiently sportive for PFAS sorption. To address this challenge, common polymer types were modified to achieve greater chemical affinity.

We chose an equilibrium method to try and avoid the limitations of methods that rely on kinetic calibrations for each PFAS complex. In this study, we explored single-layer polymers gels in order to measure the concentrations of PFAS. The target thickness of the polymer sheet was below 1 mm to allow a rapid mass transfer.

We began the development of PFAS samplers by evaluating potential materials. We explored four broad classes of polymers: Polydimethylsiloxane (PDMS), agarose (AG), cellulose acetate (CA) and cellulose triacetate (CTA) that were cast as the thin base film in the functionalized passive sampler construction in this project. We used a range of sorbent amendments to allow equilibrium sorption of a wide range of PFAS compounds: activated carbon, commercially available materials Oasis HLB and Oasis WAX, and human serum albumin. These sorbents have shown affinities to a wide range of PFAS compounds in previous research. The solid sorbents were embedded in a thin polymer sheet. A range of polymer and polymer composites were prepared to test sorption capacity and linearity. Polymers were chosen for pore size, the sorbent capacity of PFAS, and the ability to potentially include sorbents. A wide variety of polymers with and without sorbent inclusions were synthesized and tested. Our goal was to synthesize passive sampling materials having a range of properties, including:

- A reasonably rapid equilibrium from water.
- Partition coefficients close to the measured K for PFAS in natural sediments ($10^{1.5}$ to $10^{3.5}$).

- Sorption isotherms can be described across the concentration range of interest, from the ng/L range commonly found in natural uncontaminated sediment pore waters to the high ug/L concentrations found in contaminated sites.
- Capable of accumulating detectable and reproducible masses of PFAS in thin layer deployments at field-relevant concentrations.
- Ability to synthesize consistent thin films that are structurally stable in water deployments.

5.2. Polymer selection

We used four constructs to develop the passive samplers as described in the section below. For each construct, we developed 3-4 individual formulations of the polymer by altering the composition. The suitable polymers used as the base polymer in the synthesis were: PDMS, agarose, CA and CTA. Using PDMS was our first choice as that polymeric phase will also allow sampling of a wide range of hydrophobic compounds, including some of the hydrophobic PFAS. Metal nanoparticles were successfully embedded on PDMS composite films in the research conducted by Goyal et al. (2009). A passive sampler of activated carbon embedded agarose polymers was developed for methylmercury successfully (Sanders 2020). Cellulose acetate and cellulose triacetate are environmentally friendly polymers derived from acetylating cellulose, which could be the potential raw materials for synthesizing functionalized polymers for PFAS analysis. Kwon et al. investigated the incorporated silver nanoparticles in cellulose acetate polymers and their reaction chemistry in 2005.

The target thicknesses of the polymer sheet were below 1 mm to allow a rapid mass transfer. Before performing any sorption studies, the polymers were first investigated to assess rigidity and structural stability in a water environment. Only polymer formulations that were able to withstand deployment in a well-stirred bath of water for a period of 7 days and insertion and retrieval from a sediment bed were taken forward for sorption studies.

5.3. Sorbent selection

5.3.1 Activated Carbon

Work in the last two decades has demonstrated that black carbonaceous particles in sediments such as soot, coal, and charcoal very strongly bind organic compounds, and their presence in

sediments reduces exposure (Cornelissen et al., 2005), often by one order of magnitude or more compared to natural organic matter. As a black carbon type, activated carbon (AC) is a strong sorbent with a large surface area and has been used for many organic contaminants removal. Activated carbon has been applied in the equilibrium passive sampling polymer formulations developed for other contaminants in the aqueous environment like mercury and methylmercury (Sanders 2020).

At this time, AC is the best know sorbent for a wide range of PFAS compounds (Field et al., 2017). It offers a range of sorption sites including hydrophobic interaction and association with specific functional groups that can be beneficial to targeting the full range of PFAS compounds. Ochoa-Herrera and Sierra-Alvarez (2008) evaluated the activated carbon affinity for perfluorooctane sulfonate (PFOS), perfluorooctanoic acid (PFOA) and perfluorobutane sulfonate (PFBS), and the results indicated that activated carbon adsorption is a promising treatment technique for the removal of PFOS. McCleaf et al. (2017) applied AC and AE columns to evaluate PFAS affinity, and the findings showed that Linear isomers of PFOS, PFHxS, and perfluorooctane sulfonamide (FOSA) had greater column removal efficiencies using granular activated carbon (GAC). Yu et al. (2009) compared the powdered activated carbon (PAC), GAC and anion-exchange resin for PFOA and PFOS. The PAC showed the highest sorption capacity among these three materials for PFOS while the anion-exchange resin had the highest sorption capacity for PFOA. In a study that investigated PFAS sorption to activated carbon at environmentally relevant nanogram per liter concentrations conducted by Hansen et al. (2010), PAC gave higher adsorption than GAC for three perfluorosulfonates and five perfluoroacetic acids. In the present research, we started with both GAC and PAC as the sorbents in our initial polymer constructions and decided to go only with PAC, which shows better performance.

5.3.2 Oasis HLB

Oasis HLB is a commercially available solid-phase extraction sorbent. It is a strongly hydrophilic, reversed-phase and water-wettable polymer consisting of hydrophilic-lipophilic balanced copolymer of [poly(divinylbenzene)-co-N-vinylpyrrolidone]. It is the most frequently used receiving phase in commercial polar organic chemical integrative sampler (POCIS) sampling for PFAS analysis.

Kaserzon et al. (2012) evaluated the HLB embedded POCIS sampling technologies for monitoring seven PFAS compounds and demonstrated that POCIS seems to be a more practical approach for monitoring PFASs in aquatic environments than analyses of fish. Recent work by Wang et al. (2017) explored the use of immobilized ionic liquids and HLB in silica gel to develop a POCIS passive sampler for PFAS, and the HLB-sampler showed linear uptake kinetics in the first seven days for most analytes. Fedorova et al. (2013) applied Oasis HLB samplers in a PFAS study and 10 of 15 analyzed PFCs were found in the samplers, with only 5 of them detected in wastewater. These data indicated the applicability of HLB POCIS for time-integrative water sampling for perfluorinated carboxylates and perfluorinated sulfonates. Since Oasis HLB shows a good affinity for PFAS compounds in POCIS samplers, we chose it as one of our receiving phases in this passive sampler development project.

5.3.3 Oasis WAX

The Oasis WAX used for PFAS analysis is a mixed-mode weak anion exchange polymer that has been shown to be a suitable solid phase extraction (SPE) sorbent for anionic perfluorinated species in water (Taniyasu et al., 2005). This is due to the modification of Oasis HLB sorbent with piperazine groups that offer a weak anionic retention mechanism. Oasis WAX sorbent has been widely used in the analysis method for PFAS, especially short-chain perfluorinated acids (Taniyasu et al., 2005, 2008; ISO25101, 2009). Barreca et al. (2018) reported a method using Oasis WAX to detect perfluorinated compounds at pg/L levels in superficial and underground water samples. Kaserzon et al. (2012) developed a modified POCIS with Oasis WAX for perfluorinated chemicals and the data indicated WAX can be a suitable binding phase for some PFCs, but may with a more limited range of analytes. In the comparison conducted by Taniyasu et al. (2005), Oasis HLB and Oasis WAX showed similar performance for extracting PFCAs and PFSAs from water, but WAX offers advantages for relatively short-chained species.

5.3.4 Human Serum Albumin (HSA)

The distribution and accumulation of a wide range of ionizable molecules in the animal body are determined by the binding to plasma proteins. This is especially true for PFAS compounds which have been found to bind primarily to serum albumins in both humans and rats (Mallik et al. 2010; Han et al. 2003; Ng and Hungerbuhler 2014). Since human serum albumin (HSA) is the primary binding moiety inside the body, we developed our tailored polymer to include

immobilized HSA. PFAS binding to HSA is non-covalent and reversible (Han et al., 2003) allowing the construct to be amenable for adoption in equilibrium passive sampling.

5.2 Materials and methods

5.2.1. Materials for the synthesis of functional passive samplers

1) Polymer phase: Agarose (ACROS organics, NJ), polydimethylsiloxane (ACROS organics, NJ), Dow 184 silicone encapsulant clear kit (Dow, NJ), low melting point cellulose acetate (ACROS organics, NJ), cellulose triacetate (ACROS organics, NJ).
2) Binding phase: activated carbon (Calgon Carbon, 80 x 325 TOG LF, CAS #7440-44- 0, Type 3055, Moon Township, PA), Chrialpak silica-bonded human serum albumin (5 µm, Chiral Technologies Inc, West Chester, PA), human serum albumin (Sigma, St. Louis, MO), Oasis® HLB (30 µm, Waters Corporation), Oasis®WAX (30 µm, Waters Corporation).
3) Solvent: hexane (Fisher Scientific, Fair Lawn, NJ), methanol (Fisher Scientific, Fair Lawn, NJ), acetone (Fisher Scientific, Fair Lawn, NJ), methylene chloride (Fisher Scientific, Fair Lawn, NJ), Milli-Q Type 1 (18.2 MΩ) water (Millipore Sigma, Burlington MA).
4) Others: Multiple Clearance Square Applicator (Gardner, Pompano Beach, FL), glass plates, glass slides, etc.

5.2.2. Materials for single point isotherm study

The 24 target chemicals (Chemicals listed in Appendix 1) were purchased from AccuStandard as a pre-made mixture in methanol (New Haven, CT, No. PFC-24). The mix was obtained as a 2 ng/uL solution for each target chemical in methanol and this served as the stock solution for target chemicals. The internal standards (IS) used include perfluoro-[13C8] octanoic acid (13C8-PFOA), sodium perfluoro-1-[3C8] octanesulfonate (13C8-PFOS), and N-deuteriomethylperfluoro-1-octanesulfonamidoacetic acid (d3-NMeFOSAA). All internal standards (IS) were purchased from Wellington Laboratories (Guelph, Ontaria, Ca). The IS were purchased individually as a 50 ng/uL solution, diluted to 2 ng/uL in methanol, and combined to serve as the IS stock solution. The surrogate standards (SS) used include perfluoro-n-[1,2-13C2] hexanoic acid (13C2-PFHxA), perfluoro-n-[1,2-13C2] decanoic acid (13C2-PFDA) and N-deuterioethylperfluoro-1-octanesulfonamidoacetic acid (d5-NEtFOSAA). The SS were

purchased as a 50 ng/uL solution for each SS and were diluted to 2 ng/uL in methanol combined to serve as the SS stock solution.

5.2.3. Development of functional passive samplers for PFAS

The experiments designed at this stage focused on general polymer casting and selected functional particles embedded within base films. Four different materials: Agarose, PDMS, CA and CTA were used to form a polymer base for PFAS compound analysis. Different parameters were controlled to determine the best experimental conditions for the film formation, including stirring speed, time and temperature, settling time and temperature, solution system like solvent and solution ratio, polymer thickness, etc. All glass plates and appliances were cleaned with solvent before use. For the materials that can stand high temperature, like glassware and aluminum foils, cleaning was performed by heating in a furnace for 16 hours at 450°C.

Figure 5.1 Multiple Clearance Square Applicator (Gardner, Pompano Beach, FL) used for polymer casting with eight different thickness controls (5mil, 10mil, 15mil, 20mil, 25mil, 30mil, 40mil, 50 mil).

1) Agarose

Agarose gels were adapted from an existing method (Sanders et al., 2020). An amount of 0.3 g agarose powder was diluted in 20 mL MilliQ water. The selected functional absorbent for PFAS compounds like powdered activated carbon, WAX, and HLB particles were added to the solution at a designed ratio. Then the mixture was placed in a boiling water bath, covered and gently stirred for 4 min 30 sec until all the Agarose was dissolved and the solution was immediately

pipetted on a clean glass plate. For the HSA particles, high temperatures from boiling water may lead to deactivation. Therefore, the low melting point of agarose materials with a relatively low water bath temperature (60°C) was used. Two different ways were used to control the polymer thickness: A) pipetted the solution into two glass plates with a spacer (1000 μm or 484 μm) separating the plates; B) used the applicator to cast for a specific thickness. After 1 h cooling down at room temperature, agarose gels were cut into small pieces with a clean plexi-glass cutter. Two different thicknesses were designed for the polymer: 484μm and 1000μm.

2) PDMS

Two different types of PDMS were used. Type 1 (PDMS 1) was crosslinked polydimethylsiloxane (ACROS Organics), while type 2 (PDMS 2), Dow corning 184, consists of two parts: silicone elastomer base (part A) and curing agent (part B). The A: B ratio was 10 :1. The PDMS materials and the functional particles like HLB were mixed and dissolved in hexane, then stirred with a magnetic bar for mixing before casting. The mixture was cured to a flexible PDMS polymer when thoroughly mixed with liquid components. Membranes with different weight percentages of PDMS/hexane solutions (5%, 10%, 15%) were pre-crosslinked at room temperature for 30 minutes under stirring. The composites were then cast on glass plates and heated at 75℃ to complete the crosslinking. Various experimental conditions including crosslinking temperature (20°C, 60°C, 75°C, 100°C), stirring time, speed, and solution recipe were explored to determine the most optimal synthesis approach.

3) Cellulose Acetate

CA powder and the target additives for PFAS absorption were weighed and placed in a vessel with acetone. The solution was continuously stirred until these different compositions were completely dissolved to form a homogeneous solution. Then it was kept still for de-gassing. This takes 5-10 minutes. The thickness of the active layer was controlled with the polymer applicator. Then the membrane was placed for crosslinking and further dried for 1 hour, then cut into small pieces for deployment.

The CTA polymer casting process was similar to the CA experiment. To get better solubility, the solvent system needed to replace acetone with DCM or DMAc. The membrane was placed into a

vacuum drying oven for crosslinking. The thickness of the active layer was controlled with a polymer applicator.

5.2.4. Single point isotherm study

In initial isotherm experiments, a piece of test polymer was added to 100 mL deionized water bottle and spiked with PFAS at a concentration of 800 ng/L. The PFAS analytes for the laboratory intercomparison were acquired as an analytical mixture (PFC-24-10X) from AccuStandard (New Haven, CT) at a concentration of 20 µg/mL (Table A3) in 80:20 methanol-water solvent. This mixture was diluted 25:1 in LCMS grade methanol as a spike standard to yield 0.8 µg/mL concentration for each of the 24 PFAS (of which 7 were studied in detail). A 1.00 mL aliquot of the spike standard was added to each of 6 bottles containing 1.00 L of Milli-Q Type-I water to serve as the 800 ng/L nominally spiked samples, which were equally divided between Clarkson University (DoD ELAP Laboratory) and George Mason University (Foster lab). Samples were contained in 125 mL polypropylene (PP) bottles. Samples were loaded at room temperature (20°C) with orbital shaking at 45 rpm. After loading for 7 days, the PFAS concentrations on the passive sampler, water, and attached to the bottle were measured separately.

The passive samplers were first spiked with 100 uL of SS (equivalent to 100 ng of SS per tube) 100 uL of each IS (equivalent to 80 ng of each IS) in 15 mL PP centrifuge tubes. The tested passive sampler was then extracted with 10 mL X 3 volumes of the appropriate solvent. The combined 3X extracts were transferred to 40 mL glass evaporation vials using plastic pipettes for solvent evaporation to a final volume of 0.5 mL. After evaporation, the extracts were filtered through syringe filters into 1 mL PP LC-MS/MS vials.

The water samples were also spiked with SS and IS and then were extracted with Supelco Swift HLB (60 mg bed 30 mL barrel) cartridges (Millipore 57492-U). The cartridges were initially conditioned sequentially with 4 mL of 0.3% NH_4OH, 4 mL MeOH, and 4 mL of water. The 100 mL sample was extracted at 4 mL/min. The cartridge was rinsed with 2 x 4 mL of water and eluted with 2 x 0.50 mL of 0.3% NH_4OH in MeOH directly into the PP autosampler vials. During elution, the eluents were passed through a 0.2 µm (pore diameter) 13 mm PP syringe filter (Tisch SF14704) into the autosampler vials.

The extracted solvents were concentrated under a vortex stream of nitrogen gas to a final volume of 0.5 mL in a TurboVap concentrator, then analyzed by the LC-MS/MS instrument.

5.2.5 PFAS analyses.

PFAS analysis was carried out using an LC-MS/MS at George Mason University (GMU). The primary analytical instrument was a Shimadzu 8050 tandem mass spectrometer (Shimadzu, Columbia, MD). The LC-MS/MS analysis of the PFAS isotherm sample run was completed using a 50 mm x 2.1 mm (1.8 μm) UHPLC Supelco Titan C18 column in the MRM analysis mode. This method was adapted from the framework of EPA Method 537.1. QA/QC included blanks, replicates, spikes and suitable certified reference materials.

As required by the SERDP program for all PFAS-related projects, an analytical confirmation was performed and a white paper was submitted to the program (also attached in the appendix). For analytical confirmation, George Mason University (GMU) submitted a 500 mL sample of spiked Milli-Q water to Clarkson University for analysis of the 7 per- and polyfluoroalkyl substances (PFAS). Another 500 mL spiked sample was prepared for analysis at GMU. The Clarkson 500 mL spiked sample was submitted for the purpose of analytical confirmation to a Department of Defense (DoD) Environmental Laboratory Accreditation Program (ELAP)- accredited laboratory at Clarkson University (CAARES Laboratory) on 10 June 2021. Guidelines outlined by the SERDP program specify that results should ideally be within 30% of the ELAP-accredited laboratory. A comparison of the analytical results from GMU and Clarkson University was presented as a white paper and is included in this report in Table A2-4 in Appendix #2. There was only one case where an exceedance was observed in the case of PFOA (%D = 38%). To address this difference, GMU worked to correct the problem as follows: 1) 200 mg HLB cartridges were used in place of 60 mg cartridges and 2) 4 mL of MeOH were used to elute the HLB sorbent vs. the current 0.7 mL. We believe this will enhance the performance of PFOA in water analysis.

Seven model PFAS compounds that were covered in the 1-year limited scope study are listed in Table1. The seven selections out of our current list of analytes represent each of the PFAS chemical classes by functional group, carboxy (long & short chain), sulfonate (long and short chain), telomer sulfonate, & sulfamidoacetate, with which we can interpolate the behavior of the

full suite of PFAS homologues. After the year 1 proof-of-concept phase, we plan to extend our passive sampling development work to the full range of 24 PFAS compounds.

Table 5-1. Current PFAS List and targets for the 1-year limited scope proposal

PFAS	**Abbrev**	**CAS #**	**Study**
			Targets
Perfluorobutanoic acid	PFBA	375-22-4	X
Perfluoropentanoic acid		2706-90-3	
Perfluoroheptanoic acid		375-85-9	
Perfluorooctanoic acid	PFOA	335-67-1	X
Perfluorononanoic acid		375-95-1	
Perfluorodecanoic acid		335-76-2	
Perfluoroundecanoic acid		2058-94-8	
Perfluorododecanoic acid		307-55-1	
Perfluorotridecanoic acid		72629-94-8	
Perfluorotetradecanoic acid	PFTreA	376-06-7	X
N-methyl perfluorooctanesulfonamidoacetic acid	NMeFOSSA	2355-31-9	X
N-ethyl perfluorooctanesulfonamidoacetic acid		2991-50-6	
Perfluorobutane sulfonic acid	PFBS	375-73-5	X
Perfluorohexane sulfonic acid		355-46-4	
Perfluorooctane sulfonic acid	PFOS	1763-23-1	X
Sodium 1H,1H,2H,2H-perfluoro-1-hexanesulfonate		757124-72-4	
Sodium 1H,1H,2H,2H-perfluoro-1-octanesulfonate		27619-97-2	
Sodium 1H,1H,2H,2H-perfluoro1-decanesulfonate	FtS 8:2	39108-34-4	X
1H,1H,2H,2H-Perfluoro-1-octanol		647-42-7	
1H,1H,2H,2H-Perfluoro-1-decanol		678-39-7	

5.3 Results and discussion

5.3.1 Lab synthesized functional passive samplers for PFAS compounds

A total of 15 different polymeric sheets for use as passive samplers were successfully synthesized in the lab. Photographs of the different polymer composites are shown in **Figure 5.2**. The additive adsorbent particle ratios and thickness of polymers in Figure 5.2 are listed in **Table 5-2**, with a dimension of around 1.5”x1”. The films with different base polymers show different textures. The passive samplers can be tailored into different sizes, thicknesses, water content,

distribution, and sorbent content. The cast films are uniform in thickness and texture, as shown in Figure 5.2. Even though the thickness varies among different formulations, the measured masses for different polymer types are overall comparable. The average dry mass of each type of functionalized film has been provided in Table 5-2, along with the dry ratio of polymer to additive. The structural stability was tested by soaking in a PP bottle loaded with 100 mL MillQ water and shaking on a rolling table at 110 rpm for 28 days. All the synthesized passive samplers remained stable for 28 days, which is a typical deployment period for passive HOC passive samplers.

5.3.1.1. Functional adsorbent particles embedded in polymers

As shown in **Table 5-2**, the selected adsorbent particles have different sizes: WAX and HLB particles are 30 μm, HSA particles are 5 μm, and powdered active carbon has a larger size. The portion of each absorbent particle was determined based on some preliminary experiments. **Table 5-2** shows the nominal mass of additive in each case, which is calculated assuming even distribution of additive in each film, as confirmed by microscopy analysis in **Figure 5.3**. The photos show that all types of functional particles were well embedded in each type of cast polymer. Moreover, the adsorbent was embedded in the polymers at multiple depths within the polymer thickness with good distribution, instead of surface adhesion only.

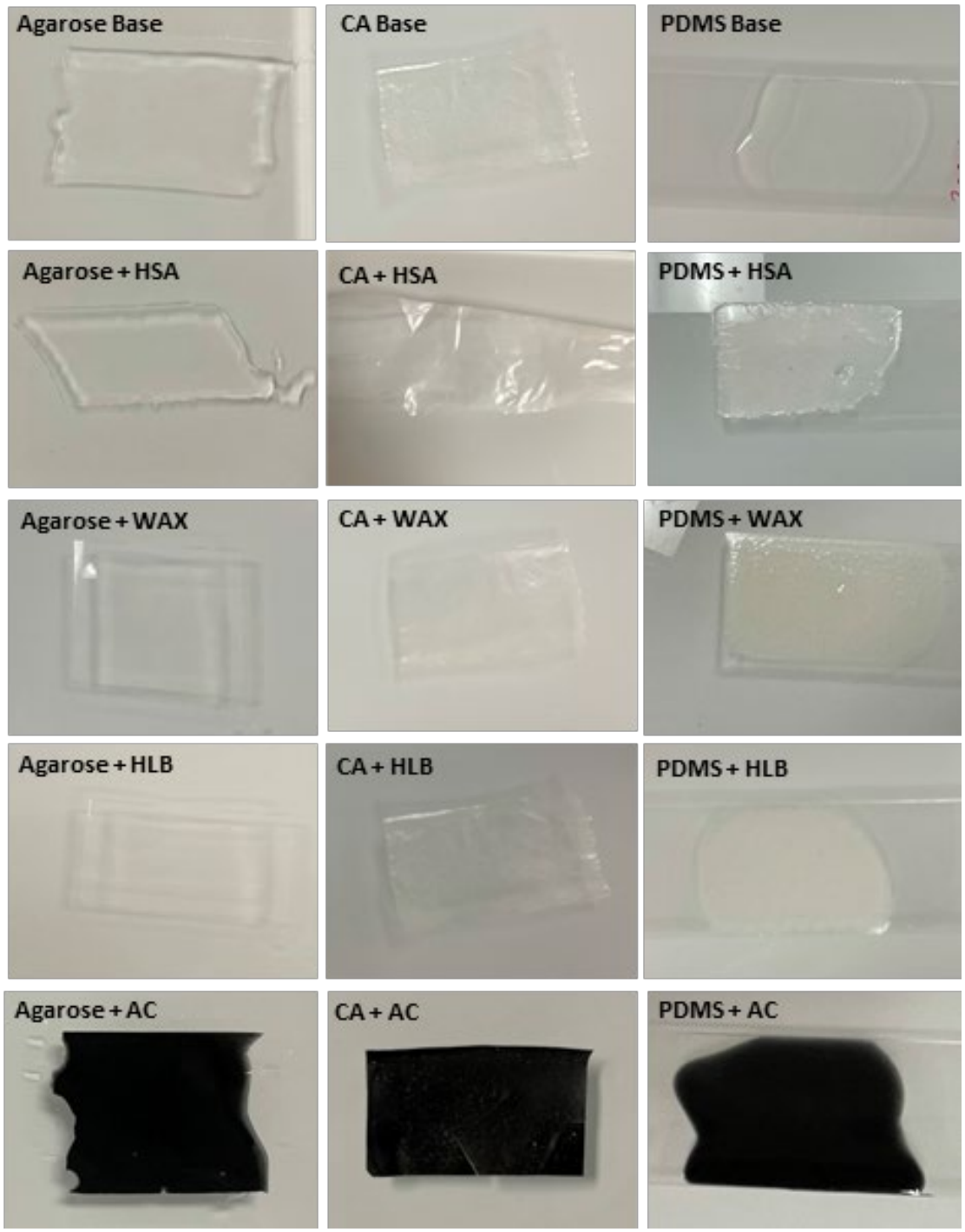

Figure 5.2 Photographs of lab-synthesized polymers to be used as passive samplers for PFAS compounds.

Table 5-2. Additive adsorbent particle ratios and thickness of lab-synthesized polymers for evaluation as passive samplers for PFAS compounds.

Polymer type	Polymer formula	Additive adsorbent particle size	Base polymer: additive particle mass ratio	Polymer thickness	Average polymer mass*	Nominal additive mass**
Agarose	Ag base	-	1	1000 µm	0.096g	0g
	ag+HLB	30 µm	10:1	1000 µm	0.104g	0.009g
	ag+WAX	30 µm	10:1	1000 µm	0.101g	0.009g
	ag+HSA	5 µm	10:2	1000 µm	0.116g	0.019g
	ag+AC	-	10:5	1000 µm	0.128g	0.042g
Cellulose Acetate	CA base	-	1	180 µm	0.117g	0g
	CA+HLB	30 µm	10:1	180 µm	0.123g	0.011g
	CA+WAX	30 µm	10:1	180 µm	0.107g	0.010g
	CA+HSA	5 µm	10:1	180 µm	0.083g	0.008g
	CA+AC	-	10:5	180 µm	0.115g	0.038g
PDMS	PDMS base	-	1	300 µm	0.126g	0g
	PDMS+HLB	30 µm	10:1	300 µm	0.170g	0.015g
	PDMS+WAX	30 µm	10:1	300 µm	0.185g	0.017g
	PDMS+HSA	5 µm	10:1	300 µm	0.133g	0.012g
	PDMS+AC	-	10:5	300 µm	0.148g	0.049g

*The average mass is the average of measured polymer mass of various batches.
** The nominal mass of additive in each case is calculated assuming evenly distribution in film.

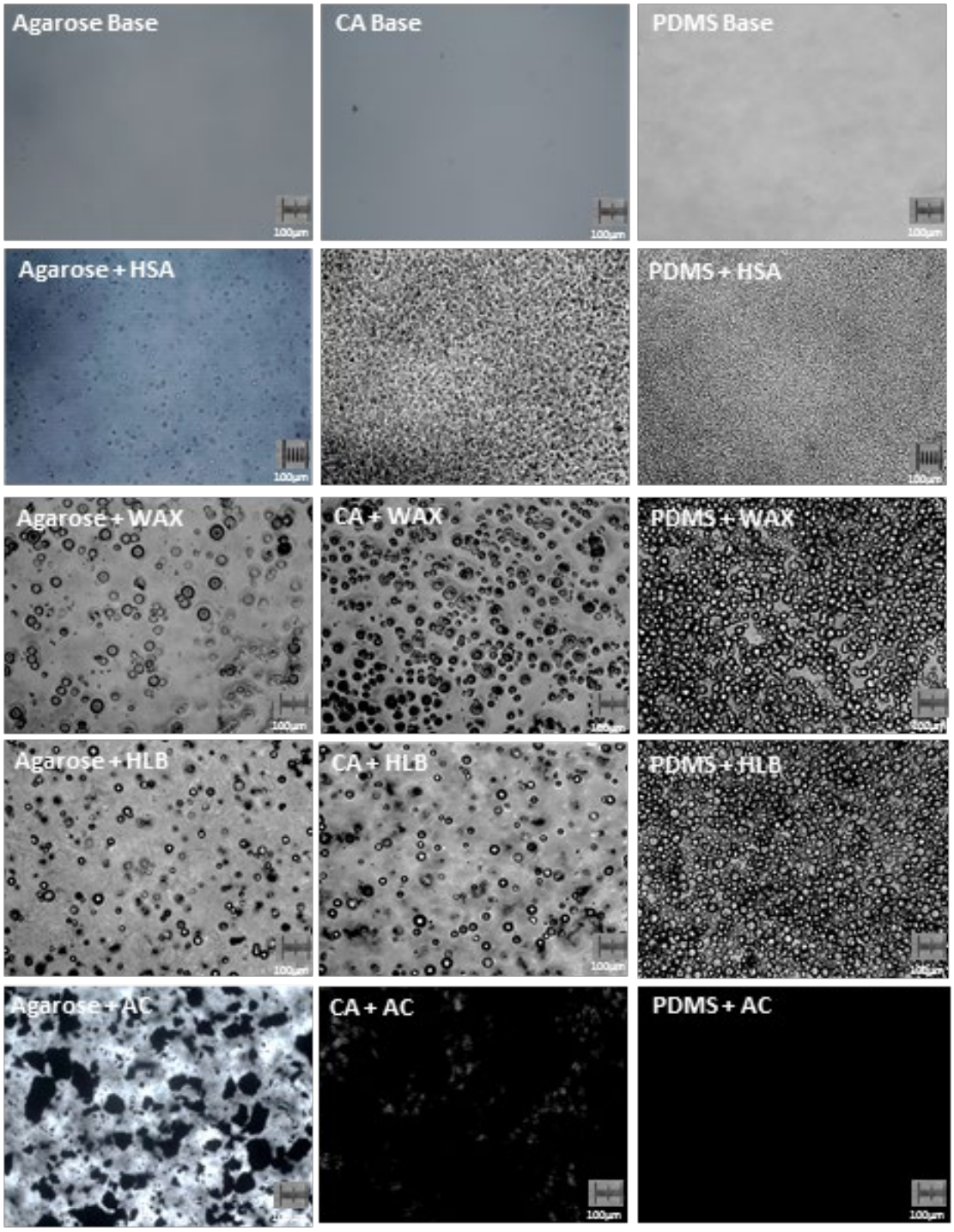

Figure 5.3 Assortment of magnified photos of lab-synthesized polymers taken by light microscopy. Scale at the bottom right of each photograph indicates 100 μm.

5.3.1.2. Agarose based passive samplers.

The first polymers tested were the agarose-based passive samplers. For this project, agarose gels containing embedded sorbent particles were prepared and found to be stable in water for at least 28 days, the typical deployment time for our lab's passive sampler deployments in the field.

After casting, the agarose gels have the highest water content and are soft with a thickness of 1000 μm. Since agarose films are the most fragile ones, an extraction experiment was conducted to determine the best extraction conditions for the Agarose based polymers. The extraction conditions checked different deployment conditions: table rolling 16 hours (110rpm), vortex 5 min (speed 7), sonication 3 min (30s pulse, 30% amplitude), and various extraction solvents (methanol, acetone and the mixture solvent). Polymers were weighed before extraction then added to 40mL glass vials prefilled with 10 mL solvent. After being extracted under different conditions, the mass of polymers was measured in the same way as before extraction. The mass of agarose films was measured under different extraction conditions as shown in **Table 5-3**. Overall, there are few differences among various mixing approaches in methanol and methanol: acetone (v:v 1:1) extractions, but acetone extraction with 3 min sonication results in a lower mass than other experiments. Therefore, we decided to use methanol as the extraction solvent and a rolling table as the extraction condition, which is the most commonly used approach. This extraction method can also remain consistent with other film types.

Table 5-3 Agarose mass ratio after to before under different mixing conditions and extraction solvent.

Remained Mass Ratio	Methanol (10 mL)	Meth (5 mL) + Ace (5 mL)	Acetone (10 mL)	DI Water (10 mL)
Rolling table 16 hours	0.96	0.98	0.96	-
Rolling table 16 hours + vertexing 5 min	0.99	0.96	0.98	0.88
Rolling table 16 hours + sonicating 3 min	0.97	0.98	0.89	0.87

Different thicknesses and embedded sorbent ratios were also explored for agarose based films. 1000 μm agarose films have shown good ability to use as passive samplers for methylmercury (Sander et al., 2020), but the thinner film has a chance of faster mass transfer. Therefore, agarose gels with a thickness of 484 μm were also explored. We also explored casting agarose films in 254 um thickness, however, the films are very fragile and lead to difficulties in handling, like transferring, extraction, and weighing (**Figure A2**). **Figure 5.4** shows the different polymer thicknesses and AC ratios for agarose samplers, with a width of 1 inch and length of 3 inches.

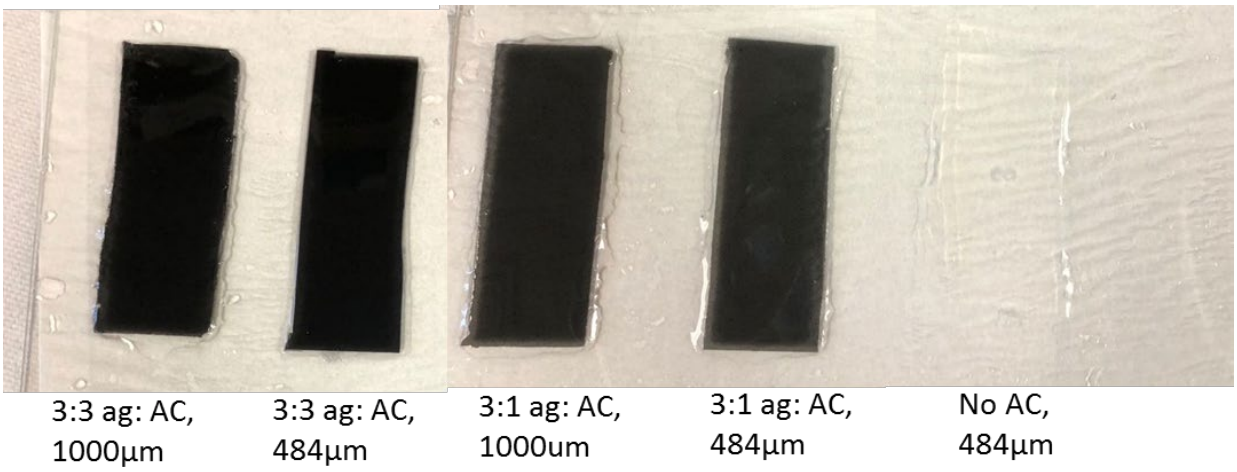

Figure 5.1 Photographs of lab-synthesized agarose base polymers and AC embedded agarose polymers with different thicknesses and AC ratios as passive samplers for PFAS compounds.

The consistency of the synthesized agarose films was also examined. The dry mass ratio for six agarose base polymer samples with a size of 1-inch x 1-inch x 1000 μm is shown in **Table 5-4**, with an average value of 2.02±0.18%. The consistent dry mass ratio among replicate passive samplers indicates a consistent casting and distribution.

Table 5-4 Mass before and after 48 hours drying at room temperature, and the dry mass ratio for agarose films with a size of 1”x1”x1000 μm.

Replicates	Polymer wet mass (mg)	Polymer dry mass (mg)	Dry Mass Ratio
#1	692	14	2.0%
#2	740	15	2.0%
#3	852	16	1.9%
#4	678	14	2.0%
#5	894	21	2.4%
#6	709	13	1.9%
Average	761	15	2.0%

The cast agarose based films are still fragile and easily break during handling. To solve this problem, we increased the dry mass ratio by doubling the agarose powder portion in the casting solution, thereby increasing the density of the polymer. The newly cast agarose samplers with a higher dry mass ratio show better rigidity. Therefore, the agarose dry mass ratio was increased in the later experiments.

With the increased dry portion, agarose films embedded with AC (ag: AC 2:1) and agarose base films with no additive were dried at room temperature for 48 hours and weighted. **Figure 5.5** shows the samplers before and after drying. The wet mass and dry mass ratios for this batch of samplers are consistent and agree with the calculated results in **Figure 5.6**. For the same size polymer pieces, the wet masses were similar indicating similarly high water content for the agarose based polymers. The agarose+AC polymer had a dry polymer to additive ratio of 2:1, which amounts to a theoretical additive content of 50% above the dry polymer mass in the film. As shown in the figure, our measured total dry mass for the agarose+AC film was 53% higher than for the agarose only film, confirming that the additive target dose was successfully incorporated for this formulation.

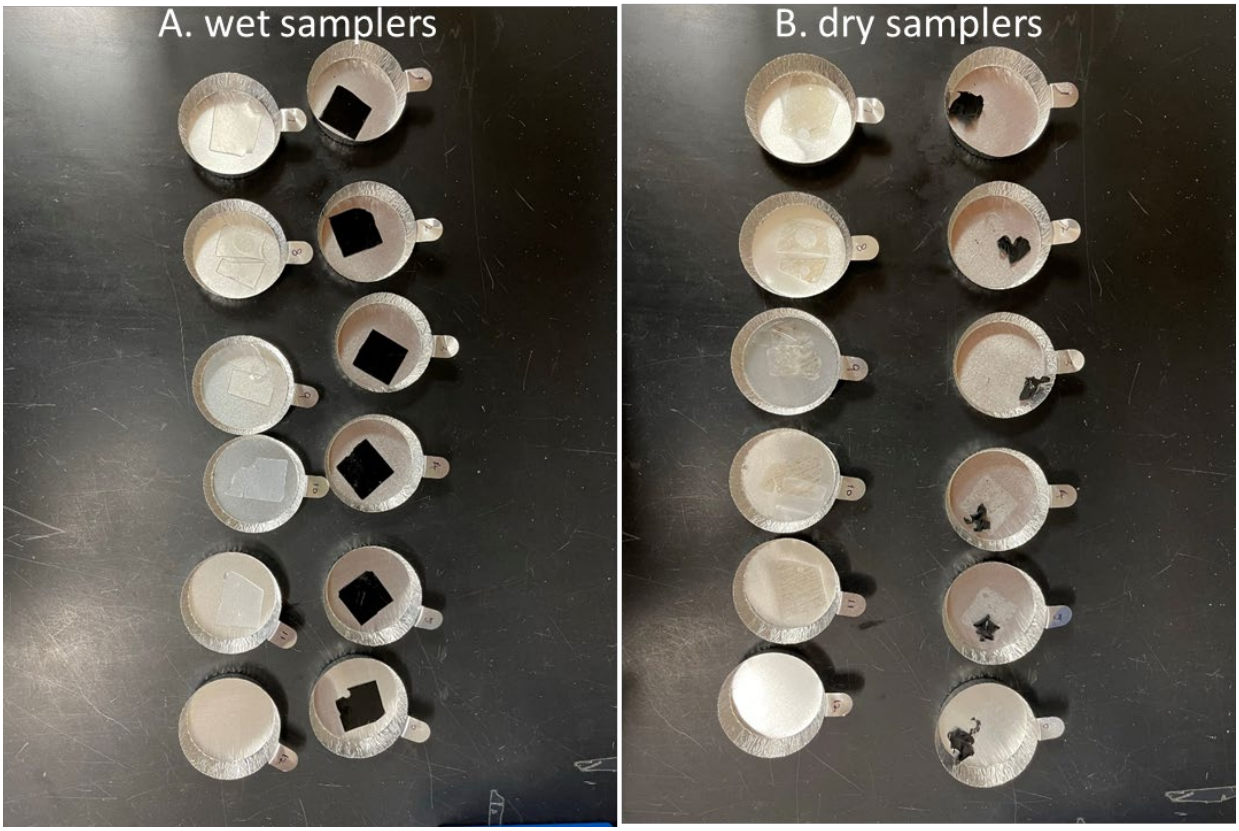

Figure 5.2 Agarose base polymer (white) and AC embedded agarose (black) polymer before (A) and after (B) 48 hours drying in room temperature.

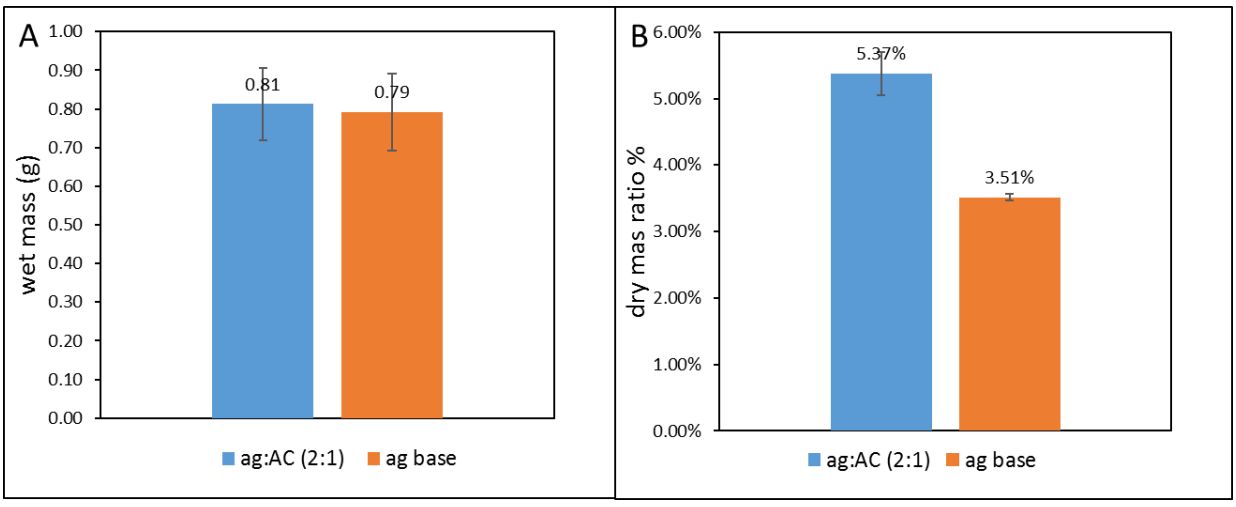

Figure 5.3 Wet mass and dry mass ratios for AC embedded agarose films (ag:AC 2:1) and base agarose gels with size of 1”x1”x1000 µm.

5.3.1.3. Cellulose acetate based passive samplers

Various solvent ratios were explored to determine the best synthesis approach. The lab-synthesized cellulose acetate based films were more rigid than the agarose polymer and did not need high temperature in the synthesis process. After 28 days of soaking in water, they remain intact and stable, indicating a potential for deployment as passive samplers. The thickness of CA films can vary from tens of micrometers to hundreds of micrometers. However, the casting solution is mainly acetone, which evaporates very fast, and may cause some problems in the uniformity of the cast films, like thickness and particle distribution when we make thick films. Therefore, after exploring different thicknesses, we moved forward with using the 15 mil groove from the applicator to cast the films. The thickness of these films was measured to be 180 μm.

The CA films will dissolve in acetone; therefore, only methanol was used for the extraction. More than 99% of the mass remained after methanol extraction for 16 hours on a rolling table with a speed of 110 rpm.

The synthesis of cellulose triacetate polymers was also explored. However, despite similar properties to CA films, they dissolve in methanol when extracted. Therefore, the CTA films were not used in the subsequent experimental phase.

5.3.1.4 PDMS based passive samplers

Two different ways of casting PDMS films were explored. It turns out that using the corning materials (PDMS 2), which contains both silicone elastomer base (part A) and curing agent (part B), is more efficient, easier to perform, and can control the film dimensions better. Therefore, we used this approach for the subsequent phases of our project.

To determine the best synthesis approach, various crosslinking temperatures (20°C, 60°C, 75°C, 100°C), stirring time, speed, and solution recipe were tested. The prepared PDMS solutions were cast on 3”x1” glass plates, pre-cleaned by hexane and methanol, to get a PDMS layer of 300 μm thickness. The PDMS samplers were robust, easy to process, and stable for a 28 days’ deployment. To determine the best extraction condition, the remaining mass ratio was measured under different extraction solvents: 99% for the methanol, 98% for the acetone, and 98% for the 50:50 mixtures.

5.3.2 Single point isotherm study with polymers

Single point isotherm studies were performed to evaluate the sorption capacity of the lab synthesized passive samplers to PFAS compounds to enable initial screening of the polymers. A total of 13 polymeric films synthesized in the lab were used to determine the single point isotherms for our target PFAS compounds: CA base, CA+HLB, CA+WAX, CA+HSA, CA+AC, ag base, ag+HLB, ag+WAX, ag+HSA, ag+AC, PDMS base, PDMS+HLB, PDMS+AC. High temperature (75°C) was used in the PDMS based passive sampler synthesis process, which will deactivate the HSA particles. Therefore, the PDMS+HSA was not used in this study stage. We also explored developing the passive samplers using direct serum albumins instead of silica-bonded HSA. The direct HSA protein particles can be embedded in cellulose acetate films, however, within seven days' deployment in water, the HSA tend to leach off from the agarose passive samplers. This is probably due to the large pore size of the agarose films, and the binding was not strong. On the other hand, the HSA protein embedded cellulose acetate films show good rigidity and stay stable after seven days in water. Further polymer chemistry work is needed to embed HSA directly into polymers.

In our first and second batch of single point isotherm experiments, the mass balance results and surrogate recoveries were out of the criteria shown in Appendix **Figure A3** and **Figure A4**. We modified our analytical method to solve this problem and redid a batch of single point isotherm studies. In the third and fourth batches, the surrogate recovery results were within 80%-120% for most samples as shown in **Figure 5.7**. Total measured mass extracted from passive sampler, water and bottle rinse summed agree with spike amount, 80 ng, for the majority of passive samplers as shown in **Figure 5.8** and **Figure 5.9**. In the fourth experiment batch, we also explored the CA polymers embedded with direct HSA proteins and compared them with the other polymers. In these two batches, the mass from the bottle rinse portion decreased compared with preliminary experiments in our lab in the early stage. Overall, the results from these two batches are in good agreement. The passive sampler extracted mass was relatively low compared to the PFAS mass in water for some compounds, and some were not detected in the fourth batch. This was possibly due to the limited passive sampler amount added to each sample (<50 mg dry mass/sample). Therefore, for subsequent experiments, we tripled the passive sampler amount by combining three pieces in one sample and extracted together to improve the results. Different passive samplers show various affinities to different PFAS compounds. In the third batch, 8:2

FTS and NMeFOSS showed good responses, but they failed to show absorption in the fourth batch, especially in the agarose films. 8:2 FTS and NMeFOSS are weak responses on LCMS, and with low PSD masses, it created some initial difficulties in getting good signal in phase 1 experiments. This has been corrected by adding more PSD mass in the subsequent isotherm experiments to partition more PFAS mass into the solid phase. The aqueous concentrations, passive sampler extracted concentrations, and calculated log K_d values are plotted in **Figure 5.8** and **Figure 5.9**. The log K_d values fell within the range of 1.5-4 for most samples. For the HSA particles, the commercially available ones which were 5 µm and bonded to silica particles, show consistent results with the direct HSA protein for the PFAS affinity.

Nevertheless, the silica bonded particles were more stable, easy to process, and had better distributions in the polymer casting solutions. So we moved forward with the silica-bonded 5 µm HSA particles in the subsequent research phases. Based on the results, four types of synthesized films: CA+WAX, ag+AC, CA+HSA and PDMS+HLB were selected for further studies since they have, more consistently, relatively higher K_d values than the rest of passive samplers, which indicate a better absorption for the PFAS.

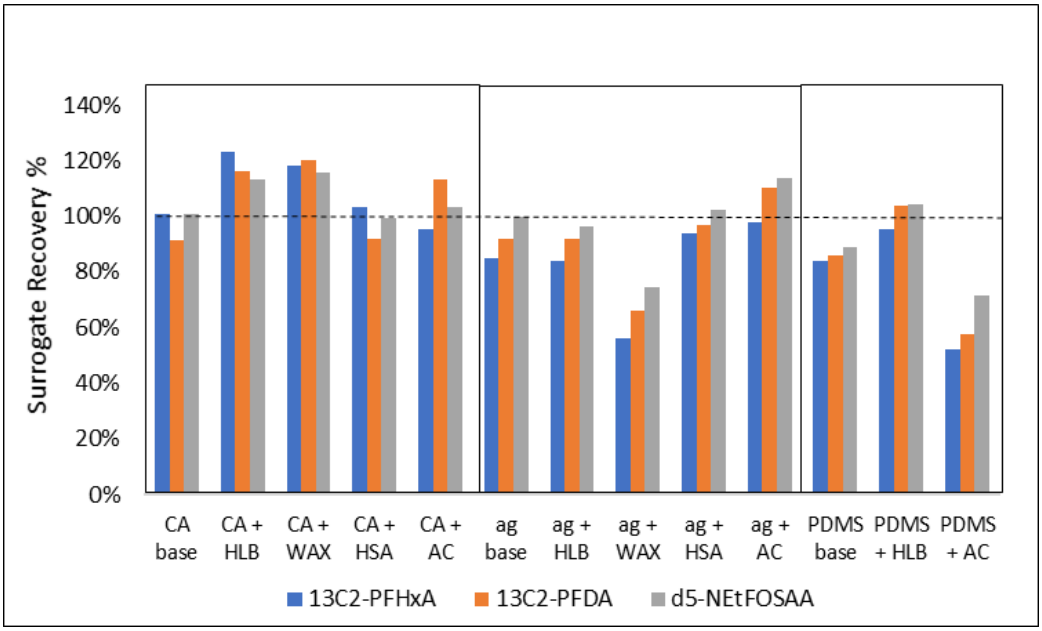

Figure 5.7 Surrogate recoveries of perfluoro-n-[1,2-13C2]hexanoic acid (13C2-PFHxA), perfluoro-n-[1,2-13C2]decanoic acid (13C2-PFDA) and N-deuterioethylperfluoro-1-octanesulfonamidoacetic acid (d5-NEtFOSAA) for the thirteen synthesized PFAS passive samplers.

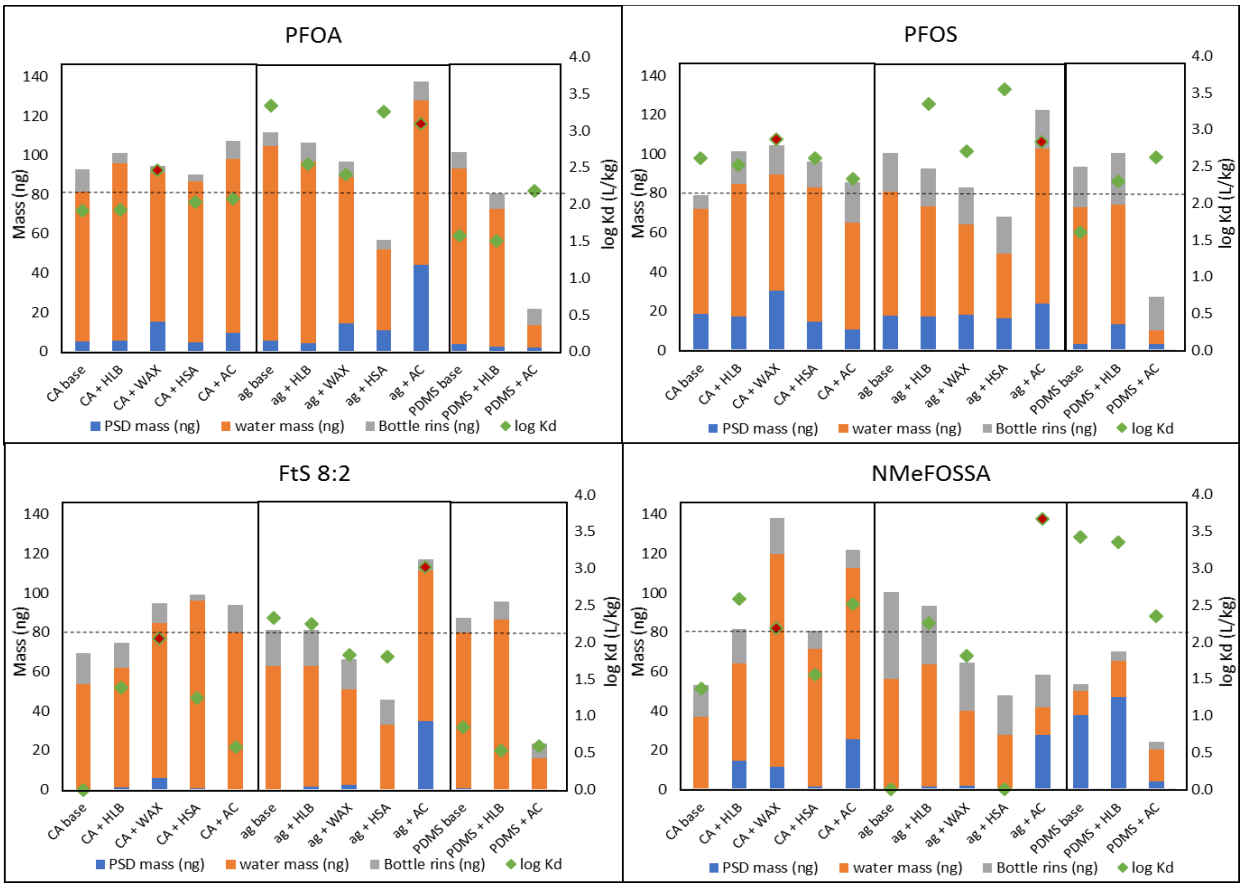

Figure 5.8 PFAS mass extracted from passive samplers, water and bottle rinse solutions for the first batch of 13 synthesized polymers, and the single point isotherm results at spiking level 800ng/L for four PFAS compounds: PFOA, PFOS, FtS 8:2, and NMeFOSSA. The red data point indicating the selected films for next steps.

In a few cases, the base polymer showed nearly the same effectiveness as the polymer with amendment, but this was not observed consistently for all experiments or all PFAS. For example, the CA and agarose base polymers appeared to be equally effective for PFOS as the amended polymers in the experiment shown in Figure 5.8, however, this was not the case for the data shown in Figure 5.9 for agarose or for some of the other compounds for CA. We noted some inconsistencies in the mass measurement of polymers after extraction (especially in the high water content polymers) and resolved the challenge by consistently measuring the mass before extraction in subsequent experiments. We also recognized the need to increase the mass of polymer for each batch as described earlier.

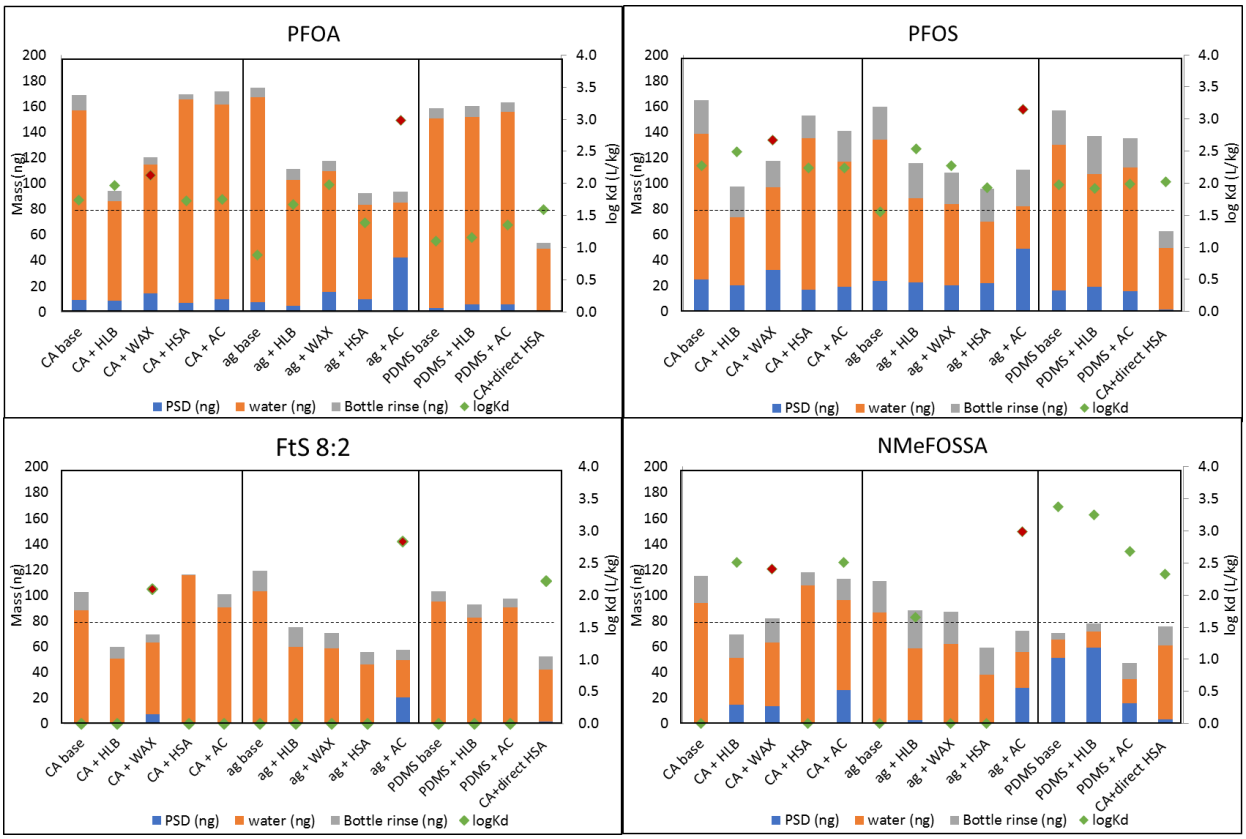

Figure 5.9 PFAS mass extracted from passive samplers, water and bottle rinse solutions for the second batch of 14 synthesized polymers, and the single point isotherm results at spiking level 800ng/L for four PFAS compounds: PFOA, PFOS, FtS 8:2, and NMeFOSSA. The red data points indicate polymer formulations selected for the next steps.

5.4 Implications

In this research, we demonstrate for the first time that several composite polymers can be synthesized that provide adequate sorption of PFAS from aqueous solution at equilibrium. Thus, conceptually, we can develop an equilibrium passive sampler for PFAS in water that is able to respond to the dissolved concentration of PFAS. The casting approach allows adjusting size and sorbent ratios to meet target PFAS concentrations. The selected polymer composites remain stable in water for a typical period of deployment.

A material with a log K_d of 3 for PFAS, exposed to an aqueous PFAS concentration of 5 ng/L (a moderate-to-low value for contaminated sediment pore water), would be capable of accumulating 500 pg of PFAS (a readily detectable amount) in a 100 mg mass of the polymer.

For most materials under consideration, the size is roughly less than 2”x1”. Several advanced materials have achieved this degree of sorption within 7 days of deployment in a single point isotherm study for various PFAS compounds. This constitutes a promising proof of concept for an equilibrium-based, polymeric passive sampling system for PFAS in sediment pore water. Before the ultimate goal of developing an equilibrium passive sampler for PFAS is achieved, a few critical questions remain to be answered and are discussed in the following chapters.

5.5 Literature Cited

Barreca S, Busetto M, Vitelli M, et al. Online solid-phase extraction LC-MS/MS: A rapid and valid method for the determination of perfluorinated compounds at sub ng· L− 1 Level in natural water[J]. *Journal of Chemistry*, 2018.

Cornelissen G, Gustafsson Ö, Bucheli T D, et al. Extensive sorption of organic compounds to black carbon, coal, and kerogen in sediments and soils: mechanisms and consequences for distribution, bioaccumulation, and biodegradation[J]. *Environmental science & technology*, 2005, 39(18): 6881-6895.

Fedorova G, Golovko O, Randak T, et al. Passive sampling of perfluorinated acids and sulfonates using polar organic chemical integrative samplers[J]. *Environmental Science and Pollution Research*, 2013, 20(3): 1344-1351.

Field J, C Higgins, R Deeb and J Conder. 2017. FAQs Regarding PFASs Associated with AFFF Use at US Military Sites. http://www.dtic.mil/dtic/tr/fulltext/u2/1044126.pdf.

Goyal, A., Kumar, A., Patra, P. K., Mahendra, S., Tabatabaei, S., Alvarez, P. J., ... & Ajayan, P. M. (2009). In situ synthesis of metal nanoparticle embedded free standing multifunctional PDMS films. *Macromolecular rapid communications*, 30(13), 1116-1122.

Han, X.; Snow, T.A.; Kemper, R.A.; Jepson, G.W. Binding of perfluorooctanoic Acid to Rat and Human Plasma Proteins. *Chem. Res. Toxicol*. 16, 775-781. 2003.

Hansen M C, Børresen M H, Schlabach M, et al. Sorption of perfluorinated compounds from contaminated water to activated carbon[J]. *Journal of Soils and Sediments*, 2010, 10(2): 179-185.

ISO25101. Water quality. Determination of perfluorooctanesulfonate (PFOS) and perfluorooctanoate (PFOA) – Method for unfiltered samples using solid phase extraction and liquid chromatography/ mass spectroscopy, ISO/TC147/SC2/WG56; 2009

Kaserzon S L, Kennedy K, Hawker D W, et al. Development and calibration of a passive sampler for perfluorinated alkyl carboxylates and sulfonates in water[J]. *Environmental science & technology*, 2012, 46(9): 4985-4993.

Kwon J W, Yoon S H, Lee S S, et al. Preparation of silver nanoparticles in cellulose acetate polymer and the reaction chemistry of silver complexes in the polymer[J]. *Bulletin of the Korean Chemical Society*, 2005, 26(5): 837-840.

Mallik, R.; Yoo, M.J.; Briscoe, C.J.; Hage, D.S. Analysis of Drug-Protein Binding by Ultrafast Affinity Chromatography Using Immobilized Human Serum Albumin. *J Chromatogr* A. 2010 April 23; 1217(17): 2796–2803.

McCleaf P, Englund S, Östlund A, Lindegren K, Wiberg K, Ahrens L. Removal efficiency of multiple poly-and perfluoroalkyl substances (PFASs) in drinking water using granular activated carbon (GAC) and anion exchange (AE) column tests. *Water research*. 2017 Sep 1;120:77-87.

Ng, CA; Hungerbuhler, K. Bioaccumulation of Perfluorinated Alkyl Acids: Observations and Models. *Environ. Sci. Technol*. 46, 4637-4648. 2014.

Ochoa-Herrera V, Sierra-Alvarez R. Removal of perfluorinated surfactants by sorption onto granular activated carbon, zeolite and sludge[J]. *Chemosphere*, 2008, 72(10): 1588-1593.

Sanders, J. A Novel Equilibrium Passive Sampler for Methylmercury and Other Advances in Monitoring and Activated Carbon Remediation for Mercury and PCBs. Ph.D. Dissertation, University of Maryland Baltimore County, 2018.

Sanders J P, McBurney A, Gilmour C C, et al. Development of a novel equilibrium passive sampling device for methylmercury in sediment and soil porewaters[J]. *Environmental Toxicology and Chemistry*, 2020, 39(2): 323-334.

Taniyasu S, Kannan K, So M K, et al. Analysis of fluorotelomer alcohols, fluorotelomer acids, and short-and long-chain perfluorinated acids in water and biota[J]. *Journal of Chromatography* A, 2005, 1093(1-2): 89-97.

Taniyasu S, Kannan K, Yeung L W Y, et al. Analysis of trifluoroacetic acid and other short-chain perfluorinated acids (C2–C4) in precipitation by liquid chromatography–tandem mass spectrometry: Comparison to patterns of long-chain perfluorinated acids (C5–C18)[J]. *analytica chimica acta*, 2008, 619(2): 221-230.

Yu Q, Zhang R, Deng S, et al. Sorption of perfluorooctane sulfonate and perfluorooctanoate on activated carbons and resin: Kinetic and isotherm study[J]. *Water research*, 2009, 43(4): 1150-1158.

Wang, L., Gong, X., Wang, R., Gan, Z., Lu, Y., Sun, H. Application of an immobilized ionic liquid for the passive sampling of perfluorinated substances in water. *Journal of Chromatography* A. 1515, 2017, 45-53.

6.0 Research Objective #2: Equilibrium partitioning studies with a selected group of PFAS compounds covering a range of properties

6.1 Introduction

To better understand the sorption of PFAS onto synthesized passive sampler polymers, sorption isotherms were studied in more detail across a range of concentrations in this chapter. PFAS adsorption isotherms relate the amount adsorbed to the adsorbent to the water concentration of PFAS. This chapter aims to evaluate the passive sampler's affinity for PFAS and ability to accumulate detectable and reproducible amounts in proportion to aqueous concentrations and develop a relationship between absorbed PFAS and freely dissolved PFAS that can be described based on typical sorption isotherm models. An adsorption isotherm is a functional curve that describes the phenomenon of a substance's retention (or release) or mobility from aqueous media to a solid phase (Foo and Hameed, 2010).

PFAS adsorption isotherms have been captured using a variety of adsorption isotherm models (Sima and Jaffe, 2021), including the Linear (Milinovic et al., 2015; Miao et al., 2017), Langmuir (Zhang et al., 2019; Saeidiet al., 2020) and Freundlich (Li et al., 2019; Saeidiet al., 2020) models.

The partition coefficients should be close to the measured partitioning for PFAS in natural sediments. The uptake isotherms should be described across the concentration range of interest, from the pg/L to the high ng/L concentrations found in the most contaminated waters. The measured log K_d (L/kg) values are around 2-3 for the POCIS-WAX and POCIS-HLB films developed by Gobelius et al. (2019). The majority of literature POCIS samplers for PFAS have a K_d range of 1.5-3.5 in the review paper by Godlewska et al. (2020). Hartmann et al. (2021) designed a passive sampler for PFAS using weak ion-exchange resin Oasis WAX and showed a good affinity for PFAS in DI water, especially for long-chain PFAS, with log K_d (L/kg) values >4.

In this task, the binding capacity of selected polymeric membrane composites were measured. Several sets of isotherms were performed as we learned about the properties of our materials and began to build that best approximated PFAS equilibrium with the water.

6.2 Adsorption isotherm models

6.2.1 Linear isotherm models

The linear model (Henry's isotherm model) can be presented as:

$$C_s = KC_w$$

where C_s (ng/g) and C_w (ng/L) are adsorbed concentrations in the sorbent and water at equilibrium, K (L/g) is the partition coefficient. The linear model is the simplest adsorption isotherm model as the partial pressure of the adsorptive gas is proportional to the amount of surface adsorbate (Ayawei et al., 2017). The mechanisms of partitioning processes in a linear model can be electrostatic interactions, van der Waals interactions, and hydrophobic interactions (Guo and Wang, 2019).

6.2.2 Langmuir isotherm models

The Langmuir model is commonly used for absorption isotherms and was developed to present the gas adsorption in the solid phase (Langmuir, 1916, 1918). The Langmuir model can be expressed as:

$$C_s = \frac{C_{s,max} K C_w}{1 + KC_w}$$

where K (L/g) is the adsorption rate and desorption rate ratio, $C_{s,max}$ (ng/g) is the maximum adsorption capacity estimated. The Langmuir model assumes that the thickness of the adsorbed layer is one molecule and the adsorption process takes place at a similar and equivalent definite localized site and a homogeneous adsorbent surface with similar adsorption energy for each site. Even when the adsorbent materials have uneven forms and non-uniform surfaces in the microscope, the Langmuir isotherm can still be used to represent adsorption (Guo and Wang, 2019; Mondal and Majumder, 2019; Liu et al., 2018).

6.2.3 Freundlich isotherm models

The reversible and non-ideal adsorption process can be described by the Freundlich models. Unlike the Langmuir model, the Freundlich isotherm model is not limited to monolayer formation, allowing it to be applied to multilayer adsorption. The Freundlich model is given by the equation:

$$C_s = KC_w{}^n$$

Where K($L^n ng^{1-n}/g$) and n are constants, the Freundlich model will reduce to the linear model when n = 1. The Freundlich model can describe the chemical adsorption with about 50% coverage fraction and the physical adsorption process and can be applied to represent the multi-layer adsorption on heterogamous surfaces (Wang and Guo, 2020; Zaheer et al., 2019).

6.2.4 Freundlich-Langmuir mix (Sips) models

The Sips model is a combination of both the Langmuir and Freundlich models (Sips, 1948). Sips model can describe the homogeneous or heterogeneous systems and is the most applicable 3-parameter isotherm model for monolayer adsorption (Ebadi et al., 2015). Sips model can be presented by:

$$C_s = \frac{C_{s,max} K C_w^n}{1 + K C_w^n}$$

where $C_{s,max}$ (ng/g) is the maximum adsorbed amount, K ($L^n mg^{-n}$) and n are the Sips constants. When n= 1, the Sips model becomes the Langmuir model, and when C_0 is low, it becomes the Freundlich model. According to Wang and Guo (2020), the Sips model represents the monolayer adsorption of one adsorbate molecule onto 1/n adsorption sites.

6.3 Materials and methods

In initial isotherm experiments, a piece of test polymer was added to 100 mL of deionized water and spiked with PFAS at one of a series of concentrations typically spanning two orders of magnitude. Seven spiking concentration levels were used for the isotherm study: 80, 120, 190, 310, 490, 800, and 2000 ng/L, which led to a total mass of spiked amounts at 8, 12, 19, 31, 49, 80 and 200 ng in each sample. Three replicates were used at each spiking level for agarose films. Samples were loaded at room temperature (20°C) with orbital shaking at 45 rpm (**Figure 6.1**). After loading for seven days, the PFAS concentrations on the passive sampler, water, and attached to the bottle were measured separately. K_{ps} for each developed passive sampler was calculated as described in Chapter 5 for the single point isotherm study.

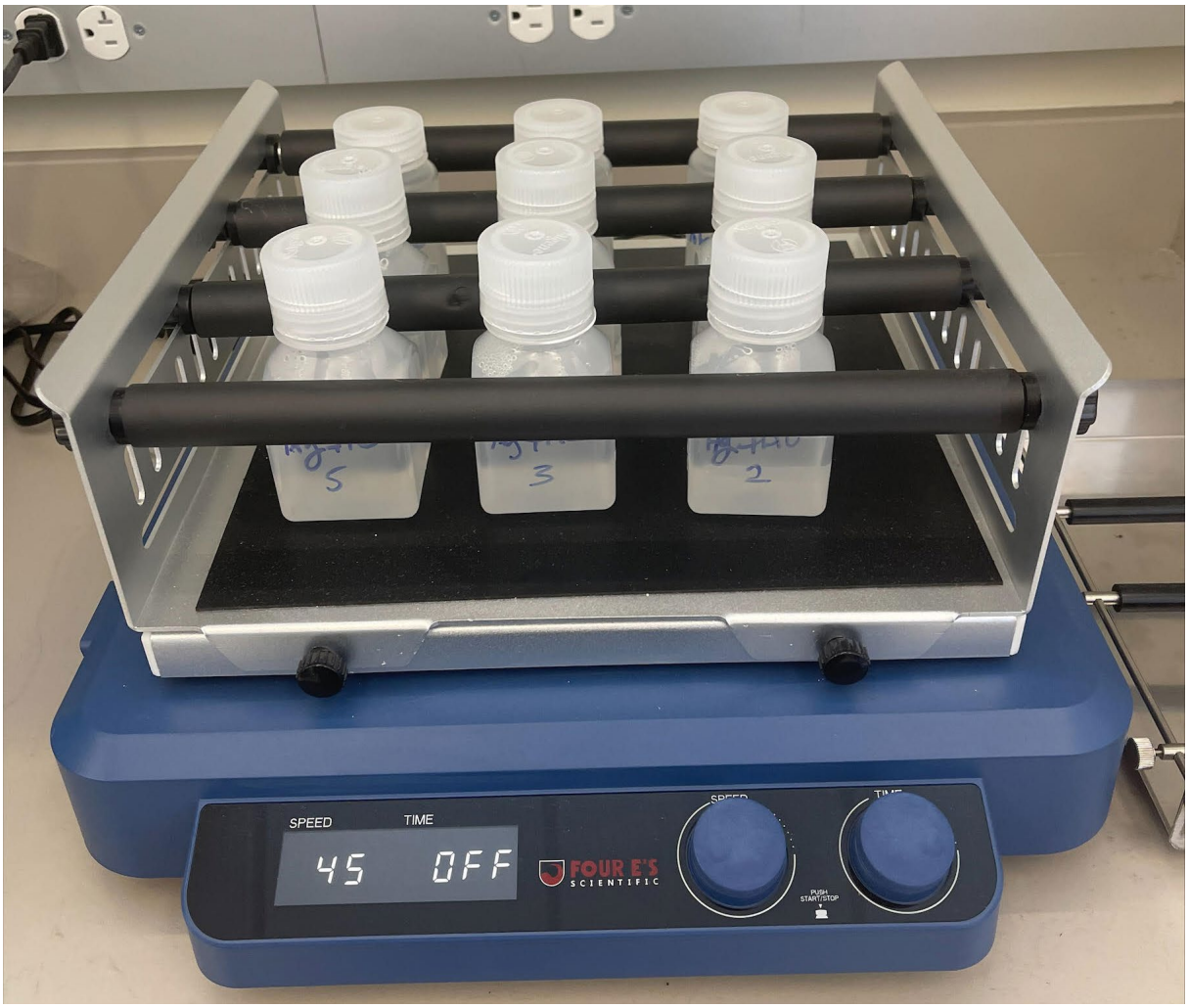

Figure 6.1 Photograph of ongoing isotherm study for passive samplers on a shaking table.

6.3.1 Water Extraction

The PFAS were analyzed in water and passive sampler polymers (PS). The PSs were removed from the exposure water bottle and placed into a 50 mL Falcon tube. Water contained in 125 mL polypropylene (PP) bottles was spiked with internal standards (500 ng) and surrogate standards (500 ng) prior to extraction. The water was extracted using an Oasis WAX (150 mg) solid-phase extraction (SPE) cartridge at a flow rate of 5 mL/min. Upon extraction, the empty bottle was rinsed with an additional 5 mL of deionized water (Milli-Q), which was also passed through the Oasis WAX cartridge.

The SPE cartridges were first rinsed with Milli-Q and eluted with 1X5 mL of 1% NH_4OH in methanol, and the methanol was collected in a 15 mL Falcon tube (to which 25 µL of

concentrated acetic acid was added). Graphitized carbon (10 mg) was added to the tube, which was vortexed/shaken for 5 min. The tube was centrifuged (2000 rpm), and the supernatant was transferred to a fresh 40 mL glass vial. The extract was concentrated in a TurboVap and transferred to a 1.5 mL LCMS vial using a syringe fitted with a syringe filter (0.2 µm PP). The water extraction procedure is summarized in **Figure 6.2**.

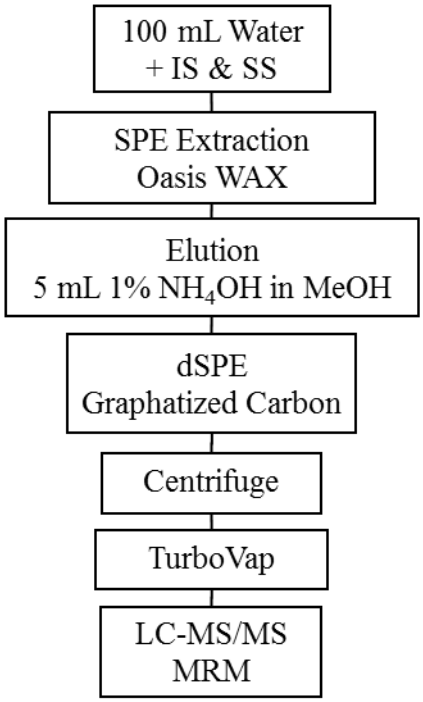

Figure 6.2 Water analysis method flow chart.

6.3.2 Passive Sampler Film Extraction

Passive samplers (PSs) were removed from the water and placed in 15 mL Falcon tubes. The PSs were spiked with internal standards (500 ng) and surrogate (500 ng) standards. Subsequently, the PSs were extracted with 2X5 mL of 0.3% NH_4OH in methanol. The tubes were placed in a sonication bath and vortex every 10 min. The solvent was transferred to a 40 mL glass vial using a plastic pipette and concentrated in a TurboVap to 0.5 mL. The concentrated extract was transferred to a 1.5 mL LCMS vial via syringe fitted with a 13 mm syringe filter (0.2 µm PP). The PS extraction procedure is summarized in **Figure 6.3**.

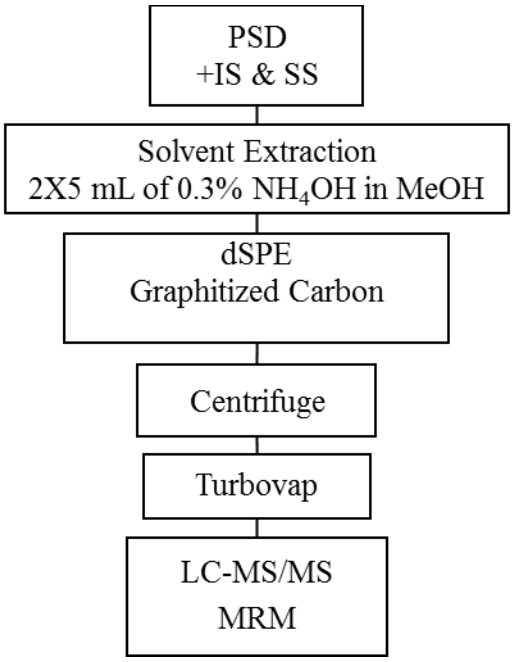

Figure 6.3 Passive sampler membrane analysis method flow chart.

6.3.3 Bottle Rinse

The empty water bottles were rinsed with 2x10 mL of 0.3% NH_4OH in methanol. The extract was transferred to a 40 mL glass vial, and the solvent is concentrated to 0.5 mL in a TurboVap. The concentrated extract was transferred to a 1.5 mL LCMS vial via syringe fitted with a 13 mm syringe filter (0.2 µm PP).

6.3.4 Liquid Chromatography-Triple Quadrupole Mass Spectrometry (LC-MS/MS) analysis method

Quantitative analysis was performed using a Shimadzu 8050 LC-MS/MS (Shimadzu, Columbia, MD) with combined electrospray (positive and negative modes) and APCI ionization (DUIS) in the presence of a Corona needle. Chromatographic separations were performed using a 50 mm x 2.1 mm (id), 1.8 µm (particle dia.) Titan C18 UHPLC column (Supelco, Bellefonte, PA) in conjunction with a binary mobile phase of 2 mM ammonium acetate in Milli-Q water (A) and 2 mM ammonium acetate in methanol (B). Data analysis and quantitation were performed using LabSolutions software (ver. 5.91, Shimadzu, Columbia, MD).

6.3.5 Quality Assurance Procedures

The quality assurance (QA) protocol includes laboratory blanks, method detection limit evaluations, matrix spikes, and surrogate standards. Laboratory blanks including all reagents and

glassware except the sample matrix serve to determine the background responses. The laboratory blanks are used as a subtraction (correction) from the sample concentrations where analytes are detected in the blanks. The method detection limits (DL) are established as a threshold peak having a Signal/Noise response of ≥ 3. For PFASs detected in the laboratory blanks, the DL values are +3 SD (standard deviations) above the levels quantified in the blanks. Lab spikes (without matrix) and matrix spikes (natural samples) containing all the analytes spiked into a mock sample are used to determine the percentage of recovery of each compound resulting from the extraction and quantitation method. All samples are spiked with surrogate (recovery) standards before beginning the extraction process in order to evaluate the performance associated with each analysis.

Besides, to make sure the extraction method is sufficient and not causing any target compound loss, two additional quality control experiments were conducted:

(1) To confirm breakthrough from cartridges during extraction:

Three samples were spiked with 800 uL of target solution to deliver 80 ng of PFAS in 100 mL of MiliQ water and spiked with 100 uL of surrogate standard. Bottle #1 was extracted through two SPE Cartridges (front and back), while the other two were extracted using one cartridge (front).

(2) To determine the elution times needed in the process:

Each cartridge was eluted with 0.1% ammonium hydroxide in methanol. A total of five elution were processed for the experiment. The bottle was rinsed at last and analyzed as well. The eluted samples were concentrated to 1 mL and analyzed like all other samples on the LC-MS.

6.4 Results and discussion

6.4.1. QA/QC

The calibration curve for the target PFAS had good linear regression with R^2 ranging from 0.98- to 1.0. The recoveries of analytical method for all PFASs for the water and the passive sampler were in a reasonable range and are shown in Appendix **Figure A5** and **Figure A6**. The bottle rinsed concentrations were negligible compared with the concentration in water and passive sampler for all spiking levels. Meanwhile, no target analytes were detected (S/N <3) in contamination controls (without the addition of PFASs), indicating that there was no contamination introduced during adsorption experiments.

The comparison results of two cartridges (front and back) used with one cartridge (front) are shown in **Figure 6.4**. Less than 30% breakthrough from the first cartridge indicates that the cartridges we were using were sufficient for the exposure and extraction.

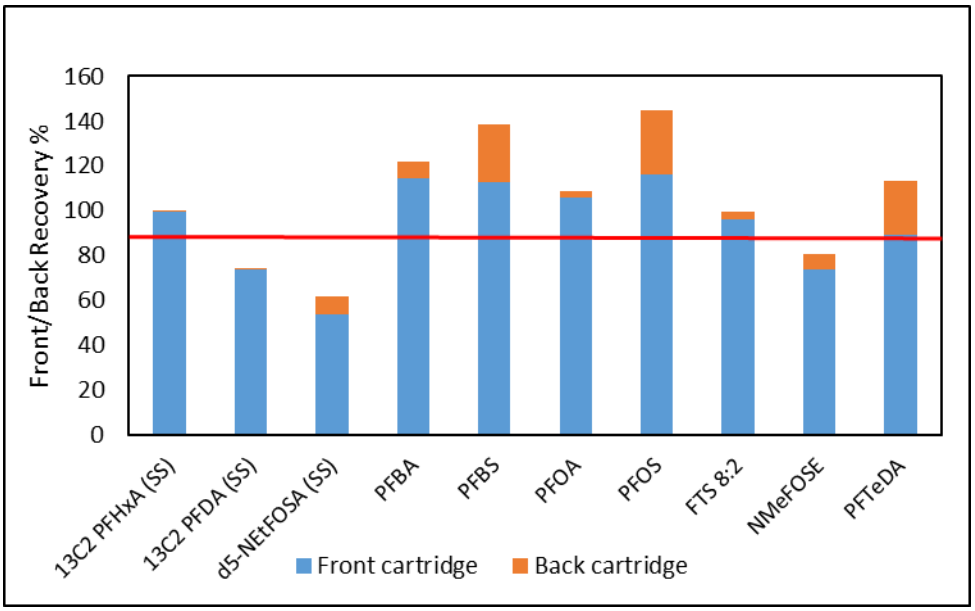

Figure 6.4 Front/Back cartridge recovery% for various PFAS and Surrogates (SS).

Figure 6.5 shows the fractional recovery percentage for each PFAS compound during the five elutions. As can be seen, the majority of the PFAS was removed in the first elution. Therefore, one elution is sufficient for the analysis.

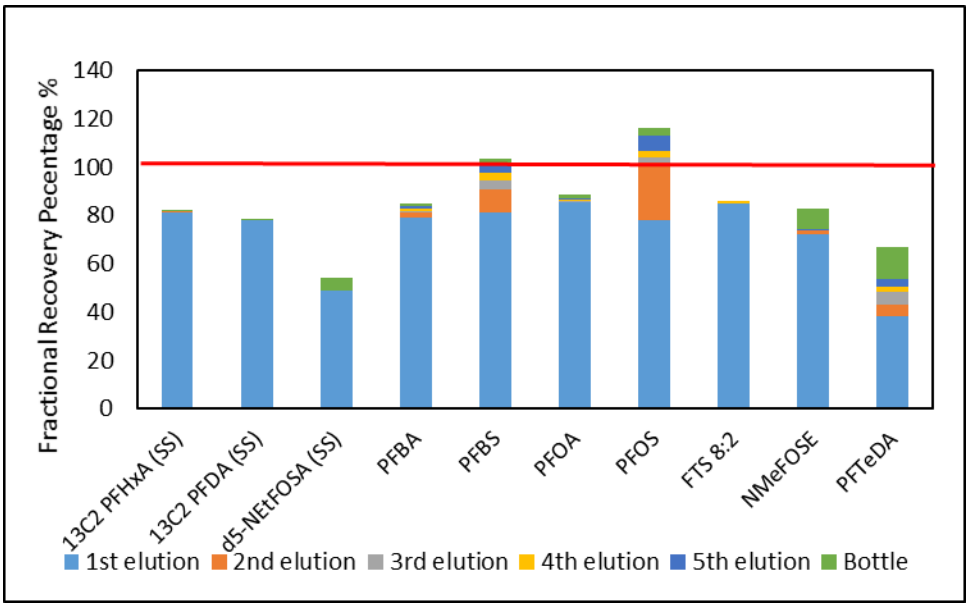

Figure 6.5 Fractional recovery percentage of target PFAS and Surrogates (SS) within five elusions.

6.4.2 Isotherm models fitting

The sorption of PFAS from the water was modeled in polymers using nonlinear curve-fitting to sorption isotherms (using Origin 2022). Linear, Langmuir, Freundlich, and Sips sorption models were evaluated. **Figure 6.6** to **Figure 6.9** show the C_{ps} vs. C_w and the model fitted isotherms for selected PFAS compounds obtained from different passive samplers: AC embedded agarose (ag+AC) polymer, WAX embedded cellulose acetate (CA+WAX) polymer, human serum album embedded cellulose acetate (CA+HSA) polymer, and HLB embedded PDMS (PDMS+HLB) polymer, separately. Overall, the model fitting results for these PFAS compounds have an R^2 0.88-0.96 for ag+AC, 0.64-0.98 for CA+WAX, 0.84-0.99 for CA+HSA, and 0.41-0.95 for PDMS+HLB among various PFAS compounds. Thus, the isotherms for each PFAS adsorbed by synthesized passive samplers can be represented well by the Linear, Langmuir, Freundlich, or the mix (Sips) model. The parameters for each fitted model are listed in **Table 6.1** to **Table 6.4**.

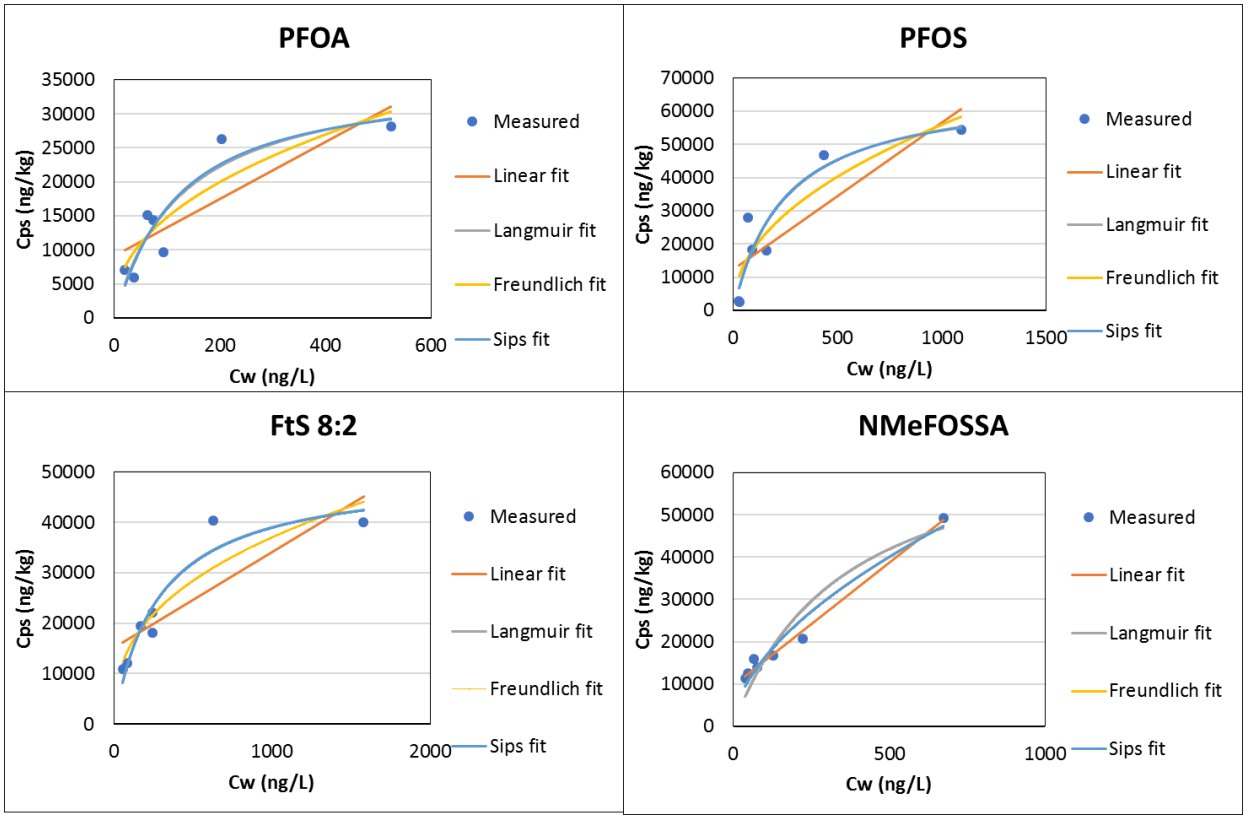

Figure 6.6 Experimental C_{ps} vs C_w and the fitted models (Linear, Langmuir, Freundlich, and Sips models for PFAS using **ag+AC polymer**, clockwise: PFOA, PFOS, NMeFOSSA, FtS 8:2.

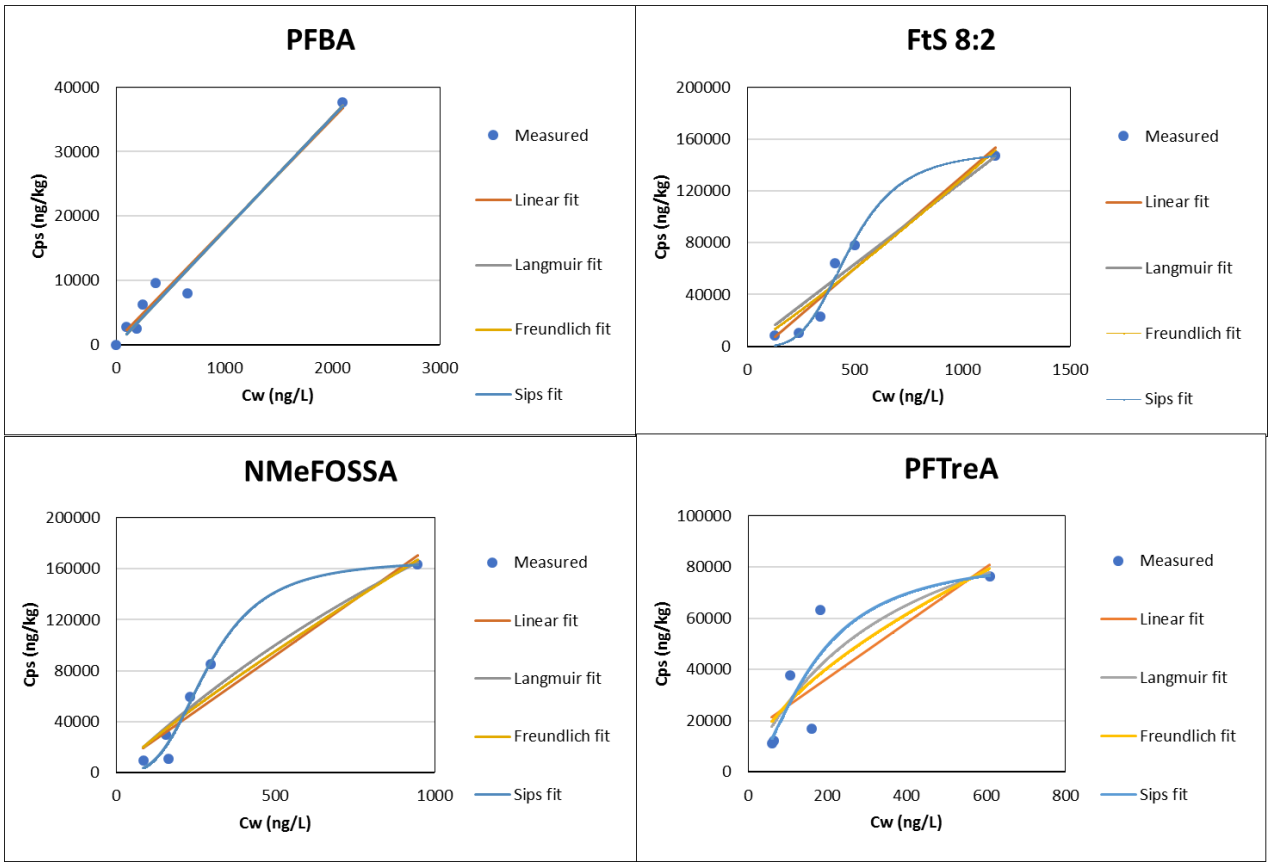

Figure 6.7 Experimental C_{ps} vs C_w and the fitted models (Linear, Langmuir, Freundlich, and Sips models for PFAS using **CA+WAX polymer**, clockwise: PFBA, FtS 8:2, PFTreA, NMeFOSSA.

.

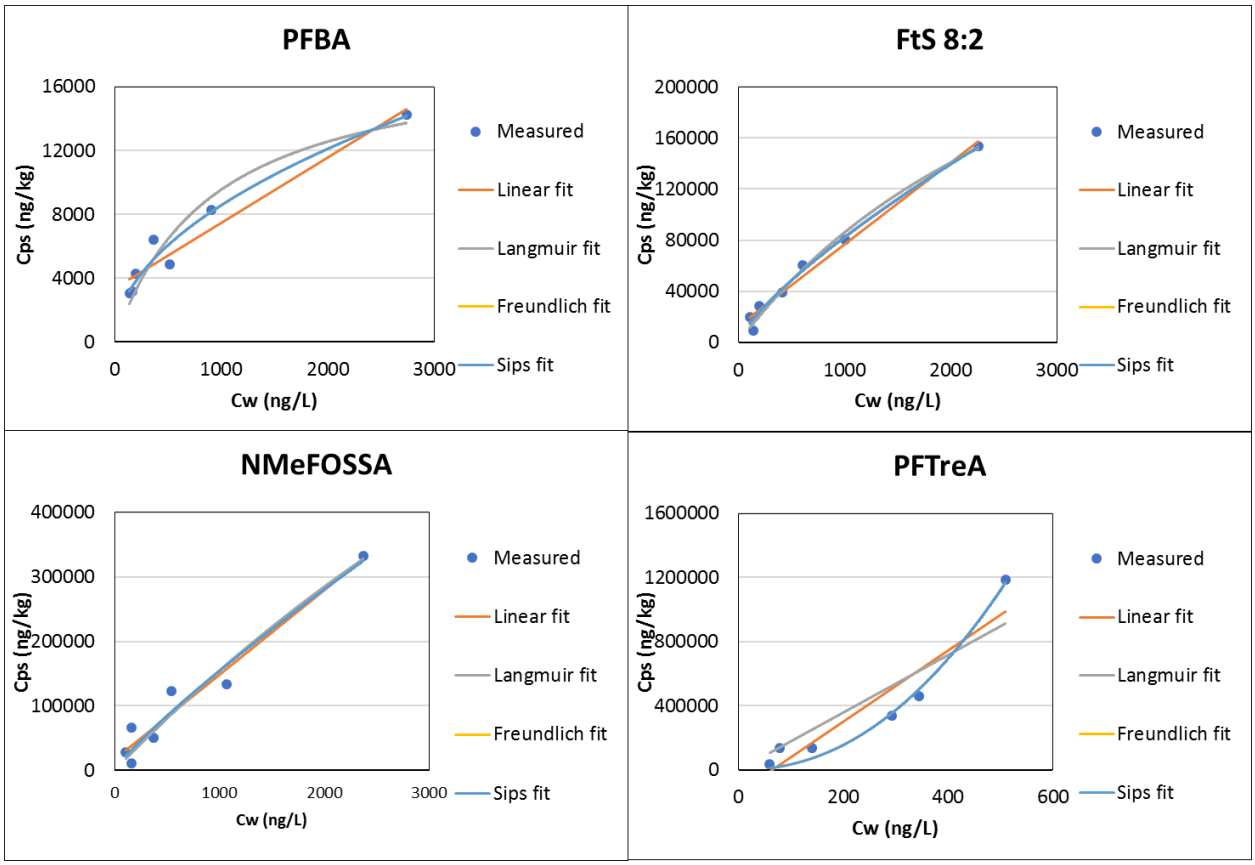

Figure 6.8 Experimental C_{ps} vs C_w and the fitted models (Linear, Langmuir, Freundlich, and Sips models for PFAS using **CA+HSA polymer**, clockwise: PFBA, FtS 8:2, PFTreA, NMeFOSSA.

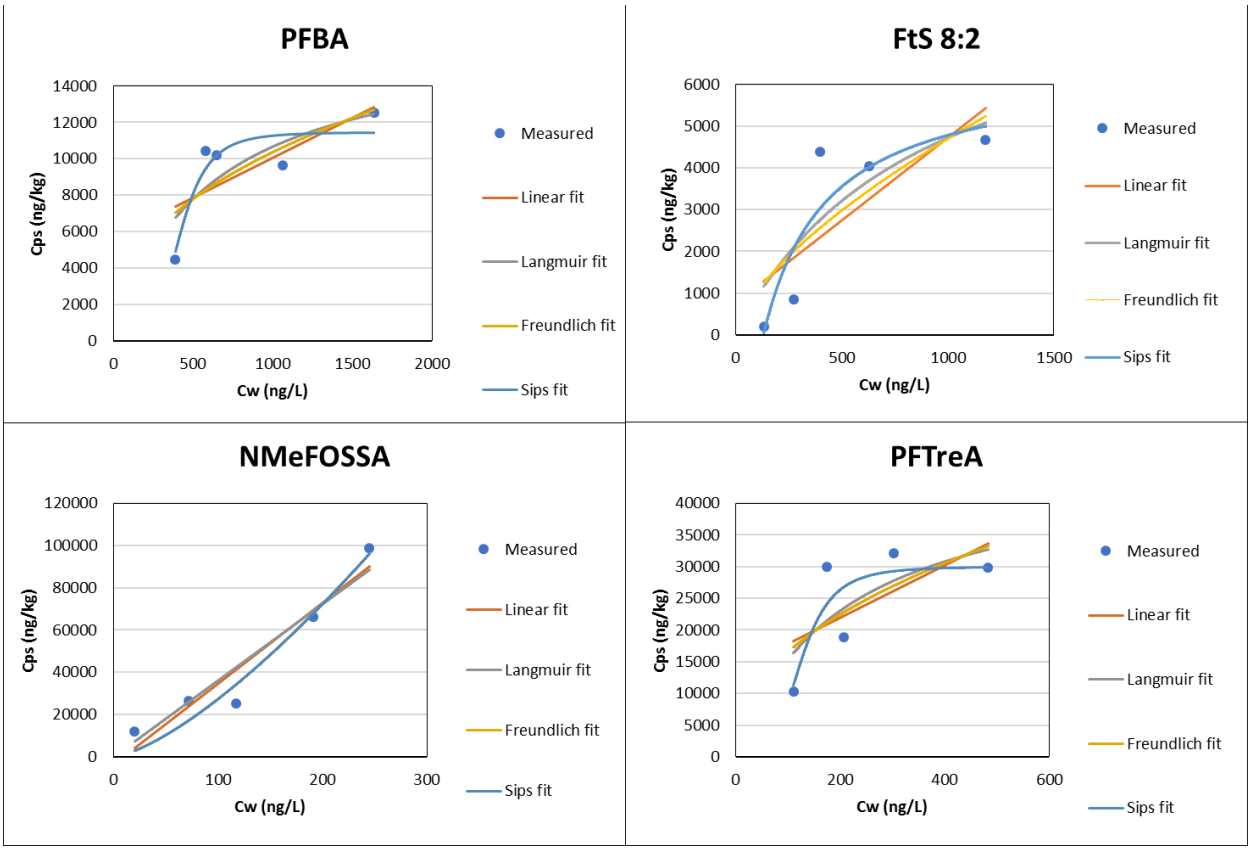

Figure 6.9 Experimental C_{ps} vs C_w and the fitted models (Linear, Langmuir, Freundlich, and Sips models for PFAS using **PDMS+HLB polymers**clockwise: PFBA, FtS 8:2, PFTreA, NMeFOSSA.

Table 6-1 Parameters of fitted PFAS adsorption isotherms (Linear model, Langmuir model, Freundlich model, and Sips model) for **ag+AC polymer**.

	PFBA	FtS 8:2	NMeFOSSA	PFTreA
Model	Linear			
Equation	y = a + b*x			
a	9.13E+03	1.24E+04	1.52E+04	9.66E+03
b	42	44	19	58
R-Square	0.70	0.72	0.71	0.99
Model	Langmuir			
Equation	Csmax*K*Cw/(1+K*Cw)			
K	7.8E-03	4.0E-03	3.6E-03	2.2E-03
Csmax	3.66E+04	6.78E+04	4.99E+04	7.16E+04
R-Square	0.86	0.88	0.92	0.89
Model	Freundlich			

Equation	K*(Cw^n)			
K	2.02E+03	2.14E+03	2.69E+03	1.21E+03
n	0.43	0.48	0.38	0.56
R-Square	0.81	0.84	0.86	0.96
Model	Sips			
Equation	Sm*(K*C)^n/(1+(K*C)^n)			
K	9.00E-03	4.00E-03	4.00E-03	3.60E-08
Sm	3.47E+04	6.66E+05	5.02E+04	1.90E+07
n	1.09	1.03	0.99	0.56
R-Square	0.86	0.88	0.92	0.96

Table 6-2 Parameters of fitted PFAS adsorption isotherms (Linear model, Langmuir model, Freundlich model, and Sips model) for **CA+WAX polymer**.

	PFBA	FtS 8:2	NMeFOSSA	PFTreA
Model	Linear			
Equation	y = a + b*x			
a	6.35E+02	-1.09E+04	4.59E+03	1.50E+04
b	17	143	175	107
R-Square	0.97	0.93	0.90	0.64
Model	Langmuir			
Equation	Csmax*K*Cw/(1+K*Cw)			
K	7.50E-07	6.26E-07	3.99E-04	2.75E-03
Csmax	2.37E+07	2.04E+08	6.04E+05	1.24E+05
R-Square	0.97	0.91	0.92	0.72
Model	Freundlich			
Equation	K*(Cw^n)			
K	18	63	409	1660
n	0.99	1.1	0.88	0.6
R-Square	0.97	0.92	0.91	0.69
Model	Sips			
Equation	Sm*K*C^n/(1+K*C^n)			
K	7.49E-07	3.35E-11	1.55E-08	1.68E-04
Sm	2.47E+07	1.52E+05	1.67E+05	8.50E+04
n	0.99	3.90	3.17	1.70
R-Square	0.97	0.98	0.98	0.74

Table 6-3 Parameters of fitted PFAS adsorption isotherms (Linear model, Langmuir model, Freundlich model, and Sips model) for **CA+HSA polymer**.

	PFBA	FtS 8:2	NMeFOSSA	PFTreA
Model	Linear			
Equation	y = a + b*x			
a	3.37E+03	1.29E+04	1.71E+04	-1.41E+05
b	4	64	131	2220
R-Square	0.94	0.98	0.95	0.89
Model	Langmuir			
Equation	Csmax*K*Cw/(1+K*Cw)			
K	0.00109	2.88E-04	9.54E-05	2.59E-07
Csmax	1.83E+04	3.85E+05	1.78E+06	6.90E+00
R-Square	0.93	0.98	0.94	0.84
Model	Freundlich			
Equation	K*(Cw^n)			
K	275	433	403	1.76
n	0.5	0.76	0.86	2.15
R-Square	0.96	0.99	0.95	0.98
Model	Sips			
Equation	Sm*K*C^n/(1+K*C^n)			
K	1.88E-04	2.65E-05	1.95E-06	2.47E-09
Sm	1.44E+06	1.60E+07	2.06E+08	7.05E+08
n	0.50	0.76	0.86	2.15
R-Square	0.96	0.99	0.95	0.98

Table 6-1 Parameters of fitted PFAS adsorption isotherms (Linear model, Langmuir model, Freundlich model, and Sips model) for **PDMS+HLB polymer**.

	PFBA	FtS 8:2	NMeFOSSA	PFTreA
Model	Linear			
Equation	y = a + b*x			
a	5.65E+03	7.57E+02	-3.60E+03	1.37E+04
b	4.4	4	382	41.3
R-Square	0.53	0.58	0.92	0.41
Model	Langmuir			
Equation	Csmax*K*Cw/(1+K*Cw)			
K	0.0017	1.13E-03	1.31E-06	4.96E-03
Csmax	1.69E+04	8.90E+03	2.76E+08	4.64E+04
R-Square	0.65	0.70	0.92	0.55

Model Equation	Freundlich K*(Cw^n)			
K	604	51	43	2144
n	0.41	0.65	1.4	0.44
R-Square	0.59	0.64	0.95	0.49
Model Equation	Sips Sm*K*C^n/(1+K*C^n)			
K	6.36E-13	4.34E-13	4.23E-07	1.59E-09
Sm	1.15E+04	4.67E+03	1.02E+08	3.00E+04
n	4.66	4.94	1.40	4.20
R-Square	0.86	0.92	0.95	0.69

Partitioning of four PFAS compounds by Agarose embedded with AC films fell within our target range for logK_{ps} of 1.5 to 3.0. And sorption isotherms remained well fitted over multiple orders of magnitude (**Figure 6.6**). The Langmuir and Sips model agree with each other very well for PFAS compounds and have an R^2 value of 0.88 and 0.90, respectively. The R^2 for Freundlich model fitting averaged to be 0.87 for the four PFAS compounds. For NMeFOSSA, the Freundlich model fits with R^2 =0.96, while other compounds' data fit better in Langmuir models. The log C_{ps} vs. log C_w were plotted in Appendix **Figure A8** for linear regression.

The CA+WAX and CA+HSA polymers have the best fitting results among different films, especially for the short-chain PFAS (PFBA), with R^2 >0.93. The isotherm models do not fit the PDMS+HLB polymer as well as other passive samplers. The linear model works very well for cellulose-based polymers but not so well for agarose and PDMS films. The pore-filling can be a possible reason for the nonlinearity (Hu et al., 2018; Sun et al., 2013). The Langmuir and Freundlich isotherm models have similar fitting results with linear fitting for the majority of the PFAS complex. Overall, the Langmuir and Sips models were more suitable than the Linear model in most cases, judging from their corresponding R^2 values. However, most of the nonlinearity, where observed, was associated with the highest concentration data point.

The fitted adsorption isotherms, which describe the relationship between the adsorbent and the adsorbate equilibrium, can be used to determine the amount of adsorbed material of a specific pollutant.

We can get the single point K_d values for each PFAS compound by using the fitted partitioning parameters for each isotherm model. **Table 6.5** shows the estimated log K_d values of each PFAS

compound on various polymers when assuming C_w=50 ng/L. We can see that the estimated K_d values were generally within the desired range (log Kd of 1.5 to 3), and various models gave consistent results, especially for shorter-chain PFAS.

Table 6-2 Estimated logKd values from different isotherm fitting for PFAS compounds when Cw is equal to 50 ng/L.

Ag+AC polymers	Linear fit	Langmuir fit	Freundlich fit	Sips model fit
PFOA	2.35	2.31	2.34	2.31
PFOS	2.47	2.36	2.43	2.35
FtS 8:2	2.51	2.38	2.18	2.19
NMeFOSSA	2.40	2.25	2.34	2.34
CA+WAX polymers	Linear fit	Langmuir fit	Freundlich fit	Sips model fit
PFOA	1.47	1.25	1.24	1.25
FtS 8:2	-	2.11	1.97	-
NMeFOSSA	2.43	2.37	2.41	1.10
PFTreA	2.61	2.48	2.54	2.29
CA+HSA polymers	Linear fit	Langmuir fit	Freundlich fit	Sips model fit
PFOA	1.85	1.28	1.59	1.58
FtS 8:2	2.51	2.04	2.23	2.22
NMeFOSSA	2.67	2.23	2.37	2.37
PFTreA	-	-	2.20	2.19
PDMS+HLB polymers	Linear fit	Langmuir fit	Freundlich fit	Sips model fit
PFOA	2.07	1.42	1.78	-
FtS 8:2	1.28	0.98	1.11	-
NMeFOSSA	2.49	2.56	2.31	2.31
PFTreA	2.50	2.27	2.38	1.11

6.5 Implications

A series of concentrations typically spanning two orders of magnitude from 80 ng/L to 2000 ng/g were spiked to the lab synthesized passive samplers for the isotherm study for PFAS compounds. The C_{ps}-C_w data were evaluated using several common sorption isotherm models, which provide a relationship between absorbed PFAS and freely dissolved PFAS. The Langmuir model provided the best fit for the full range of concentrations evaluated. This work lays the foundation of passive sampling technology and provides the capability of ag+AC, CA+WAX, CA+HSA passive samplers to be used to measure the freely dissolved concentration and further bioaccumulation of PFAS compounds. Besides, the estimated K_d values are within the desired range, demonstrating again that the casted functionalized passive samplers have good sorption of the PFAS compounds tested.

6.6 Literature Cited

Ayawei, N., Ebelegi, A., Wankasi, D., 2017. Modelling and interpreatation of adsorption isotherms. *J. Chem*. 2017, 1-11.

Ebadi, R., Saadi, Z. Fazaeli, R., Fard, N.E., 2015. Monolayer and multilayer adsorption isotherm models for sorption from aqueous mdia. Kor. *J. Chem. Eng*. 32, 787-799.

Foo, K.Y., Hameed, B.H., 2010. Insights into the modeling of adsorption isotherm systems. *Chem. Eng*. J. 156 (1), 2–10

Gobelius, L., Persson, C., Wiberg, K., & Ahrens, L. (2019). Calibration and application of passive sampling for per-and polyfluoroalkyl substances in a drinking water treatment plant. *Journal of hazardous materials*, 362, 230-237.

Godlewska, K., Stepnowski, P., & Paszkiewicz, M. (2020). Application of the polar organic chemical integrative sampler for isolation of environmental micropollutants–A review. Critical Reviews in *Analytical Chemistry*, 50(1), 1-28.

Guo, X., Wang, J.L., 2019. Comparison of linearization methods for modeling the Langmuir adsorption isotherm.*J. Mol. Liq*. 296, 111850.

Guo, X., Wang, J.L., 2019. The phenomenological mass transfer kinetics model for Sr^{2p} sorption onto spheroids primary microplastics. *Environ. Pollut*. 250, 737-745.

Hartmann, H., Hefner, C., Carter, E., Liles, D., Divine, C., & Edmiston, P. L. (2021). Passive sampler designed for per‐and polyfluoroalkyl substances using polymer‐modified organosilica adsorbent. *AWWA Water Science*, 3(4), e1237.

Hu, S., Zhang, D., Xiong, Y., Yang, Y., Ran, Y., 2018. Nanopore-filling effect of phenanthrene sorption on modified black carbon. Sci. Total Environ. 642, 1050–1059.

Langmuir, I., 1916. The Constitution and fundamental properties of solids and liquids. Part I. Solids. J. *Am. Chem. Soc*. 38 (11), 2221–2295.

Langmuir, I., 1918. The adsorption of gases on plane surfaces of glass, Mica and platinum. J. *Am. Chem. Soc*. 40 (9), 1361–1403.

Liu, Y., Li, H.A., Tian, Y., Jin, Z., Deng, H., 2018. Determination of the absolute adsorption/desorption isotherms of CH4 and n-C4H10 on shale from a nanoscale perspective. *Fuel* 218, 67e77.

Li, F., Fang, X.L., Zhou, Z.M., Liao, X.B., Zou, J., Yuan, B.L., Sun, W.J., 2019. Adsorption of perfluorinated acids onto soils: kinetics, isotherms, and influences of soil properties. *Sci. Total Environ*. 649, 504–514.

Miao, Y., Guo, X.T., Peng, D., Fan, T.Y., Yang, C., 2017. Rates and equilibria of perfluorooctanoate (PFOA) sorption on soils from different regions of China. *Ecotoxicol. Environ. Saf*. 139, 102–108.

Milinovic, J., Lacorte, S., Vidal, M., Rigol, A., 2015. Sorption behaviour of perfluoroalkyl substances in soils. *Sci. Total Environ*. 511, 63–71.

Mondal, S., Majumder, S.K., 2019. Honeycomb-like porous activated carbon for efficient copper (II) adsorption synthesized from natural source: kinetic study and equilibrium isotherm analysis. *J. Environ. Chem. Eng*. 7, 103236.

Saeidiet, N., Kopinke, F.D., Georgi, A., 2020. Understanding the effect of carbon surface chemistry on adsorption of perfluorinated alkyl substances. *Chem. Eng.* J. 381, 122689.

Sima MW, Jaffé PR. A critical review of modeling Poly-and Perfluoroalkyl Substances (PFAS) in the soil-water environment. *Science of the Total Environment*. 2021 Feb 25;757:143793.

Sips, R. 1948. On the structure of a catalyst surface. J. *Chem. Phys*. 16, 490-495.

Sun, K., Ran, Y., Yang, Y., Xing, B., Mao, J., 2013. Interaction mechanism of benzene and phenanthrene in condensed organic matter: importance of adsorption (nanopore-filling). Geoderma 204-205, 68–74.

Wang J. and Guo X. (2020). Adsorption isotherm models: Classification, physical meaning, application and solving method. *Chemosphere*. 258, 127279.

Zaheer, Z., Aisha, A.A., Aazam, E.S. (2019). Migration and sorption of strontium in clay-sand mixtures. *J. Radioanal. Nucl. Chem*. 308, 439-445.

Zhang, D.Q., Zhang, W.L., Liang, Y.N., 2019. Adsorption of perfluoroalkyl andpolyfluoroalkyl substances (PFASs) from aqueous solution – a review. *Sci. Total Environ*.694, 133606.

7.0 Research Objectives #3&4: Testing of reversible equilibrium with matching kinetics of sorption and desorption and mechanism of accumulation in polymer

7.1 Introduction

For the time integrative equilibrium passive sampling to function, the sorption must be reversible within a reasonable period matching a typical deployment period of a few weeks. In addition, the sorption and desorption kinetics have to be comparable. Different compounds require different exposure times to equilibrium between passive sampler polymer and water. Some studies have shown that for many hydrophobic organic compounds to obtain equilibrium, passive sampler sorbent needs to be placed in the environment for weeks or months (Booji et al., 2002; Adams et al., 2007; Cornelissen et al., 2008; Ghosh et al., 2014).

For samplers where equilibrium is uncertain, some methods of evaluating the extent of equilibration are required. Performance reference compounds (PRCs) can be used to estimate the non-equilibrium uptake (Huckins et al., 1993). PRCs are pre-loaded onto a passive sampler and their release indicates the extent to which target compounds of similar characteristics are sorbing to the passive sampler. The depletion of the PRCs should be inversely related to the uptake of target compounds with comparable sorption properties and thus, the extent of PRCs' release can be used to correct the non-equilibrium exposure of passive samplers. Many studies have explored PRCs approach on passive samplers like PE, POM and PDMS using mass transfer models to describe the exchange between the environment and the passive sampler (Booij et al., 2002; Tomaszewski and Luthy, 2008; Fernandez et al., 2009; Lampert et al., 2015; Schmidt et al., 2018).

Improved mechanistic knowledge of PFAS association with passive samplers can better inform functionalized film modification and application. Different desorption models investigated in earlier work (Gustafson et al., 1994; Ghosh et., 2001) for PAHs can be adapted in our works for the functional passive samplers.

Therefore, to develop equilibrium passive samplers for PFAS complex, the sorption and desorption kinetics are essential and explored in this chapter. Based on the results of this task, if the adsorption kinetics for the polymer is predictable based on the desorption kinetics of an

analogous compound, we should be able to use stable isotope labeled performance reference compounds for checking and correcting for equilibrium. The goal is to be able to develop an approach analogous to the one used currently for passive sampling of hydrophobic compounds (Ghosh et al., 2014; Fernandez et al., 2009).

7.2 Materials and methods

7.2.1 Uptake kinetic studies

Four of the selected functionalized passive samplers were used to demonstrate equilibrium reversibility for the PFAS complex. The sampler was first placed in contact with PFAS compounds in a finite volume of water and spiked with 800 ng/L PFAS complex at time 0. Then, the concentrations of PFAS were tracked over time to estimate the adsorption kinetics. A total of nine sampling time points were used: 0 hours (control samples), 6 hours, 24 hours, 48 hours, 4 days, 7 days, 9 days, 12 days, and 14 days. The samples were extracted at each time point and analyzed by LC-MS for PFAS concentrations using the protocol described in previous chapters. In addition, the concentrations that remained in water were also analyzed at each sampling time point to help understand the uptake kinetics.

7.2.2 Desorption measurements

Another batch of passive samplers of CA+WAX, ag+AC, PDMS+HLB were used for the desorption kinetics. The synthesized films were spiked with 800 ng/L of PFAS mixture in 100 ml DI water and loaded for 7 days to achieve equilibrium. After 7 days, the loaded polymer was placed in clean water to measure the desorption kinetics. In both the adsorption and desorption cycles, the mixing environment in water was maintained the same.

The final concentrations in water and samplers were checked to evaluate if the initial sorption was reversible and the same partition constants were measured in the equilibrium's adsorption and desorption cycles. The kinetic results allow us to evaluate if a diffusion-based or first-order PRC correction method will be necessary (Sanders et al., 2018).

7.2.3 Mechanism of accumulation in polymer

The activated carbon embedded agarose films were used to test if the sorption in the functionalized polymer formulation was based on diffusion of PFAS within the polymer matrix and binding to target domains. Two different thicknesses (1000 μm and 484 μm), and three different additive AC portion (ag:AC=3:3, ag:AC=3:2, and ag:AC=3:1) were used as the

evaluation sample matrix formulation. The samples were spiked with 800ng/L target PFAS compounds with IS and SS, and loaded under the same conditions as described in previous chapter for 7 days. At the end of the deployment, the mass loaded on polymers, remaining in the water, and attached to bottles were measured and compared.

7.3 Results and discussion

7.3.1 Uptake kinetic study

Agarose+AC, CA+WAX, and PDMS+HLB polymers were used in this phase based on the single point isotherm study results. The mass balance was calculated for each compound's uptake kinetic study and shown in Appendix **Figure A7**. The sorption of PFAS from water (**Figure 7.1**) was modeled in polymers using nonlinear curve-fitting to sorption isotherms. As shown in the figure, the $\log K_d$ values for various PFAS compounds reached a steady value within 7 days' deployment, which indicates that 7 days is sufficient for PFAS sorption on passive samplers.

The kinetic results were fitted to a pseudo first-order model for PFBA, PFOA, PFOS, FtS 8:2, NMeFOSSA, and PFTreA in three types of lab synthesized passive samplers: AC embedded agarose, HLB embedded PDMS, and WAX embedded cellulose acetate films, which can be expressed as:

$$S_t = S_e(1 - e^{-\mu t})$$

where S_t and S_e are the amounts of PFAS sorbed at time t and equilibrium(ng/g), respectively. The μ is the sorption rate constant.

As given in **Figure 7.1**, the model prediction fitted well with the experimental data and the fitting parameters are summarized in **Table 7.1**. Overall, the modeling results had good agreement with the uptake rate of these six PFAS compounds in systems using the passive samplers we cast. Deviations between the model simulation and experimental data were more obviously for the PDMS+HLB films at 12 or 14 days' data, likely related to quantification problems, which were also reflected in the poor mass balance. The equilibrium K_d values for each PFAS compound on a passive sampler can also be obtained by the fitted model, which agrees with our 7-day isotherm study results discussed in the previous chapter. The adsorption kinetics appeared to be fastest for the CA-WAX sampler and slowest for AG+AC.

As shown in **Figure 7.1** and **Table 7.1**, with the increase of perfluorocarbon chain length, the fractions that cannot partition to the solid phase decreased while the fractions that can be adsorbed onto polymers increased. The results indicate that the PFASs with long perfluorocarbon chains prefer partitioning to solid phase, consistent with PFAS sorption to soils (Li et al., 2019).

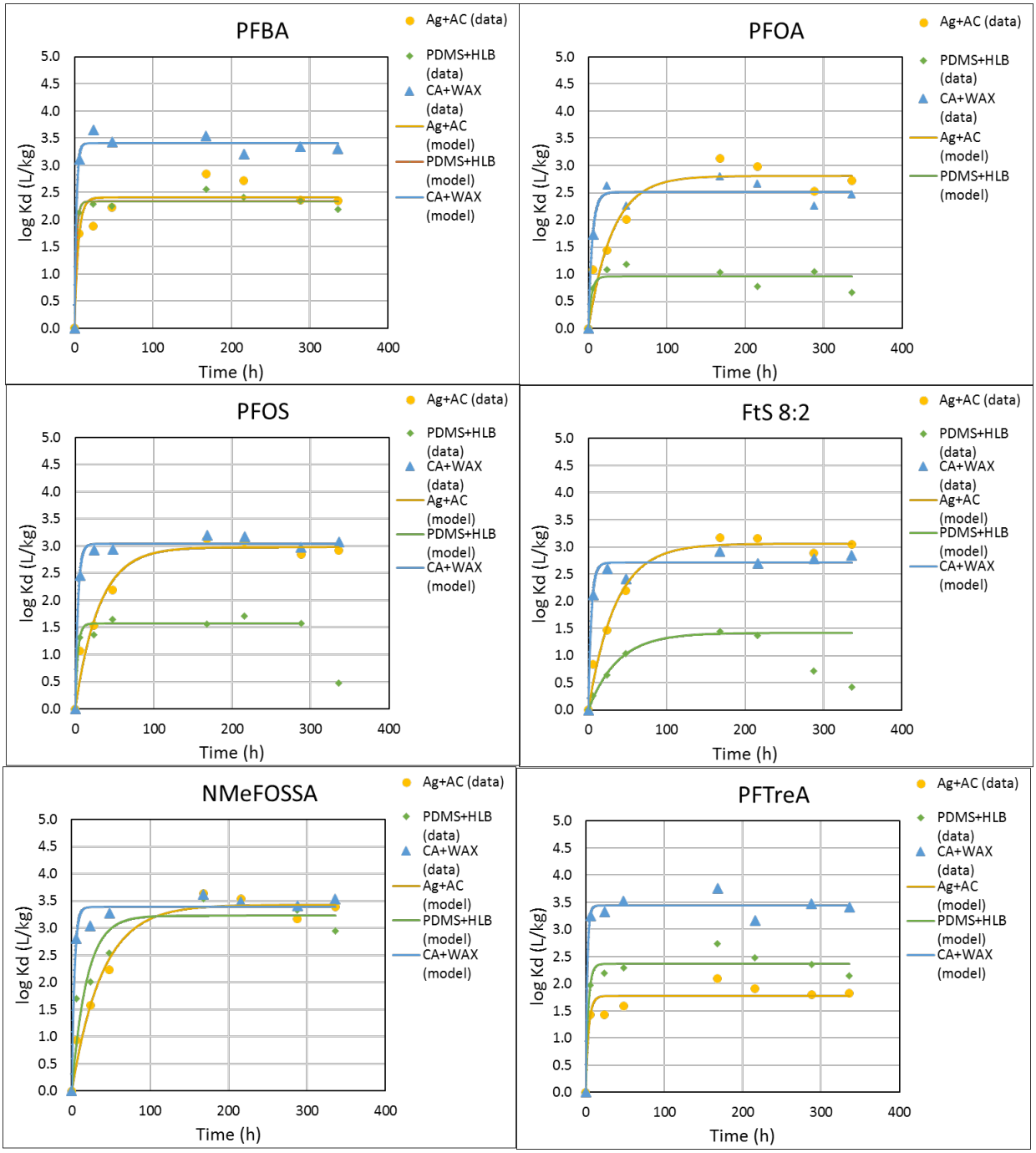

Figure 7.1 Uptake Kinetics of PFAS in three types of lab synthesized passive samplers: AC embedded agarose, HLB embedded PDMS, and WAX embedded cellulose acetate films. Experimental data have been shown by symbols, and model simulations have been shown by lines.

Table 7-1 Uptake kinetics fitted model parameters for PFAS complex on three types of synthesized passive samples: CA+WAX, PDMS+HLB, and AG+AC.

PFOA	CA+WAX	PDMS+HLB	AG+AC	**PFOS**	CA+WAX	PDMS+HLB	AG+AC
Model	pseudo first-order	pseudo first-order	pseudo first-order	Model	pseudo first-order	pseudo first-order	pseudo first-order
Equation	$S_t = S_e(1 - \exp(-\mu*t))$	$S_t = S_e(1 - \exp(-\mu*t))$	$S_t = S_e*(1 - \exp(-\mu*t))$	Equation	$S_t = S_e(1 - \exp(-\mu*t))$	$S_t = S_e(1 - \exp(-\mu*t))$	$S_t = S_e(1 - \exp(-\mu*t))$
S_e	2.51	0.96	2.8 1	S_e	3.04	1.57	2.97
μ	0.20	0.24	0.03	μ	0.27	0.30	0.03
R-Square (COD)	0.96	0.80	0.92	R-Square (COD)	0.99	0.97	0.96
FtS 8:2	CA+WAX	PDMS+HLB	AG+AC	**NMeFOSSA**	CA+WAX	PDMS+HLB	AG+AC
Model	pseudo first-order	pseudo first-order	pseudo first-order	Model	pseudo first-order	pseudo first-order	pseudo first-order
Equation	$S_t = S_e(1 - \exp(-\mu*t))$	$S_t = S_e(1 - \exp(-\mu*t))$	$S_t = S_e(1 - \exp(-\mu*t))$	Equation	$S_t = S_e(1 - \exp(-\mu*t))$	$S_t = S_e(1 - \exp(-\mu*t))$	$S_t = S_e(1 - \exp(-\mu*t))$
S_e	2.71	1.42	3.06	S_e	3.39	3.22	3.43
μ	0.25	0.027	0.029	μ	0.28	0.05	0.025
R-Square (COD)	0.97	0.99	0.98	R-Square (COD)	0.98	0.88	0.97
PFTreA	CA+WAX	PDMS+HLB	AG+AC	**PFBA**	CA+WAX	PDMS+HLB	AG+AC
Model	pseudo first-order	pseudo first-order	pseudo first-order	Model	pseudo first-order	pseudo first-order	pseudo first-order
Equation	$S_t = S_e(1 - \exp(-\mu*t))$	$S_t = S_e(1 - \exp(-\mu*t))$	$S_t = S_e(1 - \exp(-\mu*t))$	Equation	$S_t = S_e(1 - \exp(-\mu*t))$	$S_t = S_e(1 - \exp(-\mu*t))$	$S_t = S_e(1 - \exp(-\mu*t))$
S_e	3.44	2.37	1.78	S_e	3.41	2.34	2.41
μ	0.48	0.29	0.26	μ	0.40	0.39	0.20
R-Square (COD)	0.98	0.95	0.91	R-Square (COD)	0.99	0.98	0.89

7.3.2. Reversibility test

The $\log K_d$ (L/kg) values after 7 days' desorption in AG+AC films and CA+WAX films were calculated for each PFAS compound and shown in **Figure 7.2**, along with the uptake kinetic curves. As can be seen, the $\log K_d$ values after 7 days' desorption fit the kinetic curve well, which indicates good reversibility and "stable" status after 7 days' desorption in DI water. Moreover, it shows the possibility of predicting the adsorption kinetics based on the desorption kinetics and the feasibility of using stable isotope labeled PFAS compounds as PRCs.

The ability of PFAS to desorb from passive samplers depends on the sorption mechanism between PFAS and polymers, soil surface characteristics, and sorption time (Askeland et al., 2020; Gagliano et al., 2020; Xiao et al., 2019). The desorption ratio, which is calculated by the remaining concentration at the end of the desorption divided by the equilibrium concentration/loaded concentration, of PFBS, FtS 8:2, NMeFOSSA and PFTreA in ag+AC and CA+WAX polymers is shown in **Table 7.2**. The C/C_0 ratio (%) of PFBS, NMeFOSSA and PFTreA have small values (<15%), which indicates the sorption of these compounds in both ag+AC and CA+WAX films is highly reversible.

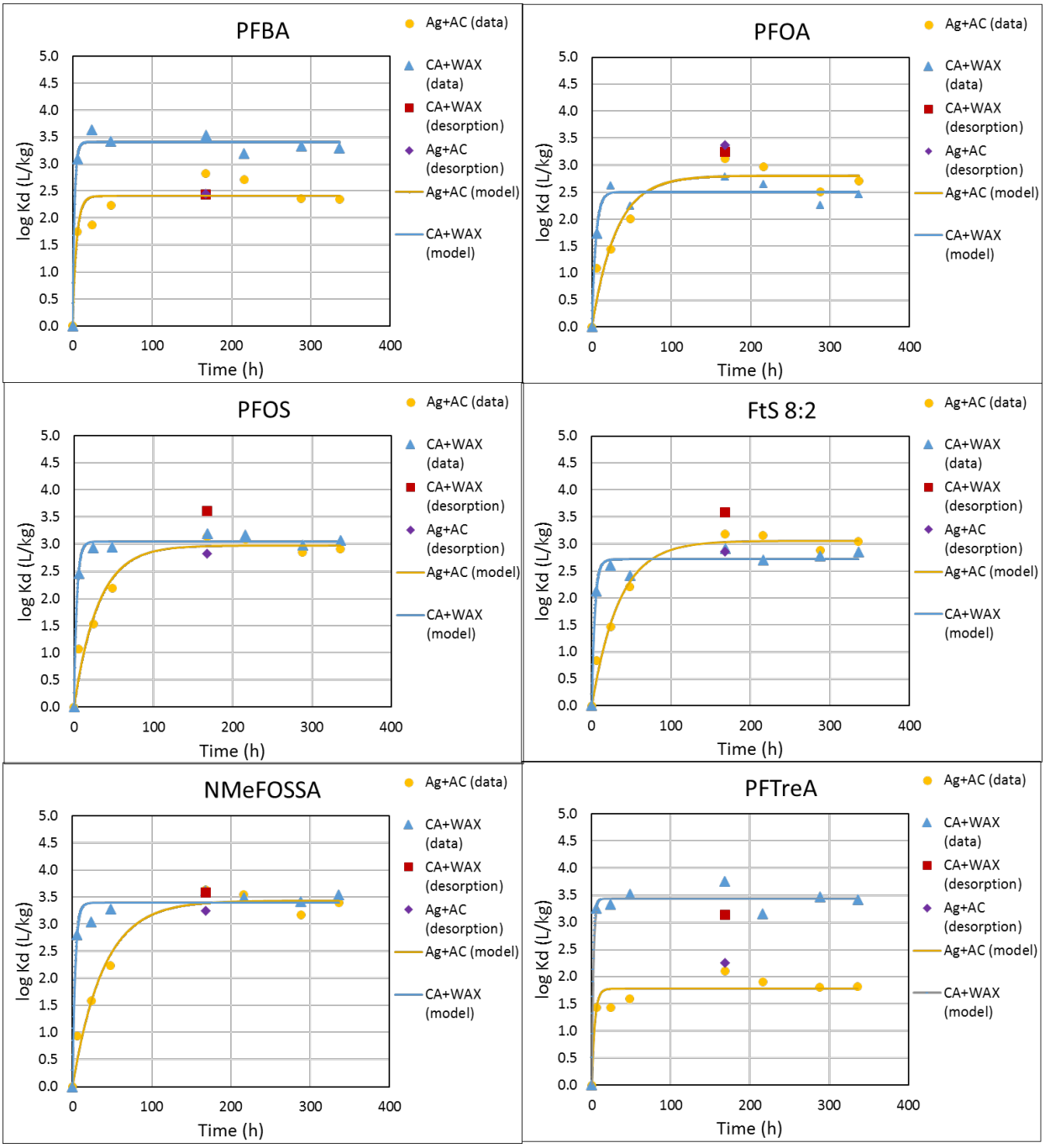

Figure 7.2 LogK$_d$ values calculated for 7 days' desorption compared with uptake Kinetics of PFAS in AC embedded agarose and WAX embedded cellulose acetate films.

Table 7-2 Desorption ratio (C/C_0) % for PFBS, FtS 8:2, NMeFOSSA, and PFTreA in ag+AC and CA+WAX films

Desorption ratio (C/C_0)%	PFBS	FtS 8:2	NMeFOSSA	PFTreA
Ag+AC	1%	27%	2%	3%
CA+WAX	9%	12%	2%	15%

7.3.3 Mechanism of accumulation

To explore the mechanism of PFAS accumulation, we measured the absorption of two different thicknesses and four different functional partial (AC) portions in the agarose films within 7 days. The two different film thicknesses were 484µm and 1000µm, while the four different ag: AC ratios were: 3:0 (base agarose polymer with no AC added), 3:1, 3:2, and 3:3. Two batches of experiments were conducted for this object.

The mass balance results of three PFAS compounds in the first batch are shown in **Figure 7.3**. The measured total PFBA and PFBS amount are less than we spiked (80 ng), and the majority of the target compounds were found in water instead of passive samplers. Some data points are missing in this batch, for example, data for polymers with the ratio of AG:AC=3:1, 484µm. Furthermore, we calculated $\log K_d$ values for the three PFAS compounds for different polymer formulas. As shown in **Figure 7.4**, the log K_d values are similar for the two thickness of the polymer, which is what we would expect to see if the sorption mechanism involves penetration of the compounds within the polymer. The log K_d values in agarose base polymer with no AC added are lower than those with AC, indicating better sorption to PFAS due to the AC particles embedded. However, the differences in calculated log K_d values for different AC ratios are insignificant. The low mass extracted may be the main reason for these results. So we repeated this experiment to confirm the observation.

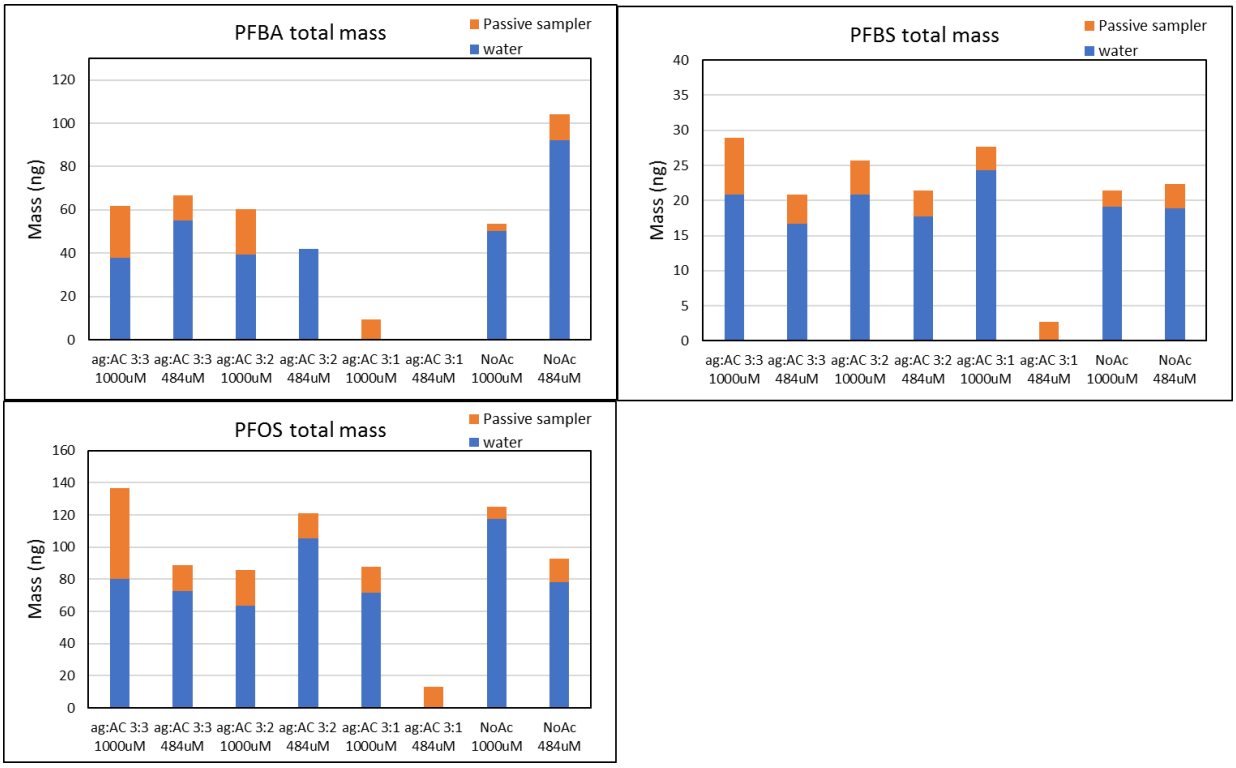

Figure7.3 Mass balance results for Activated carbon embedded agarose film with various casting formulation (thickness and AC ratio) in the first batch. Clockwise: PFBA, PFBS, PFOS.

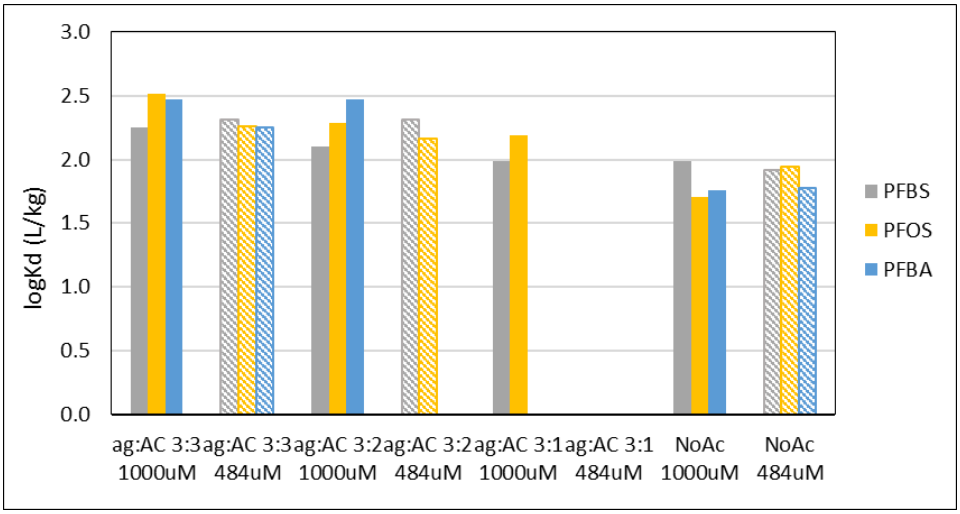

Figure 7.4 Calculated K_d values for activated carbon embedded agarose film with various casting formulation (thickness and AC ratio) in the first batch.

In the second batch, the loaded mass of three PFAS compounds: PFOS, PFOA, and FtS 8:2 for each passive sampler formulation and the mass balance is shown in **Figure 7.5**. We also measured the mass attached to the bottle by rinsing the bottle and extracted the rinsed water in this batch. The majority of the spiked PFAS complex have been loaded to the agarose films within 7 days, and the total measured mass for the majority of compounds ranged from 80-120% compared with the spiking amount, indicating good extraction for the samples and mass balance. Furthermore, K_d values were calculated for each polymer formulation for these three PFAS compounds (**Figure 7.6**). When the film thickness is the only variable, the 1000 μm polymer has comparable K_d values with the 484 μm ones. This is possible because the sorption happens throughout the interior of the polymer and is not limited by the polymer's external surface area. Thus, there is some indication that the sorption process is internal to the polymer, and the mass of the polymer explains the difference in sorption capacity.

While the second set of experiments seemed to reconfirm that the sorption was not limited to the external surface area of the polymer, the K_d values were similar across the polymer formulations. Overall, our assessment is that these two batches of experiments, which were conducted in the early stage of this project, when we faced some analytical challenges and relatively high variability in the overall mass balance, may need to be redone in future work with greater analytical quality control. Thus, the mechanism of accumulation study needs to be replicated with tighter QA/QC in further study.

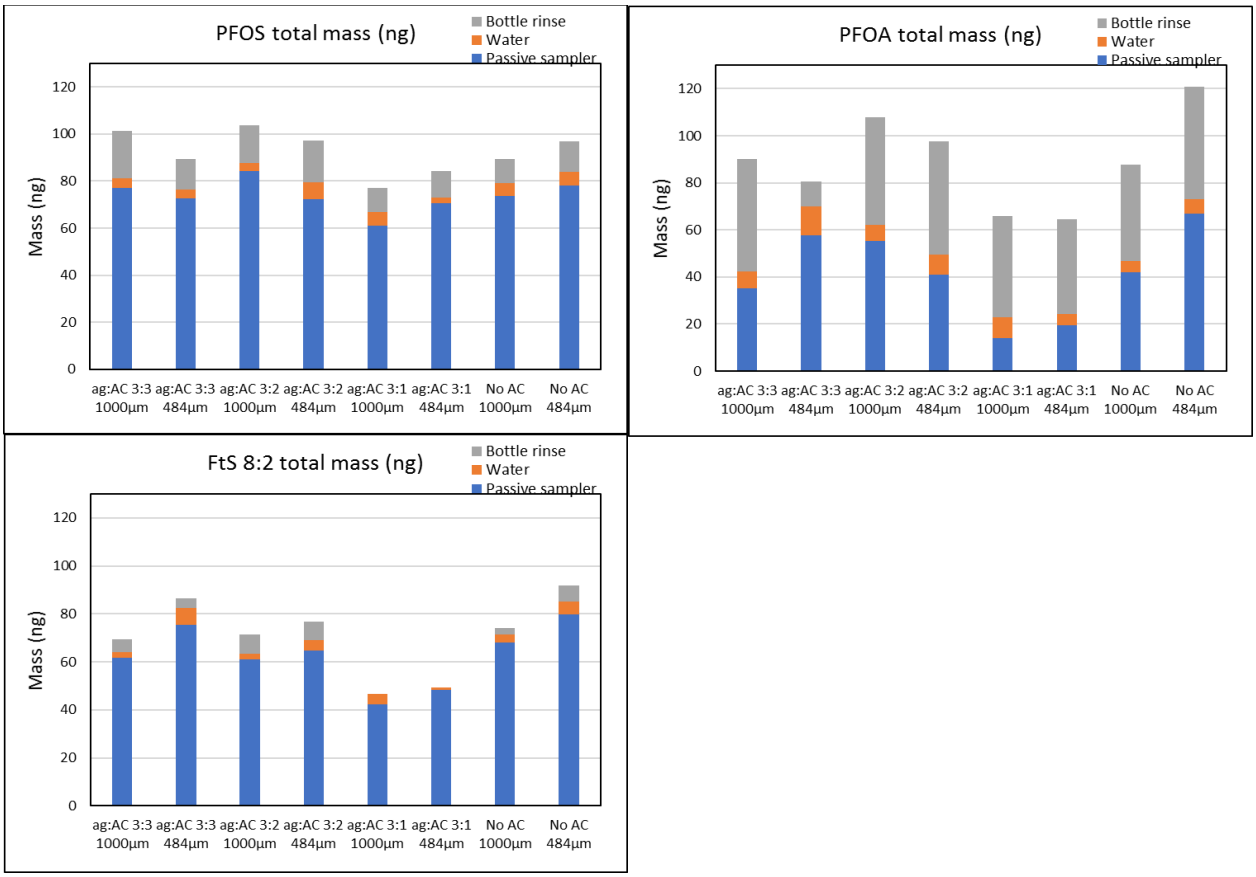

Figure 7.5 Mass balance results for Activated carbon embedded agarose film with various casting formulation (thickness, and AC ratio) in the second batch. Clockwise PFAS complex: PFOS, PFOA, FtS 8:2.

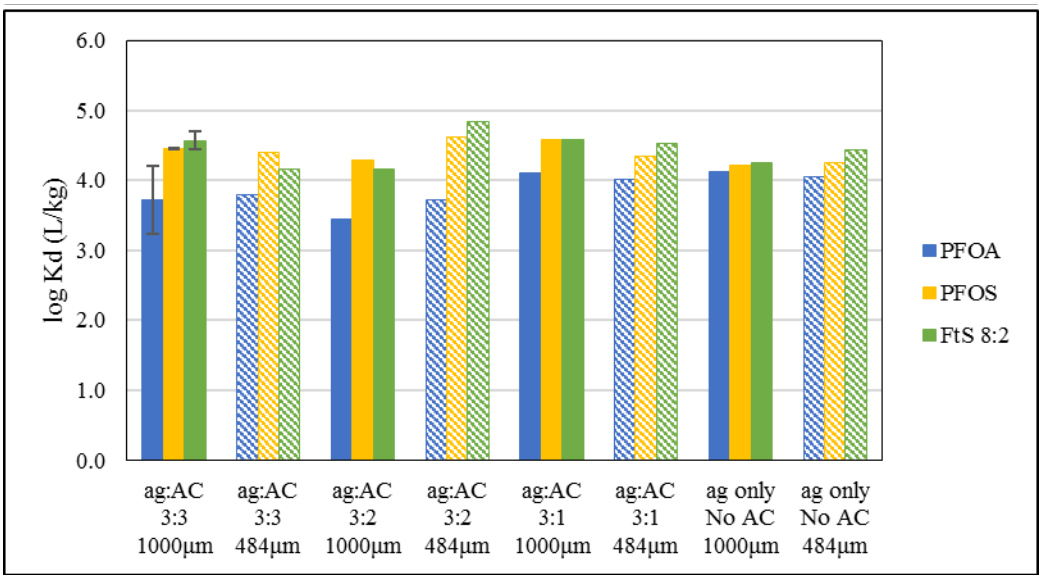

Figure 7.6 Calculated K_d values for activated carbon embedded agarose film with various casting formulation (thickness and AC ratio) in the second batch.

7.4 Implications

The uptake kinetics and the desorption have been explored for the selected passive samplers in this chapter. A total of 9 time points within 14 days were used for the uptake kinetic study, and the data were fitted for first-order models. The fitted first-order kinetic models will be essential to determine the deployment period for passive sampling approaches. For all target PFAS compounds, the uptake happens quickly and 7 days appears to be sufficient for loading from the aqueous medium. The single time point desorption kinetics matched reasonably well with the adsorption kinetics, which provides promising early indication that desorption kinetics can be used to predict the adsorption kinetics for an analogous compound. Therefore, we may be able to use stable isotope labeled PFAS compounds as PRCs, and further determine the fraction to steady state.

Further work is needed to fully understand the mechanism of sorption of the full range of PFAS compounds to the passive samplers.

7.5 Literature cited

Adams, R.G., Lohmann, R., Fernandez, L.A., Macfarlane, J.K., Gschwend, P.M., 2007. Polyethylene devices: Passive samplers for measuring dissolved hydrophobic organic compounds in aquatic environments. Environmental science & technology 41, 1317 1323.

Askeland, M., Clarke, B.O., Cheema, S.A., Mendez, A., Gasco, G., Paz-Ferreiro, J., 2020. Biochar sorption of PFOS, PFOA, PFHxS and PFHxA in two soils with contrasting texture. Chemosphere 249, 126072.

Booij, K., Smedes, F., van Weerlee, E.M., 2002. Spiking of performance reference compounds in low density polyethylene and silicone passive water samplers. Chemosphere 46, 1157-1161.

Cornelissen, G., Pettersen, A., Broman, D., Mayer, P., Breedveld, G.D., 2008. Field testing of equilibrium passive samplers to determine freely dissolved native polycyclic aromatic hydrocarbon concentrations. Environmental toxicology and chemistry / SETAC 27, 499.

Fernandez, L.A., MacFarlane, J.K., Tcaciuc, A.P., Gschwend, P.M., 2009. Measurement of freely dissolved PAH concentrations in sediment beds using passive sampling with low-density polyethylene strips. Environmental science & technology 43, 1430-1436.

Gagliano, E.G., Sgroi, M., Falciglia, P.P., Vagliasindi, F.G.A., 2020. Removal of poly- and perfluoroalkyl substances (PFAS) from water by adsorption: role of PFAS chain length, effect of organic matter and challenges in adsorbent regeneration. Water Res. 171, 115381.

Gustafson, K. E.; Dickhut, R. M.. Molecular diffusivitiy of polycyclic aromatic hydrocarbons

in aqueous solution. J. Chem. Eng. Data.1994, 39, 281-285.

Ghosh U, Talley JW, Luthy RG. Particle-scale investigation of PAH desorption kinetics and thermodynamics from sediment. Environmental science & technology. 2001 Sep 1;35(17):3468-75.

Ghosh, U., Kane Driscoll, S., Burgess, R.M., Jonker, M.T.O., Reible, D., Gobas, F.,Choi, Y., Apitz, S.E., Maruya, K.A., Gala, W.R., Mortimer, M., Beegan, C., 2014. Passive sampling methods for contaminated sediments: Practical guidance for selection, calibration, and implementation. Integrated environmental assessment and management.

Huckins, J.N., Manuweera, G.K., Petty, J.D., Mackay, D., Lebo, J.A., 1993. Lipid Containing Semipermeable-Membrane Devices for Monitoring Organic Contaminants in Water. Environmental science & technology 27, 2489-2496.

Lampert, D., C. Thomas and D. Reible. 2015. “Internal and external transport significance for predicting contaminant uptake rates in passive samplers.” Chemosphere 119: 910-916.

Li, F., Fang, X.L., Zhou, Z.M., Liao, X.B., Zou, J., Yuan, B.L., Sun, W.J., 2019. Adsorption of perfluorinated acids onto soils: kinetics, isotherms, and influences of soil properties. Sci. Total Environ. 649, 504–514.

Sanders, J. A Novel Equilibrium Passive Sampler for Methylmercury and Other Advances in Monitoring and Activated Carbon Remediation for Mercury and PCBs. Ph.D. Dissertation, University of Maryland Baltimore County, 2018.

Schmidt, S. N., Wang, A. P., Gidley, P. T., Wooley, A. H., Lotufo, G. R., Burgess, R. M., Ghosh, U., Fernandez. L. A., and Mayer, P. 2017. Cross validation of two partitioning-based sampling approaches in mesocosms containing PCB contaminated field sediment, biota, and activated carbon amendment. Environmental science & technology, 51(17), 9996-10004.

Tomaszewski, J. E. and R. G. Luthy. 2008. Field deployment of polyethylene devices to measure PCB concentrations in pore water of contaminated sediment. Environmental Science & Technology 42(16): 6086-6091.

Xiao, F., Jin, B., Golovko, S.A., Golovko, M.Y., Xing, B., 2019. Sorption and desorptionmechanisms of cationic and zwitterionic per- and polyfluoroalkyl substances in natural soils: thermodynamics and hysteresis. Environ. Sci. Technol. 53, 11818–11827.

8.0 Conclusions and recommendations for further research.

In this 1-year SERDP project, we developed equilibrium passive samplers as a proof-of-concept before addressing the subsequent questions regarding the ability to predict concentrations in more complex water chemistries, applicability in the field, and interpretations of field deployments. We have successfully formed novel functional passive samplers for PFAS in the lab experiments with adjustable polymer shapes and thicknesses. The target PFAS compounds equilibrium partitioning and transport mechanism have been evaluated for each synthesized polymer. The motivation for embedding fine sorbent particles in a thin polymer sheet lies in the enhancement of mass transfer and progress towards achieving equilibrium partitioning with water. The sampler-water partition coefficients for PFAS were in a desirable range given analytical and practical considerations ($10^{1.5}$–$10^{4.0}$). Sampler equilibration time in water and sediments/soils was less than 1 week in a well-mixed deployment. Sampling was kinetically influenced by interactions with sorbent particles and not limited by diffusion through the gel. We also demonstrated desorption of PFAS, indicating that this sampler is capable of reversible equilibrium measurements. We believe that the initial results presented in this report show great promise for pursuing the concept of equilibrium passive sampling for PFAS compounds. Several of these materials can be produced in thin films with sufficient capacity for PFAS analysis, but this will need additional testing.

Further work is needed to operationalize the passive sampling system explicitly designed to quantify the time-weighted average bioavailable PFAS concentration in a reproducible fashion.

Recommendations for future work to advance the technology development for passive sampling of PFAS are listed below:

1) Extend our passive sampling development work to the full range of 24 PFAS compounds.

2) Several analytical challenges were encountered in our current setup. For a follow up study we would like to involve a DOD ELAP certified lab more closely with our work to enable more accurate measurements, and also address technology transition at an early stage.

3) Test the developed polymers in more complex natural water matrices that include a range of pH, ionic strengths, and DOC concentrations.

4) Develop enriched stable isotope spikes as performance reference compounds in these samplers. This work will also explore the minimum number of PRCs that can be employed to allow accurate determination of extent of equilibrium for the full range of PFAS compounds.

5) Extend testing to natural sediments with a select set of passive samplers. Include measurement of total pore water PFAS and variables needed for equilibrium modeling of PFAS complexation. Measurements in sediments, surface water, and groundwater can also be explored.

6) Explore enabling reproducible measurements of bioavailable PFAS compounds and allowing improved risk assessment and management for PFAS-contaminated sites by accurately measuring C_{free} and estimating biouptake and toxicity using developed functionalized passive samplers.

9.0 Appendices

Appendix #1. Standard Operating Procedures (SOP) for the PFAS Passive Sampler Extraction and LC-MS/MS Analysis of PFAS

1. Summary

Water will be sampled using passive sampling devices. The project is focused on developing passive sampler technology optimized for PFAS analysis ***in situ***. The polymeric membrane prototypes will be tested in amended water samples to determine kinetic and thermodynamic properties. The membranes are solvent extracted using methanol:acetone (1:1) (exact composition to be determined through the research) to recover PFAS sorbed to the membranes. Experiments will be conducted to determine sorption isotherms between water and passive samplers. The passive samplers are solvent extracted, the extracts are reduced in volume to 0.5 mL, and the concentrated extract is filtered and analyzed by LC-MS/MS. Water samples in isotherm experiments are extracted by solid phase extraction and analyzed by LC-MS/MS. Seven PFAS have been selected as model compounds for detailed isotherm characterization, which are shown 2. below.

2. Chemical List

PFAS Targets	Abbrev	CASN
1. Perfluorobutanoic acid*	PFBA	375-22-4
2. Perfluoropentanoic acid	PFPA	2706-90-3
3. Perfluorohexanoic acid	PFHxA	307-24-4
4. Perfluoroheptanoic acid	PFHpA	375-85-9
5. Perfluorooctanoic acid*	PFOA	335-67-1
6. Perfluorononanoic acid	PFNA	375-95-1
7. Perfluorodecanoic acid	PFDA	335-76-2
8. Perfluoroundecanoic acid	PFUdA	2058-94-8
9. Perfluorododecanoic acid	PFDoA	307-55-1
10. Perfluorotridecanoic acid	PFTrDA	72629-94-8
11. Perfluorotetradecanoic acid*	PFTeDA	376-06-7
12. N-methyl perfluorooctanesulfonamidoacetic acid*	NMeFOSSA	2355-31-9
13. N-ethyl perfluorooctanesulfonamidoacetic acid	NEtFOSSA	2991-50-6
14. Perfluorobutane sulfonic acid*	PFBS	375-73-5

15. Perfluoropentane sulfonic acid	PFPeS	2706-91-4
16. Perfluorohexane sulfonic acid	PFHxS	355-46-4
17. Perfluoroheptane sulfonic acid	PFHpS	375-92-8
18. Perfluorooctane sulfonic acid*	PFOS	1763-23-1
19. Perfluorononane sulfonic acid	PFNS	68259-12-1
20. Perfluorodecane sulfonic acid	PFDS	335-77-3
21. Perfluorodecane sulfonamide	PFOSA	754-91-6
22. Sodium 1H,1H,2H,2H-perfluoro-1-hexanesulfonate	FtS 4:2	757124-72-4
23. Sodium 1H,1H,2H,2H-perfluoro-1-octanesulfonate	FtS 6:2	27619-97-2
24. Sodium 1H,1H,2H,2H-perfluoro1-decanesulfonate*	FtS 8:2	39108-34-4

---

3. Instrumentation

3.1. LC-MS/MS

PFAS are quantitively analyzed by LC-MS/MS. The primary analytical instrument is a Shimadzu 8050 tandem mass spectrometer (Shimadzu, Columbia, MD). The instrument is equipped with dual Nexera 20ADXR UHPLC pumps, SIL-20ACXR autosampler (105 vial capacity), and DUIS dual probe set with ESI and corona needle configuration. The instrument was purchased in December 2017 by George Mason University. It is housed at the Potomac Science Center in Woodbridge, VA, a 50,000 sf research facility at GMU. The LC-MS/MS is tuned according to instrument specifications and is performed annually under a currently active preventative maintenance (PM) contract with Shimadzu.

3.2. Data System

The Shimadzu 8050 is equipped with Lab Solutions (ver. 5.91) data system for instrument acquisition (Realtime Analysis) and complete data processing (PostRun and Quant Browser).

4. Reagents

4.1. Methanol and 5 mM Ammonium Acetate as Mobile Phase A

Fisher Optima LC-MS grade methanol (Fisher No A456-500). To prepare, 0.385 g of Ammonium Acetate (Sigma Aldrich No 73954) is dissolved in 1L of LC-MS grade methanol.

4.2. Reagent Water

Milli-Q Type 1 (18.2 MΩ) water (Millipore Sigma, Burlington MA).

4.3. Reagent water and 5 mM Ammonium Acetate Solution as Mobile Phase B

To prepare, 0.385 g of Ammonium Acetate (Sigma Aldrich No 73954) is dissolved in 1L of reagent water.

4.4. Liquid Nitrogen

Liquid nitrogen is the source of the nebulizing and heating gases for the ESI liquid spray interface.

4.5 Ultra High Purity Nitrogen

Ultra-high purity nitrogen is used in the TurboVap evaporator used to concentrate solvent extracts to 0.5 mL.

4.6 Argon

High purity Argon is used as the collision gas in the LC-MS/MS.

5. Supplies

5.1. Autosampler vials

Polypropylene 1 mL vials with polypropylene caps (Agilent No. 5182-0567 and 5182-0542) are used in analysis.

5.2 Plastic pipettes

Low-density polyethylene disposable (Fisher 13-711-7) pipettes are used for sample transfer.

5.3. Syringe filters

13-mm polypropylene syringe filters (0.22 um pore size) are used to filter sample extracts prior to LC-MS/MS analysis (Tisch SF14704).

5.4 Micro syringes

10, 25, 50, 100, 250 and 500 uL glass microsyringes are used in preparing stock and calibration standards for and spiking samples with IS and SS.

5.5 Centrifuge Tubes

50-mL and 15-mL polypropylene centrifuge tubes are used to extract PFAS from the passive samplers.

5.6 Solid Phase Extraction

Supelco Swift HLB (60 mg bed 30 mL barrel) cartridges (Millipore 57492-U).

6. Standard Solutions

All standards used are >96% pure.

6.1. Target Chemical Standards

The 24 target chemicals are purchased from AccuStandard as a pre-made mixture in methanol (New Haven, CT, No. PFC-24). The mix is obtained as a 2 ng/uL solution for each target chemical in methanol and this serves as the stock solution for target chemicals. Salt forms of the targets are corrected to the corresponding acid concentrations using molecular weight ratios (certified concentration x MW acid/MW salt).

6.2. Internal Standards

The internal standards (IS) used include perfluoro-[13C8] octanoic acid (13C8-PFOA), sodium perfluoro-1-[3C8] octanesulfonate (13C8-PFOS), and N-deuteriomethylperfluoro-1-octanesulfonamidoacetic acid (d3-NMeFOSAA). All internal standards are purchased from Wellington Laboratories (Guelph, Ontaria, Ca). The IS are purchased individually as a 50 ng/uL solution and are diluted to 2 ng/uL in methanol and combined to serve as the IS stock solution.

6.3. Surrogate Standards

The surrogate standards used include perfluoro-n-[1,2-13C2]hexanoic acid (13C2-PFHxA), perfluoro-n-[1,2-13C2]decanoic acid (13C2-PFDA) and N-deuterioethylperfluoro-1-octanesulfonamidoacetic acid (d5-NEtFOSAA). The IS are purchased as a 50 ng/uL solution for each individual SS and are diluted to 2 ng/uL in methanol combined to serve as the SS stock solution.

6.4. Calibration Standards

Eight calibration standards are prepared as dilutions of targets, IS and SS combined in methanol (with 4% reagent water) at concentrations ranging from 0.2 to 0.004 ng/uL

(subject to modification) according to the particular experiment. Internal standards are present at a constant concentration of 0.08 ng/uL.

7. Procedures

7.1. Passive Sampler Membrane Extraction

The passive membrane samples are first spiked with 100 uL of SS (equivalent to 100 ng of SS per tube) 100 uL of each IS (equivalent to 80 ng of each IS) in 15 mL PP centrifuge tubes. The tested passive sampler is then extracted with 10 mL X 3 volumes of the appropriate solvent. The combined 3X extracts are transferred to 40 mL glass evaporation vials using plastic pipettes for solvent evaporation to final volume 0.5 mL. Following evaporation, the extracts are filtered through syringe filters into 1 mL PP LC-MS/MS vials.

7.2. Water preparation

Individual water samples (100 mL) from isotherm experiments are placed in 125 mL PP bottles and spiked with 100 μL of each SS (equivalent to 100 ng of each SS per vial) and 100 μL of each IS (equivalent to 80 ng of each IS). The water samples are extracted with Supelco Swift HLB (60 mg bed 30 mL barrel) cartridges (Millipore 57492-U). The cartridges are initially conditioned sequentially with 4 mL of 0.3% NH_4OH, 4 mL MeOH, and 4 mL of water. The 100 mL sample is extracted at 4 mL/min. The cartridge is rinsed with 2 x 4 mL of water and eluted with 2 x 0.50 mL of 0.3% NH_4OH in MeOH directly into the PP autosampler vials. The eluents are passed through a 0.2 μm (pore dia.) 13 mm dia. PP syringe filter (Tisch SF14704) during elution into the autosampler vials.

7.3. Solvent Evaporation

The solvent from step 7.1. is concentrated under a vortex stream of nitrogen gas to a final volume of 0.5 mL in a TurboVap concentrator.

7.4. Syringe filtration

The membrane extracts and the water samples diluted in methanol are filtered using 0.2 um PP syringe filters into LC-MS/MS autosampler vials. A 10 mL glass syringe is used to hold the sample during filtration. The syringe and filter are pre-rinsed with 2 x 5 mL of methanol prior to sample filtration.

7.5. Sample Analysis

Samples are analyzed using the analytical column and the following conditions shown in Table 1. A sample chromatogram is provided in Figure 1.

7.6. Analytical Column

The UHPLC analytical column used is a Supelco Titan C18 column (2.1 mm x 100 mm) packed with 1.9 μm d_p stationary phase particles (Millipore Sigma 577124-U).

7.7. MRM Transitions and Voltages

The LC-MS/MS is used in the MRM analysis mode. Product and precursor ions are optimized for each of the target chemicals and IS/SS standards using Lab Solutions optimization protocols. Precursor and corresponding product ions are established for the PFAS according to instrument optimization specifications via infusion experiments. A resulting MRM method is constructed culminating in one primary MRM ion (quantitation ion) and two MRM confirmation ions used in sample quantitation. Each of the confirmatory ions has and established relative abundance to the primary ion used for chemical confirmation. Following MRM optimization, the MRM method is used with a mid-range PFAS calibration standard to establish compound retention times and to check optimal peak performance. MRM evaluation is repeated until all PFAS compounds are accounted for in the method. We currently have an active PFAS MRM method at GMU that incorporates 24 of the target chemicals listed in Part 2 above. Upon initiation of this project, the 3 missing PFAS target chemicals will be added to the MRM method.

7.8. Calibration

Calibration is performed using the internal injection standard (IS) method. The list of IS is provided in Section 6.2. Three isotopically labelled IS compounds will be used that correspond the range of functional groups encountered in the PFAS mixture. A set of 8-standards are used for instrument quantitation, of which one standard is below the detection limit (DL) of the method. All calibration curves are forced through the origin as specified in EPA 537. Internal standards are checked for target suppression by evaluating the RDP, which must be <20%. Calibration acceptance criteria include the following: (i) RPD <20% for all IS, (ii) each target chemical should calculate between 70-130% of the true value (accuracy) at all dilutions, (iii) except the lowest CAL point should calculate to within 50-150% of the true value. If these criteria are not met, the instrument must be

recalibrated. Failure to meet these criteria in recalibration will result in remediation of the problem through preventative maintenance (PM) procedures such as source cleaning, UHPLC column evaluation and other steps outlined in the 8050 troubleshooting guidelines.

7.9 Retention Time Window Establishment

The position will be set using the midpoint standard of the calibration curve. The windows will be established at the beginning of the analytical sequence. On days when full calibration is not performed, the initial CCV is used.

8. Quality Checks

8.1 Mass Spectral Acquisition Rate

A minimum of 10 spectral scans are established for each target, IS and SS. Loop times are established for the minimum peak width to allow a minimum of 20 scans per peak.

8.2 Sample PFAS Identification

PFAS Target chemical identifications include a primary MRM quantitation ion and at least one secondary MRM confirmation ion. The ion ratios between primary and secondary ions will not exceed 50-150% of the established ratios for positive identifications. The ion ratios will be established through the calibration procedure. The MRM ions for PFAS analysis are provided in Table 4.

8.3 Sample Quantitation

The signal to noise ratio will be ≥10 for all ions used for quantitation. The quant ion and confirmation ions will maximize simultaneously (± 2s). Any PFAS not meeting these criteria will be flagged as biased high.

8.4. Initial Calibration Checks

Linear calibration will be checked for r^2 values ≥ 0.98 for each target. Any PFAS not meeting this criterion will be flagged.

8.5. Retention Time Windows

The RT of each target and SS must fall within ± 0.5 min of the established RTs in the most recent calibration. This will apply to every sample, standard, blank and QA sample.

8.6. Initial Calibration Verification

Target concentrations must be within 7 to 130% of the true expected values in the current calibration. This is performed after each calibration using a mid-range standard prior to sample analysis.

8.7. Continuing Calibration Verification

Continuing calibration checks (CCVs) are performed prior to sample analysis, following the injection of each batch of 10 samples, and at the end of the analytical sequence. The CCV consists of a mid-range calibration standard placed in a separate vial from the original calibration solutions. The CCV vial is quantitated as a sample and IS peaks are checked relative to the initial calibration solutions. The absolute areas of the IS peaks must be 50-150% of those in the previous (n-1) CCV injection or within 50-150% of the average areas of the initial calibration for that group of samples. Failure of the CCV criterion will require reanalysis of the samples that follow it.

8.8. Instrument Blanks

Blank samples assess the cleanliness of the analysis and the contributions of interfering substances or peaks potentially biasing the results. Instrument blanks are evaluated through the injection (5 μL) of 50/50 mobile phase in an LC-MS/MS vial. The concentration of each target must be ≤ ½ of the LOQ. Instrument blanks will be determined with each batch of samples.

8.9. Method Blank

Sample matrix blank is analyzed for the target chemicals. No targets detected at >one-half LOQ or >1/10th the amount measured in any sample will be accepted, whichever value is greater.

8.10. Surrogate Standards

Surrogate standards are amended to each sample to gauge the performance of individual analyses. In this study, SS will be added to passive sampler extraction solutions at the initial point of analysis. Percent recovery of the SS will be determined as %R = (A/B) x 100, where A is the quantitated SS and B is the amended SS quantity. Surrogate recoveries in the range of 50-150% will pass the method performance criterion for SS. If a sample fails the SS criterion, it will be reanalyzed. Any sample data where SS does not meet the above criterion will be flagged for that particular sample.

8.11. Laboratory Matrix Spike

Sample matrix is spiked with all 24 target chemicals at the mid-calibration concentration and recoveries are determined. A duplicate is performed for each preparatory batch.

8.12. Detection limits

Detection (DL) and quantitation limits (QL) are determined for each PFAS target using the LabSolutions (v. 5.91) software provided with the 8050 LC-MS/MS. DL and QL are based on a signal-to-noise (S/N) ratio of 3 for DL and 10 for QL. Only quantified concentrations greater than the QL will be reported as a number value. Any detection below the DL is recorded as 0.00 and any result between DL and QL is reported as <QL.

Table A1-1. LC Method Conditions

Time	% 5 mM Ammonium Acetate in Methanol
Initial	10
0.1	10
3.0	30
9.0	70
9.5	95
10	95
10.1	10
13.1	10

Table A1-2. ESI-MS Conditions

Interface type	ESI-negative
Interface Voltage	3 kV
Nebulizing gas	N_2, 2.0 L/min
Heating gas	N_2, 10 L/min
Drying gas	N_2, 10 L/min
CID gas	Ar
Interface temperature	300 °C

Table A1-3. Target Retention Time and Internal Standard Assignments

No.[a]	Name	IS Group	RT (min)
1	PFBA	1	2.40
2	PFPeA	1	3.68
3	PFBS	2	3.92
4	4-2 FTS	2	4.50
5	13C2 PFHxA (SS)	1	4.56
6	PFHxA	1	4.56
7	PFPeS	2	4.64
8	PFHpA	1	4.98
9	PFHxS	2	4.99
10	6-2 FTS	2	5.27
11	13C8 PFOA (IS-1)		5.30
12	PFOA	1	5.30
13	PFHpS	2	5.31
14	13C8 PFOS (IS-2)		5.48
15	PFOS	2	5.50
16	PFNA	2	5.62
17	PFNS	1	5.64
18	13C2 PFDA (SS)	1	5.96
19	PFDA	1	5.96
20	8-2 FTS	2	5.96
21	N-MeFOSAA	3	6.14
22	d3-NMeFOSAA (IS-3)		6.14
23	PFDS	2	6.29
24	PFUnA	1	6.32
25	d5-N-ETFOSAA (SS)	3	6.32
26	NEtFOSAA	2	6.33
27	PFOSA	3	6.43
28	PFDoA	1	6.81

29	PFTriA	1	7.63
30	PFTreA	1	8.53

[a]Peaks assignments in Figure A1.

Table A1-4. MRM Parameters

Name	PreC	MRM 1	MRM 2	Q1	CE	Q3
PFBA	213	169		12	9	18
PFPeA	263	219		14	9	15
PFBS	299	80	99	16	38	24
4-2 FTS	327	307	81	18	19	15
13C2 PFHxA (SS)	315	270	119	22	9	13
PFHxA	313	269	119	17	9	19
PFPeS	349	80	99	18	38	26
PFHpA	363	319	169	11	10	23
PFHxS	399	80	99	21	39	11
6-2 FTS	427	407	81	13	23	15
13C8 PFOA (IS-1)	421	376	421	23	10	19
PFOA	413	369	169	22	9	18
PFHpS	449	80	99	23	45	25
PFOS	499	80	99	19	55	10
PFNA	463	419	219	14	10	15
PFNS	549	80	99	28	53	23
13C8 PFOS (IS-2)	507	80	99	26	50	11
13C2 PFDA (SS)	515	470	220	20	11	17
PFDA	513	469	169	28	9	24
8-2 FTS	527	507	81	28	25	26
N-MeFOSAA	570	419	219	30	20	20
d3-NMeFOSAA (IS-3)	573	419	483	22	20	21
PFDS	599	99	80	32	46	10
PFUnA	563	519	269	30	11	28

d5-N-ETFOSAA (SS)	589	419	531	22	20	21
NEtFOSAA	584	419	526	32	19	15
PFOSA	498	78	169	15	36	11
PFDoA	613	569	319	22	12	22
PFTriA	663	619	169	24	12	24
PFtreA	713	669	169	38	14	26

[a]Precursor ion (m/z)

[b] Primary daughter ion (m/z)

[c]Secondary daughter ion (m/z)

[d]Q1 pre bias (V)

[e]Collision energy (V)

[f]Q3 pre bias (V)

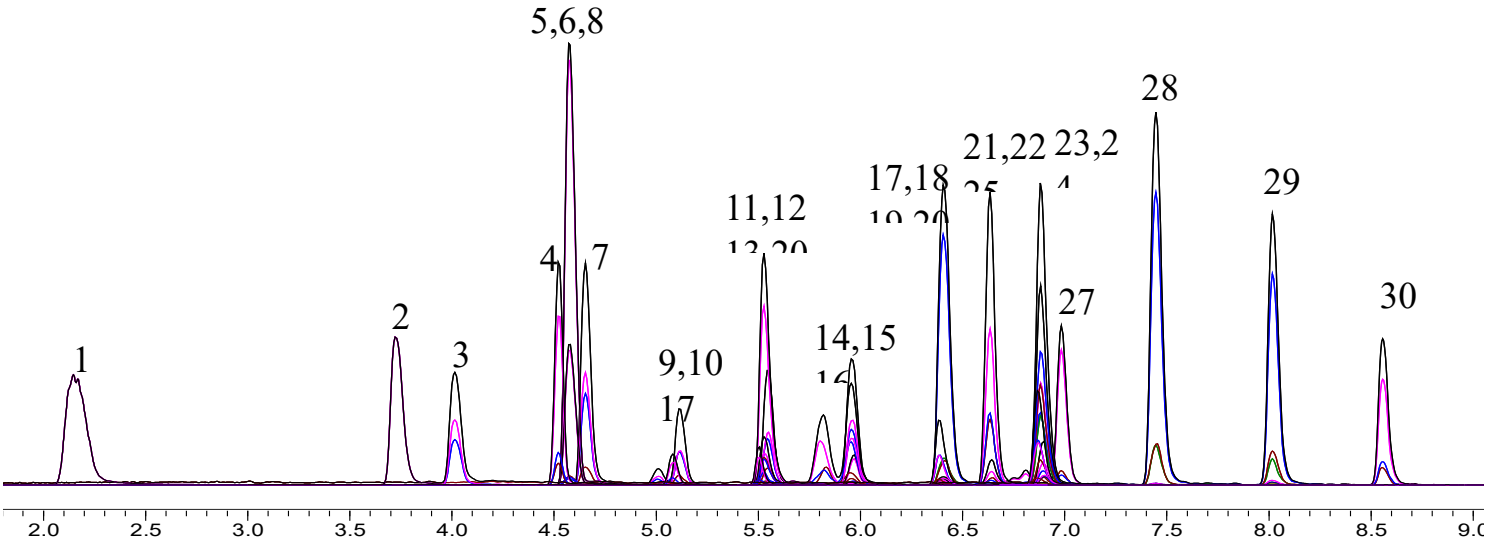

Figure A1. Sample LC-MS/MS chromatogram (ntensity vs. retention time, min) of PFAS targets and standards. Refer to Table 3 for peak assignments.

Appendix #2. Analytical Confirmation White Paper

ER20-C2-1336

Development of novel functionalized polymeric thin films for equilibrium passive sampling of PFAS compounds in surface and groundwater

Greg Foster and Batool Murtadha, Department of Chemistry and Biochemistry and Potomac Environmental Research and Education Center, Potomac Science Center, Woodbridge, VA 22191

Upal Ghosh (PI) and Songjing Yan, Department of Chemical, Biochemical and Environmental Engineering, University of Maryland Baltimore County, Baltimore, MD 21250

1. Study Introduction

The present SERDP project is focused on developing passive sampler technology optimized for PFAS analysis in situ. Several types of passive sampling devices are being tested as a pilot study. Water is amended with seven selected PFAS model compounds to determine kinetic and thermodynamic properties important in passive sampling. The pilot study experiments are being conducted to determine sorption isotherms between water and passive samplers. Water samples in isotherm experiments are extracted by solid phase extraction and analyzed for the 7 model PFAS by LC-MS/MS. As an analytical confirmation, George Mason University (GMU) submitted a 500 mL sample of spiked Milli-Q water to Clarkson University for analysis of the 7 per- and polyfluoroalkyl substances (PFAS). Another 500 mL spiked sample was prepared for analysis at GMU. The Clarkson 500 mL spiked sample was submitted for the purpose of analytical confirmation as required for PFAS projects within the Strategic Environmental research and Development (SERDP) program. Samples must be analyzed by a Department of Defense (DoD) Environmental Laboratory Accreditation Program (ELAP)- accredited laboratory at Clarkson University (CAARES Laboratory) on 10 June 2021.

2. GMU Sample Preparation and Analysis

Spiked samples were prepared in 500 mL polypropylene bottles containing 500 mL of Milli-Q water (MQW). The PFAS spike was prepared from a PFAS stock standard obtained from AccuStandard (catalog number PFC-24-10X) at a concentration of 20 □g/mL (certified concentrations for ea PFAS were included with the standard). The stock standard (1.00 mL) in a 1 mL ampule was diluted to 25.000 mL with methanol (LC-MS grade, Fisher Scientific) in a volumetric flask yielding a concentration of 0.8 □g/mL for the spike standard. The spike standard (800 □L) was delivered to 500 mL MQW in each 500 mL PP bottle, yielding a nominal concentration of 1.28 □g/L. The spike concentrations of the 7 PFAS are shown in Table 1. GMU analyzed the PFAS samples on the day following the spike preparation. Triplicate 100 mL samples (SOP) were extracted using Supel-Swift HLB preconditioned cartridges (60 mg sorbent contained in a 3 mL cartridge, Millipore Sigma) using a Supelco SPE vacuum manifold (15 torr) at a rate of 1-2 drops per second. Prior to extaction, each 100 mL water sample was spiked with isotopically labeled internal standards (IS, Cambridge Isotopes), including 13C8-PFOA (6.00 ng), 13C8-PFOS (2.00 ng) and d3-NMeFOSSA (8.00 ng) and surrogate standards (SS, Cambridge Isotopes), including 13C2-PFHxA, 13C2-PFDA, and d5-NEtFOSSA (10.0 ng each) to evaluate matrix effects, analytical variability, and analyte losses sample analysis. Following extraction, the cartridges were vacuum aspirated for 30 min at 15 torr. The HLB cartridge was eluted with 1X 0.700 mL of methanol (LC-MS grade) directly into a PP autosampler vial using a 5 mL glass syringe. The methanol was allowed to soak the HLB cartridge for 30 min prior to evacuation of the syringe. The HLB cartridge was connected via a Leuer adapter to a 13 mm (dia) PP syringe filter (0.22 □m pore size; Tisch Scientific) for the complete removal of particles. The LCMS vials were vortexed for 2 min prior to loading into the LCMS sample tray. PFAS analysis was performed using a Shimadzu 8050 liquid chromatograph-triple quadrupole-mass spectrometer (LC-MS/MS, Columbia, MD). The LC-MS/MS was operated with a DUIS interface (i.e., combined ESI-APCI) at a mass spec scan rate of 30,000 scans per second using Lab Solutions (ver. 5.91) software. The LC-MS/MS was used in the multiple reaction monitoring (MRM) acquisition mode. All seven PFAS were optimized for MRM ions using pure (>97%) individual analytical standards (Wellington Laboratories). The precursor and MRM ions selected corresponded to those reported in Table B-15 of QSM 5.3. MRM ions included a primary quantitation and two qualifier ions. The LC-MS/MS was fitted with a Supelco 10 cm x 2.1 mm (dia) Titan C18 (1.9 □m porous particle dia.) UHPLC analytical column (Millipore Sigma). A

Restek PFAS delay column (5 cm x 2.1 mm (dia), Restek) was installed between mobile phase mixer and sample injector to minimize background contamination from the LC system. LC-MS/MS calibration was performed using six analytical standards containing the seven target PFAS ranging from 2.7 to 115 ng/0.7 mL (full PP LCMS vial) along with the three IS spiked into the samples. Quality assurance samples included solvent blanks, method blanks, calibration accuracy checks, S/N checks, and detection/quantitation limit determinations. SS recoveries were used to evaluate matrix effects, analytical variability, and analyte losses during preparation. The aqueous phase consisted of 5 mM ammonium acetate (pH 6.8) in MQW (mobile phase A), and the organic phase was methanol with 5 mM ammonium acetate (mobile phase B). The mobile phase flow rate was 0.400 mL/min and the sample injection volume was 2 µL. The mobile phase gradient conditions for the separations and the DUIS-MS settings are shown in Table 2.

3. Analytical Confirmation Results

The GMU LC-MS/MS calibration results are summarized in Table 3. The R2 and %accuracy parameters met SOP specifications (0.99) except for the R2 for NMeFOSSA, which was 0.987 (and is rounded to 0.99). The GMU measured values of the 7 PFAS are shown in Table 4, and the range was 1.14 □g/L (PFBA) to 0.82 □g/L (PFOA). In Table 4 is also a comparison metric between the GMU and certified (cert) Clarkson-ELAP measurement results (% D = difference = (Ccert - Cgmu)/Ccert x 100), and the %D ranged from 3% to 38% (PFOA). The average %D was 19. The GMU values were lower than the Clarkson U-ELAP values, which is not surprising because GMU uses a solid phase extraction step versus the Clarkson U direction injection method. The GMU quantitation of recoveries were not surrogate corrected. The surrogate standard recovery values are shown in Fig. 1.

4. Conclusion

Guidelines outlined by the SERDP program specify that GMU's results should ideally be within 30% of the ELAP-accredited laboratory. There was only one case where an exceedance was

observed in the case of PFOA (%D = 38%). To address this difference, GMU is working to correct the problem as follows: 1) 200 mg HLB cartridges will be used in place of 60 mg cartridges and 2) 4 mL of MeOH will be used to elute the HLB sorbent vs. the current 0.7 mL. We believe this will enhance the performance of PFOA in water analysis.

Table A2-1. Nominal spike concentrations (μg/L) of the 7 target PFAS.

Perfluorobutanoic acid (PFBA)	1.25
Perfluorooctanoic acid (PFOA)	1.29
Perfluorotetradecanoic acid (PTreA)	1.30
N-Methylperfluorooctanesulfonamidoacetic acid (NMeFOSSA)	1.28
Perfluorobutanesulfonate (PFBS)	1.14
Perfluorooctanesulfonate (PFOS)	1.20
1H,1H,2H,2H-perfluorodecanesulfonate (FtS 8:2)	1.24

Table A2-2. LC and MS Operating Conditions

LC Gradient Conditions	
Time	**%5 mM Ammonium Acetate in Methanol**
Initial	10
0.1	10
3.0	30
9.0	70
9.5	95
10	95
10.1	10
13.1	10
MS Conditions	
Interface type	DUIS-negative
Interface Voltage	3 kV
Nebulizing gas	N_2, 2.0 L/min
Heating gas	N_2, 10 L/min
Drying gas	N_2, 10 L/min
CID gas	Ar
Interface temperature	300 °C

Table A2-3. GMU LC-MS/MS Calibration Parameters for the 7 target PFAS in Lab Comparison.

PFAS	Cal R^2	%Accuracy	QL (ng/L)
PFBA	0.994	80-100	2.4
PFBS	0.998	98-130	7.1
FtS 8:2	0.990	93-110	2.0
PFOA	0.994	96-118	1.4
PFOS	0.993	90-128	2.7
NMeFOSSA	0.987	96-124	1.5
PFTreA	0.998	82-102	3.1

Table A2-4. Summary of Laboratory Comparison Between GMU and Clarkson University.

	PFBA	PFBS	FtS 8:2	PFOA	PFOS	NMeFOSSA	PFTreA
Unit	ug/L	ug/L	ug/L	ug/L	ug/L	ug/L	ug/L
GMU-Rep 1	1.06	1.19	0.901	0.776	0.986	1.04	0.852
GMU-Rep 2	1.38	1.02	0.846	0.839	1.08	0.937	0.902
GMU-Rep 3	0.985	1.12	1.02	0.857	0.999	0.73	1.18
mean	1.14	1.11	0.92	0.82	1.02	0.90	0.98
SD	0.21	0.085	0.089	0.043	0.051	0.16	0.18
%RSD	18%	8%	10%	5%	5%	17%	18%
Clarkson	1.36	1.41	0.98	1.33	0.99	1.19	0.80
% Dif vs GMU	16%	21%	6%	38%	3%	24%	22%

Table A2-5. Summary of Clarkson University Results for The Analysis of The Shared Spiked Sample.

Quantitation Report Summary

Lab Name: CAARES Laboratory
Instrument: Thermo Scientific Instrument
User: Administrator
Batch: G_Foster_ILC_20210616

Method: G_Foster_ILC_20210616_20200624_DoD_ELAP 20200624_DoD_ELAP
Cali File: G_Foster_ILC_20210616.calx

Vial Pos	Sample ID	File Name	Level	Sample Name	File Date	Comment
Y:C7	Interlaboratory Comparison Sam	CU21_0069_1_A	N/A	Interlaboratory Comparison Sample	6/16/2021 4:06:40 PM	

			Concentration (ug/L)				
Target Compounds	RT	Manual Flag	Calculated Conc_1	Calculated Conc_2	Calculated Conc_3	Average	RSD
4:2 FTS	0.95		1.04	1.02	1.05	1.04	1.5
6:2 FTS	2.06		1.19	1.09	1.01	1.10	8.2
8:2 FTS	2.46		0.88	1.01	1.05	0.98	9.2
EtFOSAA	2.67		1.23	0.96	1.15	1.11	12.2
FOSA-1	3.13	M	0.82	0.81	0.76	0.79	4.3
MeFOSAA	2.58		1.31	1.05	1.22	1.19	11.0
PFBA	0.66		1.38	1.33	1.36	1.36	2.0
PFBS	1.32		1.41	1.36	1.47	1.41	3.7
PFDA	2.56		1.42	1.47	1.44	1.44	1.8
PFDoA	2.86		2.65	2.76	2.62	2.67	2.8
PFDS	2.92		1.52	1.27	1.14	1.31	14.8
PFHpA	1.85		1.42	1.46	1.47	1.45	1.9
PFHpS	2.46		1.24	1.16	1.14	1.18	4.3
PFHxA	1.18		1.46	1.40	1.38	1.41	3.0
PFHxS Branched	2.21		0.26	0.25	0.19	0.23	16.9
PFHxS Linear	2.27		1.27	1.38	1.16	1.27	8.5
PFNA	2.39		1.52	1.51	1.53	1.52	0.4
PFNS	2.77		0.85	0.84	0.83	0.84	1.3
PFOA	2.19		1.33	1.30	1.35	1.33	1.9
PFOS Branched	2.57		0.42	0.36	0.39	0.39	7.4
PFOS Linear	2.62		1.10	0.81	1.06	0.99	15.8
PFPeA	0.8		1.49	1.42	1.49	1.47	2.8
PFPeS	1.58		1.49	1.49	1.45	1.48	1.6
PFTeDA	3.16		0.68	0.69	0.73	0.70	4.1
PFTrDA	3.01		0.78	0.94	0.69	0.80	16.2
PFUnDA	2.71		1.24	1.24	1.30	1.26	2.6

Figure A2-1. Summary of Mean Surrogate Recoveries □ 1 Standard Deviation (N = 3).

(1 = 13C2-PFHxA; 2 = 13C2-PFDA; 3 = d5-EtMEFOSSA)

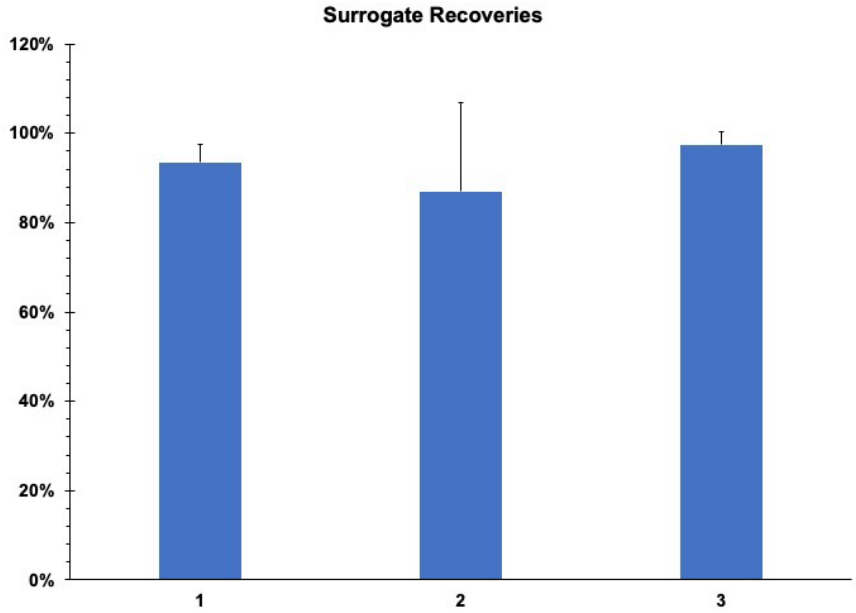

Appendix #3. QA/QC Documentation

QA/QC procedures are designed to assess the cleanliness, repeatability, performance and uncertainties of the method.

Blanks: blank samples assess the cleanliness of the analysis and the contributions of interfering substances or peaks potentially biasing the results. Blanks include instrument blanks (IB) and method blanks (MB). Instrument blanks are evaluated through the injection (5 □L) of 50/50 mobile phase in an LC-MS/MS vial. The purpose of the IB is to evaluate any background interference contributed by the instrument (including the LC-MS/MS vials) itself. The MB is used to assess any interfering substances or peaks introduced from the PIM analysis. In this case PIM membranes undergoing development at the testing site and are not exposed to PFAS mixtures are subject to quantitative analysis. IB and MB samples will be included with every set of new experiments (i.e., when a novel PIM membrane is evaluated for performance).

If target PFAS are detected in the IB samples, every effort will be made to remove those interferences in the analysis. Remedial action will include bypassing the solvent degasser in the LC-MS/MS instrument, replacing Teflon inlet lines with PEEK tubing, and adding and in-line precolumn to filter out the PFAS substances being contributed. Other remedial action is provided through EPA method 537. Any remaining PFAS detected in the blanks will be subtracted from the quantities measured in the samples if the measured concentrations are above threshold. If any PFAS are present in samples at concentration which is quantitated below a blank threshold of (blank + 3sd) will be flagged in the dataset.

Surrogate recoveries: SS are amended to each sample to gauge the performance of individual analyses. In this study, SS will be added to PIM extraction solutions at the initial point of analysis. Percent recovery of the SS will be determined as %R = (A/B) x 100, where A is the quantitated SS and B is the amended SS quantity. Surrogate recoveries in the range of 70-130% will pass the method performance criterion for SS. If a sample fails the SS criterion, it will be reanalyzed. Any sample data where SS does not meet the above criterion will be flagged for that particular sample.

Matrix spikes: A matrix spike is sample where a polymer membrane not previously exposed to PFAS is extracted in a fashion where the entire suite of 24 PFAS target chemicals + SS is amended to the sample. This sample is processed and quantitated as a MSpk sample. Matrix

spikes will be assessed as four replicates (n=4) at two concentrations (high and low). MSpk samples are evaluated in terms of the accuracy (%R) and precision (%RSD) of the result.

Continuing calibration checks (CCCs): CCCs are performed following the injection of each batch of 15 samples. The CCC consists of a mid-range calibration standard placed in a separate vial from the original calibration solutions. The CCC vial is quantitated as a sample and IS peaks are checked relative to the initial calibration solutions. The absolute areas of the IS peaks must be 70-140% of those in the previous (n-1) CCC injection or within 50-150% of the average areas of the initial calibration for that group of samples. Failure of the CCC criterion will require reanalysis of the samples that follow it. If failure of the samples occurs again, PM of the instrument is required.

Detection limits: Detection (DL) and quantitation limits (QL) are determined for each PFAS target using the LabSolutions (v. 5.91) software provided with the 8050 LC-MS/MS. DL and QL are based on a signal-to-noise (S/N) ratio of 3 for DL and 10 for QL. Only quantified concentrations greater than the QL will be reported as a number value. Any detection below the DL is recorded as 0.00 and any result between DL and QL is reported as <QL.

MRM verification: To verify the detection of a PFAS target chemical, MRM verification must be established. MRM verification is performed according to the sratio the second and third MRM ion abundances relative to MRM 1 (the quantitation ion). MRM ratios must fall within 3 sd of the values established during calibration. Any quantitation result not meeting the MRM verification that is above the QL value will be flagged. This step is performed automatically by the LabSolutions v. 5.91 software.

Table 3. Certified Concentrations of Target PFAS Compound Stock Solutions

PFAS	CAS	Certified Conc (ng/mL)
Perfluoro-n-hexanoic acid	307-24-4	2025.000
Perfluoro-n-heptanoic acid	375-85-9	1980.000
Perfluoro-n-octanoic acid	335-67-1	2016.000
Perfluoro-n-nonanoic acid	375-95-1	2006.000
Perfluoro-n-decanoic acid	335-76-2	1968.000
Perfluoro-n-undecanoic acid	2058-94-8	1999.000
Perfluoro-n-dodecanoic acid	307-55-1	1018.000

Perfluoro-n-tridecanoic acid	72629-94-8	2016.000
Perfluoro-n-tetradecanoic acid	376-06-7	2025.000
N-Methylperfluorooctanesulfonamidoacetic acid (Linear and branched)	2355-31-9	2000.000
N-Ethylperfluorooctanesulfonamidoacetic acid (Linear and branched)	2991-50-6	2016.000
Perfluoro-n-butanoic acid	375-22-4	19.600
Perfluoro-n-pentanoic acid	2706-90-3	20.140
Potassium perfluoro-1-butanesulfonate	29420-49-3	2001.000
Sodium perfluoro-1-pentanesulfonate	N/A	2019.000
Potassium perfluoro-1-hexanesulfonate	3871-99-6	2004.000
Sodium perfluoro-1-heptanesulfonate	N/A	2018.000
Potassium perfluoro-1-octanesulfonate	2795-39-3	2004.000
Sodium perfluoro-1-nonanesulfonate	98789-57-2	2001.000
Sodium perfluoro-1-decanesulfonate	2806-15-7	2007.000
Sodium 1H,1H,2H,2H-perfluoro-1-hexanesulfonate	N/A	2030.000
Sodium 1H,1H,2H,2H-perfluoro-1-octanesulfonate	N/A	2008.000
Sodium 1H,1H,2H,2H-perfluoro1-decanesulfonate	N/A	2016.000
Perfluorooctane sulfonamide	754-91-6	2043.000

Additional figures

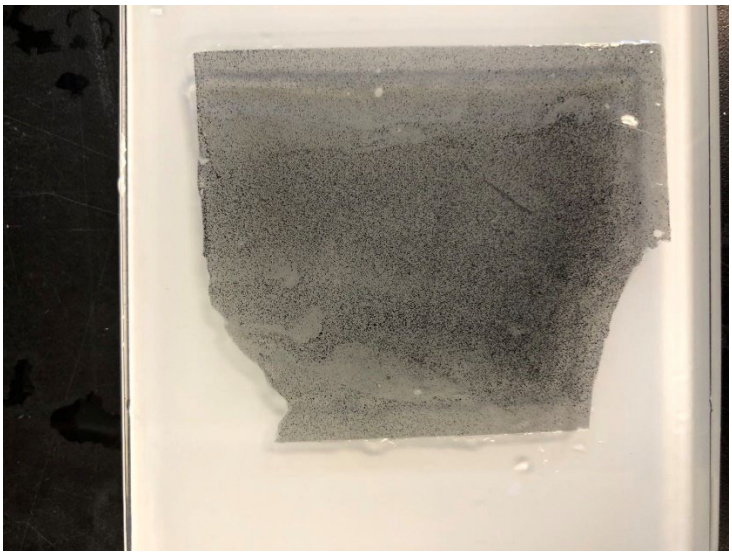

Figure A2. Lab syntheses activated carbon embedded agarose films with a thickness of 284 μm.

In our first and batch of single point isotherm study, the extracted concentrations from passive samplers were too little compared with the water concentration, and the mass balance results was not within criteria.

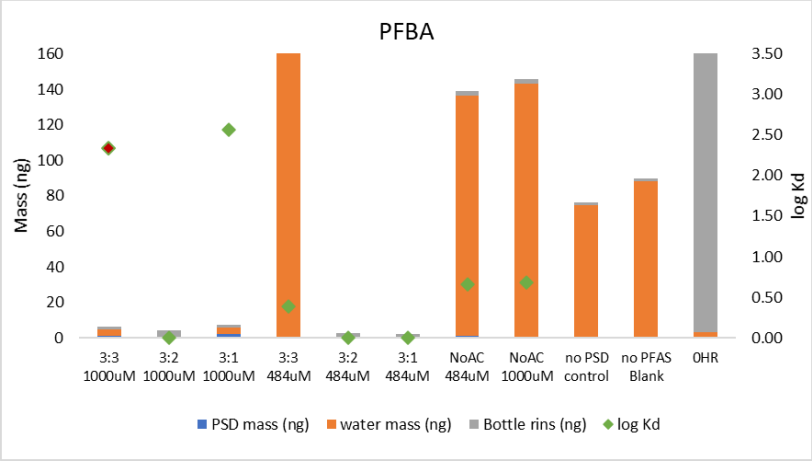
PFBA
Mass (ng)
log Kd
160
140
120
100
80
60
40
20
0
3.50
3.00
2.50
2.00
1.50
1.00
0.50
0.00
3:3 1000uM
3:2 1000uM
3:1 1000uM
3:3 484uM
3:2 484uM
3:1 484uM
NoAC 484uM
NoAC 1000uM
no PSD control
no PFAS Blank
0HR
PSD mass (ng)
water mass (ng)
Bottle rins (ng)
log Kd

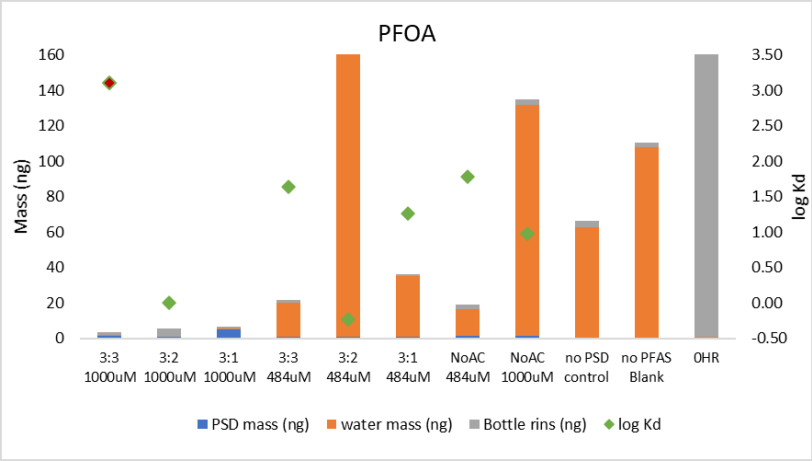
PFOA
Mass (ng)
log Kd
160
140
120
100
80
60
40
20
0
3.50
3.00
2.50
2.00
1.50
1.00
0.50
0.00
-0.50
3:3 1000uM
3:2 1000uM
3:1 1000uM
3:3 484uM
3:2 484uM
3:1 484uM
NoAC 484uM
NoAC 1000uM
no PSD control
no PFAS Blank
0HR
PSD mass (ng)
water mass (ng)
Bottle rins (ng)
log Kd

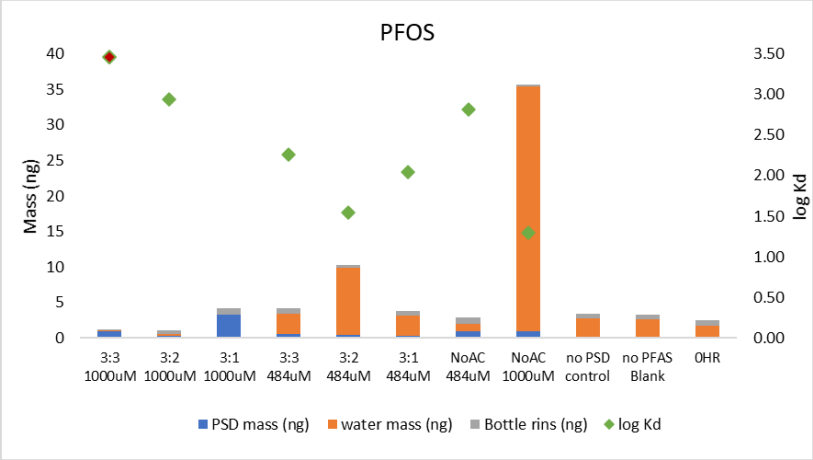
PFOS
Mass (ng)
log Kd
40
35
30
25
20
15
10
5
0
3.50
3.00
2.50
2.00
1.50
1.00
0.50
0.00
3:3 1000uM
3:2 1000uM
3:1 1000uM
3:3 484uM
3:2 484uM
3:1 484uM
NoAC 484uM
NoAC 1000uM
no PSD control
no PFAS Blank
0HR
PSD mass (ng)
water mass (ng)
Bottle rins (ng)
log Kd

Figure A3. The mass balances and K_d values from the first batch of single point isotherm study for PFBA, PFOA, PFOS, FtS 8:2, NMeFOSSA, and PFTreA.

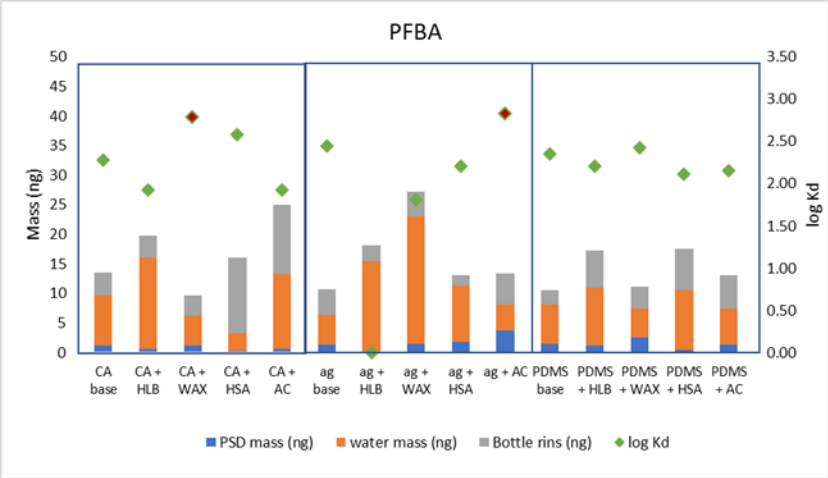
PFBA
Mass (ng)
log Kd
CA base
CA + HLB
CA + WAX
CA + HSA
CA + AC
ag base
ag + HLB
ag + WAX
ag + HSA
ag + AC
PDMS base
PDMS + HLB
PDMS + WAX
PDMS + HSA
PDMS + AC
PSD mass (ng)
water mass (ng)
Bottle rins (ng)
log Kd

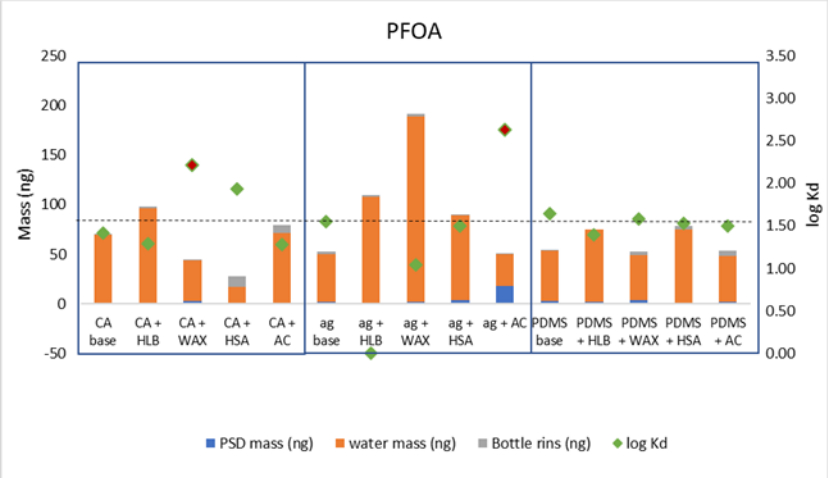
PFOA
Mass (ng)
log Kd
CA base
CA + HLB
CA + WAX
CA + HSA
CA + AC
ag base
ag + HLB
ag + WAX
ag + HSA
ag + AC
PDMS base
PDMS + HLB
PDMS + WAX
PDMS + HSA
PDMS + AC
PSD mass (ng)
water mass (ng)
Bottle rins (ng)
log Kd

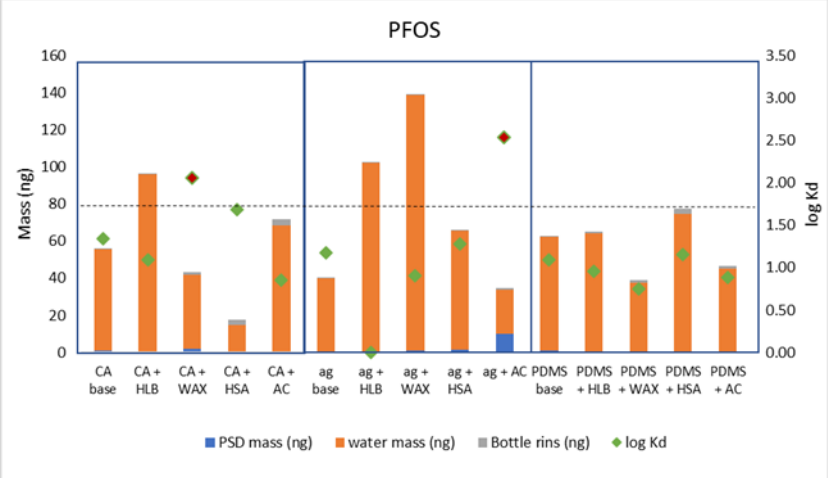
PFOS
Mass (ng)
log Kd
CA base
CA + HLB
CA + WAX
CA + HSA
CA + AC
ag base
ag + HLB
ag + WAX
ag + HSA
ag + AC
PDMS base
PDMS + HLB
PDMS + WAX
PDMS + HSA
PDMS + AC
PSD mass (ng)
water mass (ng)
Bottle rins (ng)
log Kd

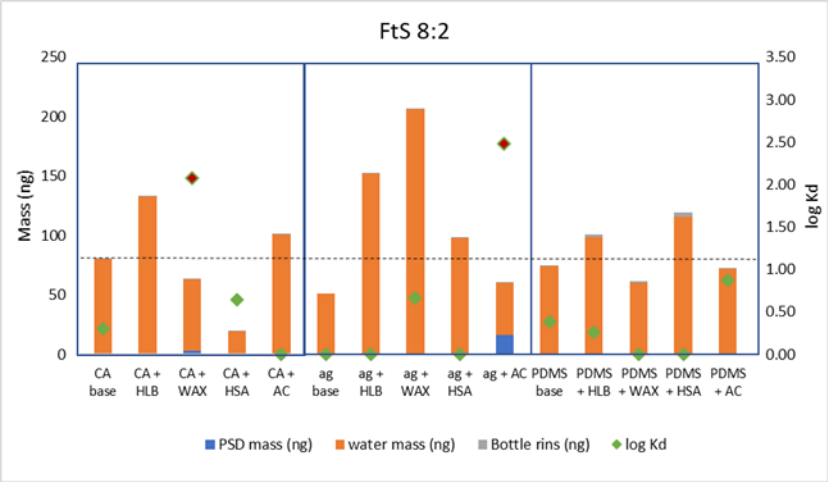

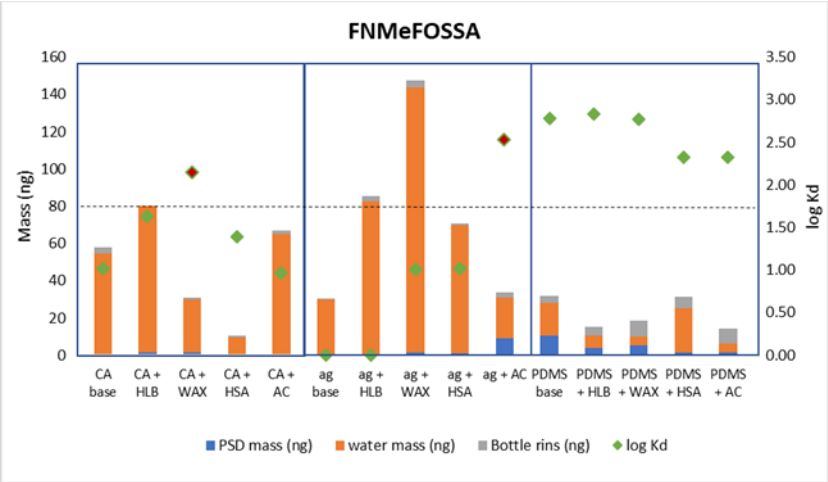

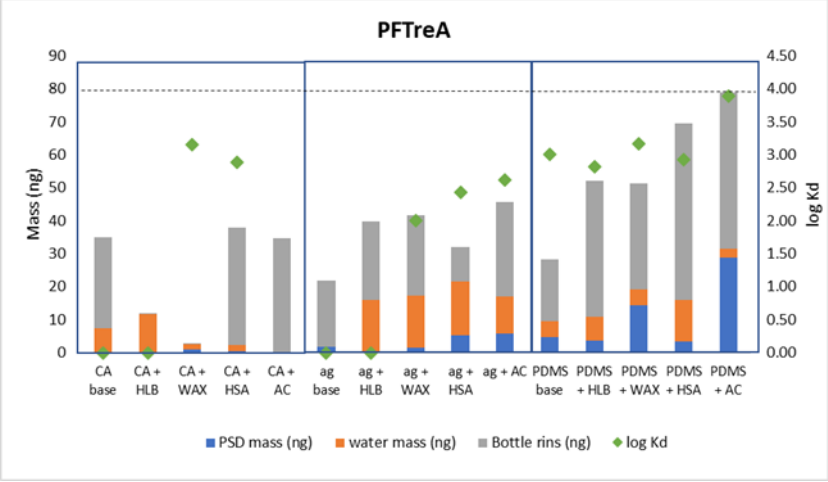

Figure A4. The mass balances and K_d values from the second batch of single point isotherm study for PFBA, PFOA, PFOS, FtS 8:2, NMeFOSSA, and PFTreA.

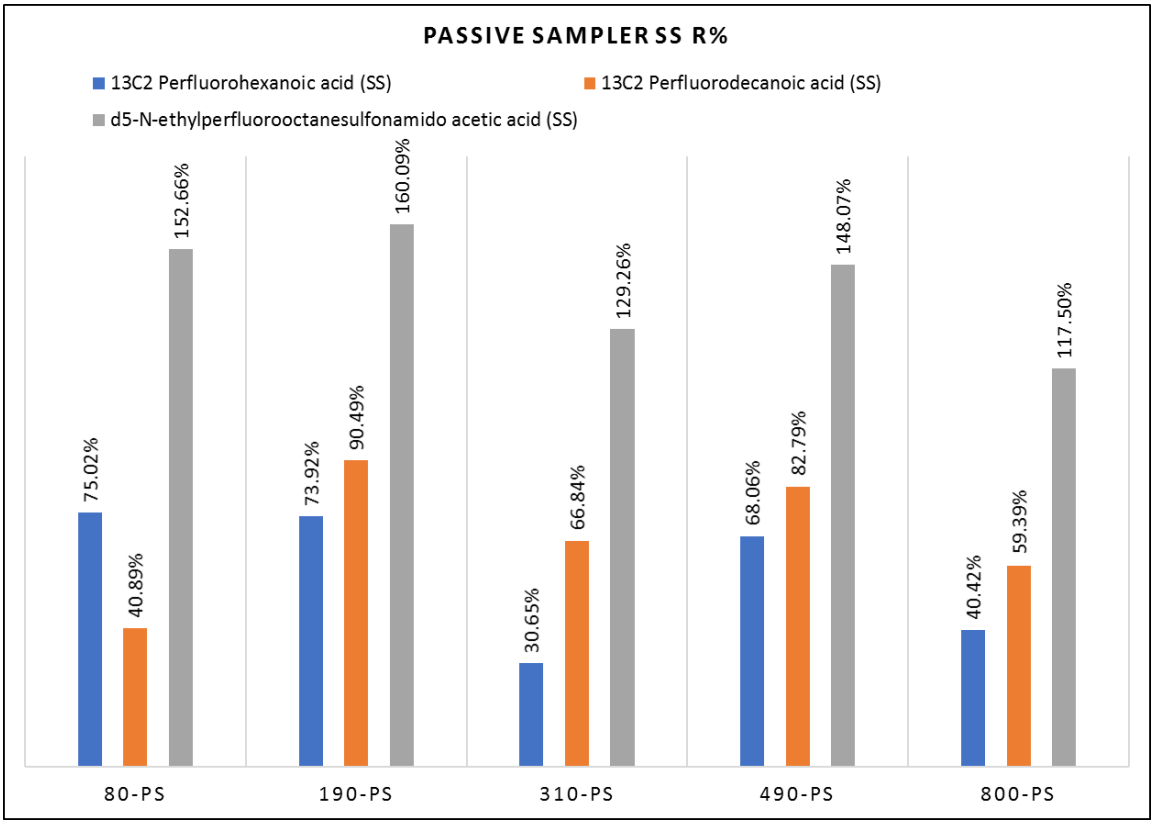

Figure A5. Surrogate recovery% for the isotherm study in PDMS+HLB passive sampler extractions.

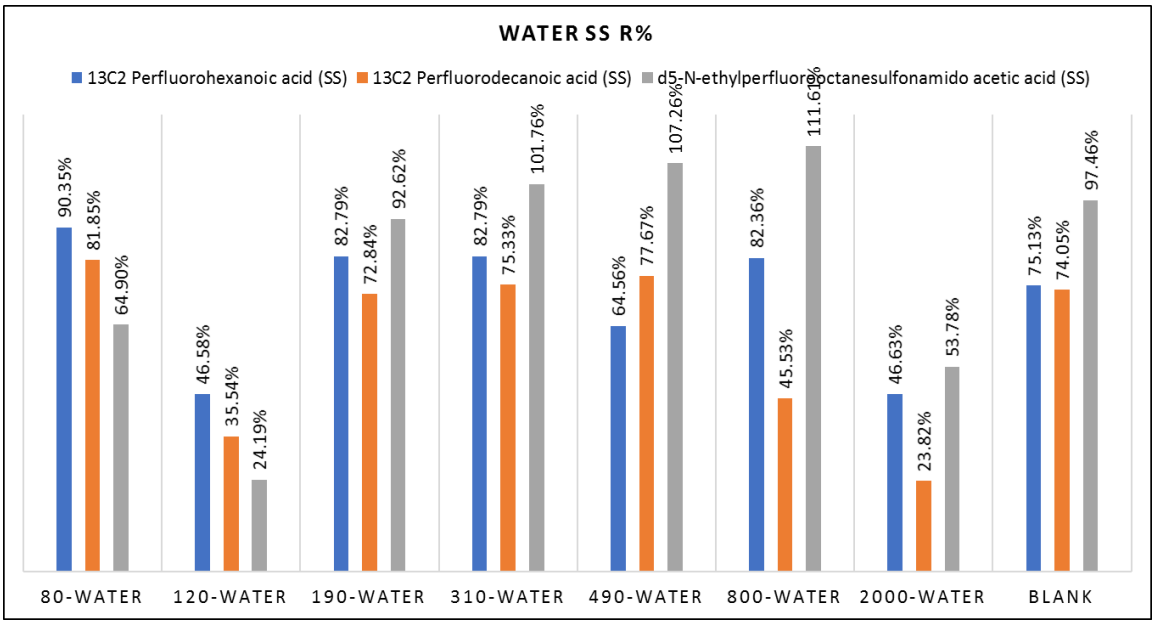

Figure A6. Surrogate recovery% for the isotherm study in PDMS+HLB passive sampler extractions.

The mass balance results for the uptake kinetic study were good for most passive samplers and PFAS compounds and shown in **Figure A7**.

PFBA

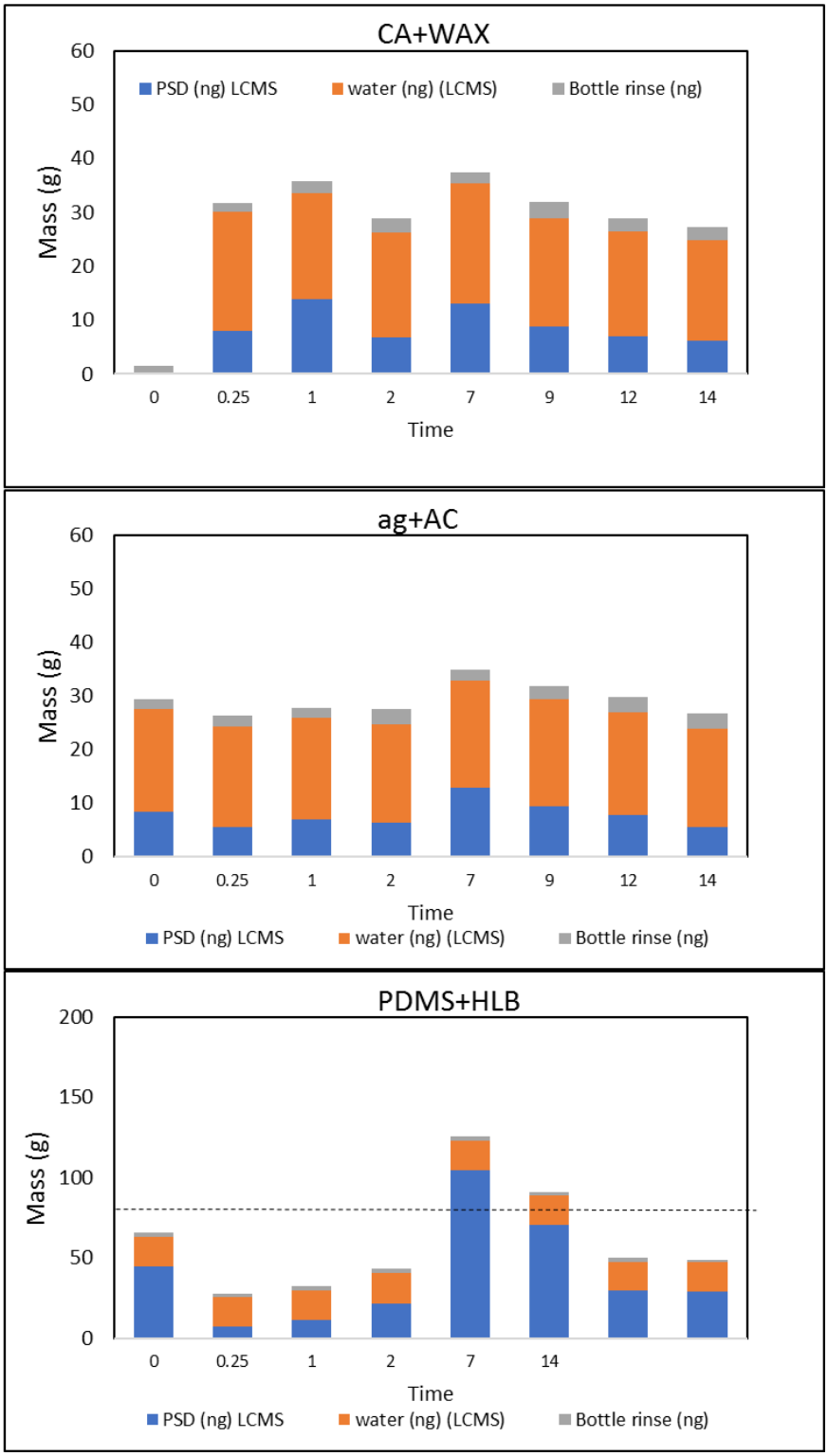
CA+WAX
PSD (ng) LCMS
water (ng) (LCMS)
Bottle rinse (ng)
Mass (g)
Time
ag+AC
PDMS+HLB

PFOA

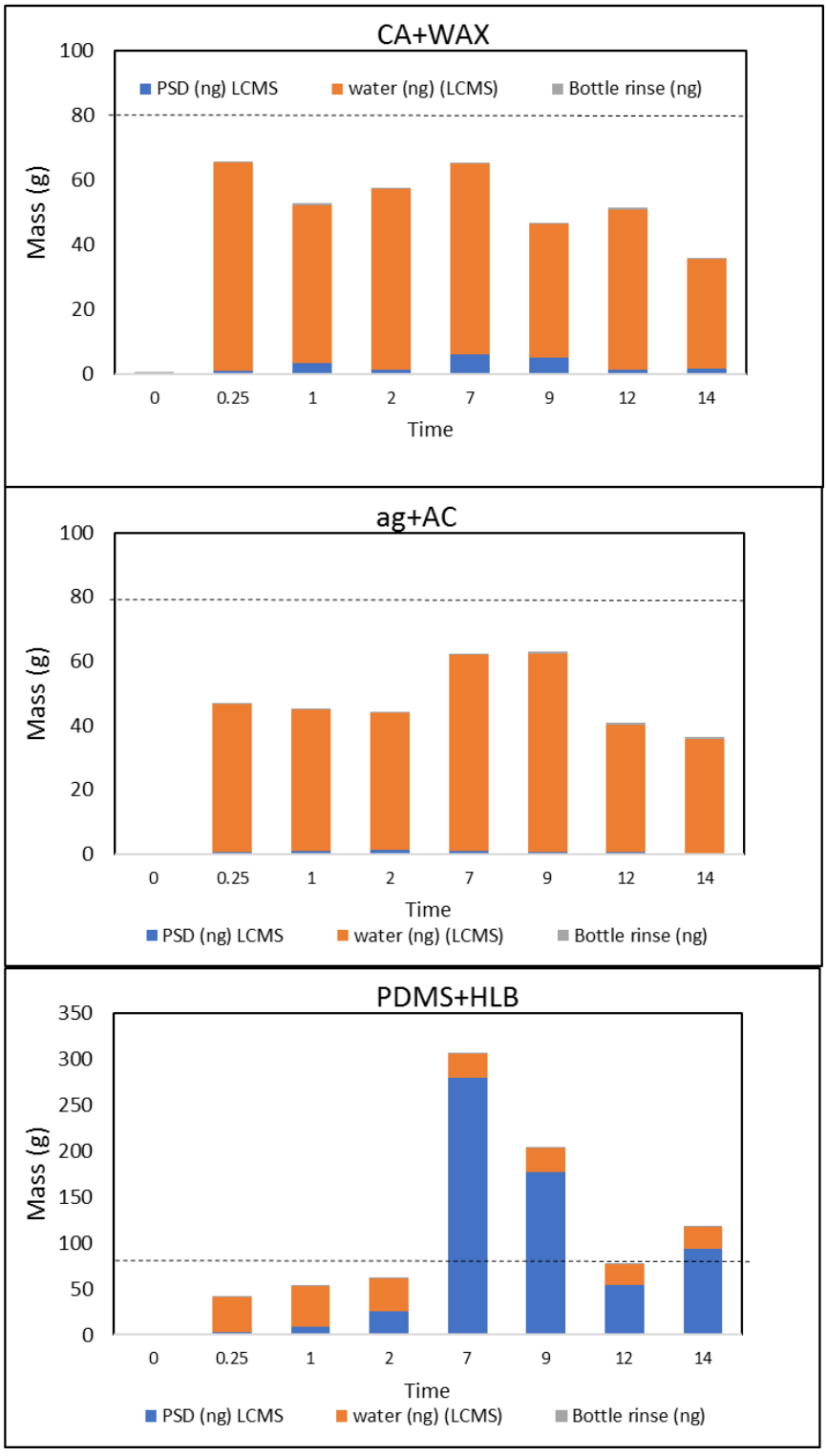
CA+WAX
100
80
60
40
20
0
Mass (g)
PSD (ng) LCMS
water (ng) (LCMS)
Bottle rinse (ng)
0
0.25
1
2
7
9
12
14
Time
ag+AC
100
80
60
40
20
0
Mass (g)
0
0.25
1
2
7
9
12
14
Time
PSD (ng) LCMS
water (ng) (LCMS)
Bottle rinse (ng)
PDMS+HLB
350
300
250
200
150
100
50
0
Mass (g)
0
0.25
1
2
7
9
12
14
Time
PSD (ng) LCMS
water (ng) (LCMS)
Bottle rinse (ng)

PFOS

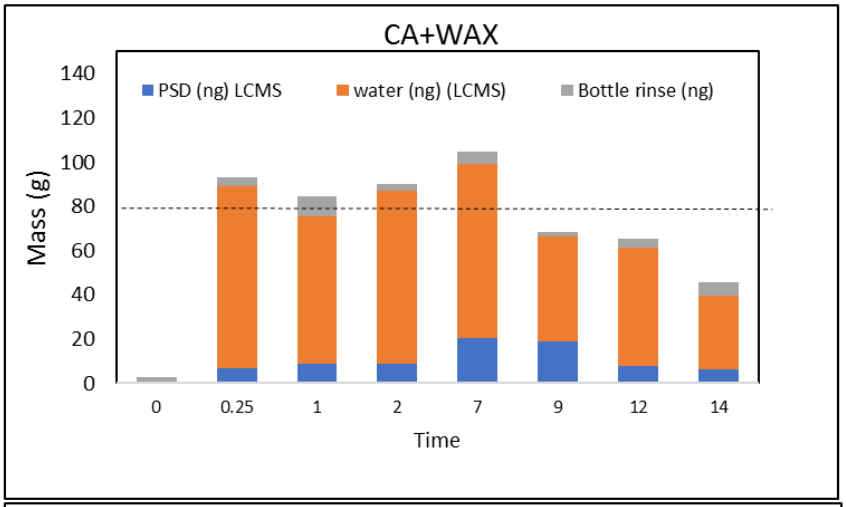
CA+WAX
PSD (ng) LCMS
water (ng) (LCMS)
Bottle rinse (ng)
Mass (g)
140
120
100
80
60
40
20
0
0
0.25
1
2
7
9
12
14
Time

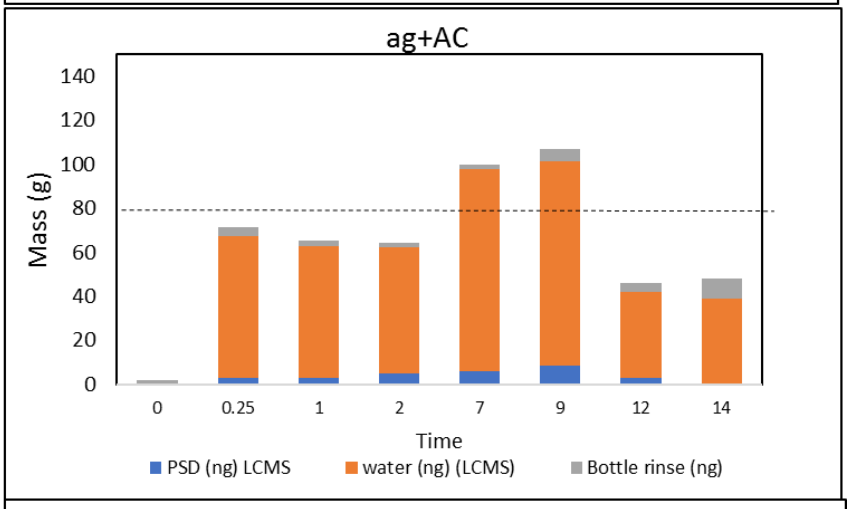
ag+AC
Mass (g)
140
120
100
80
60
40
20
0
0
0.25
1
2
7
9
12
14
Time
PSD (ng) LCMS
water (ng) (LCMS)
Bottle rinse (ng)

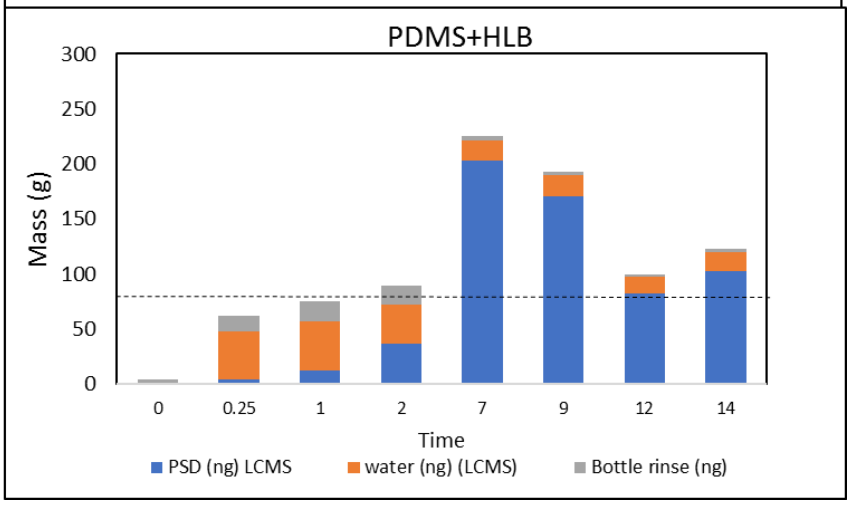
PDMS+HLB
Mass (g)
300
250
200
150
100
50
0
0
0.25
1
2
7
9
12
14
Time
PSD (ng) LCMS
water (ng) (LCMS)
Bottle rinse (ng)

FtS 8:2

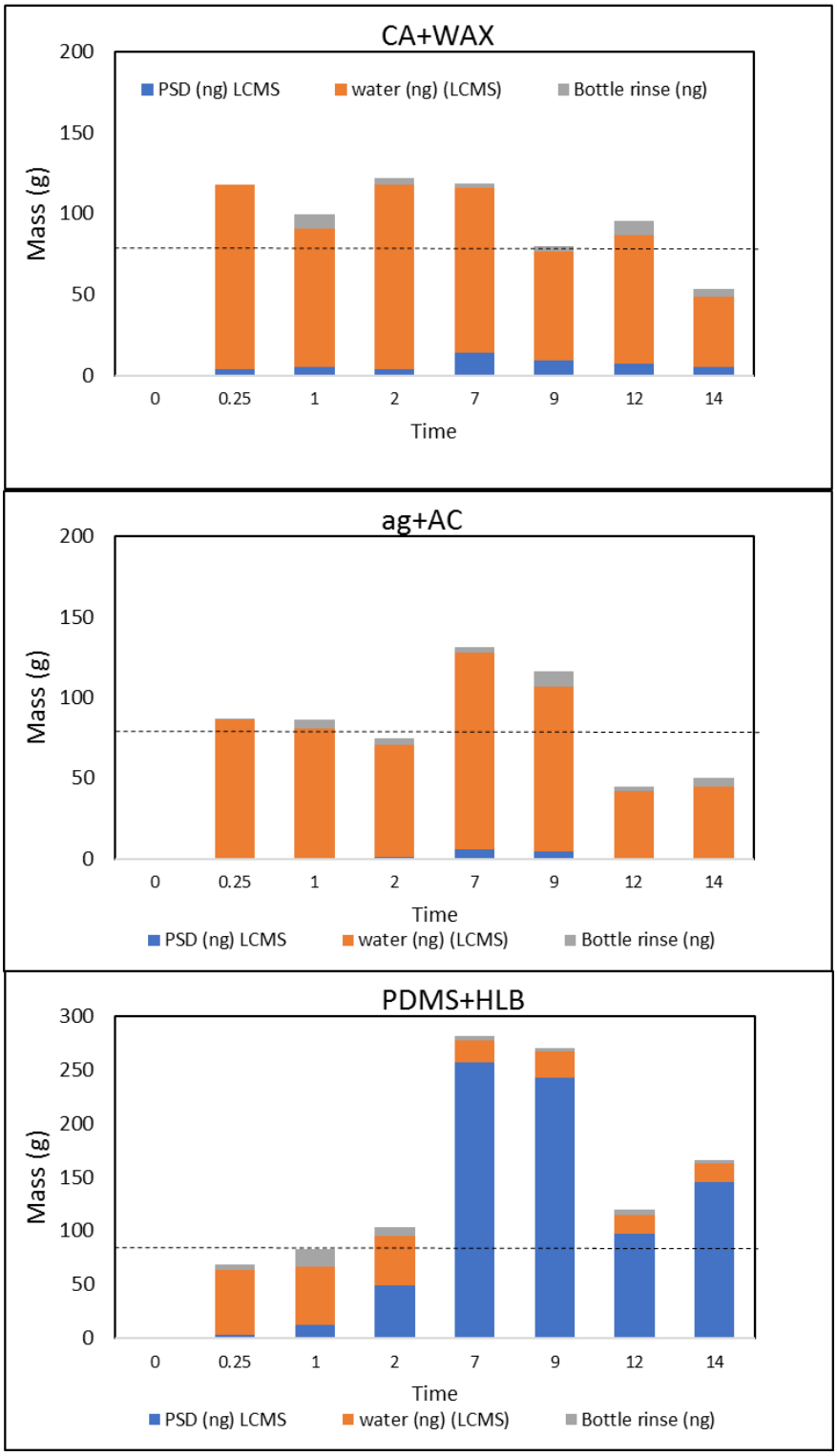
CA+WAX
PSD (ng) LCMS
water (ng) (LCMS)
Bottle rinse (ng)
Mass (g)
Time
0
0.25
1
2
7
9
12
14
ag+AC
PDMS+HLB

NMeFOSSA

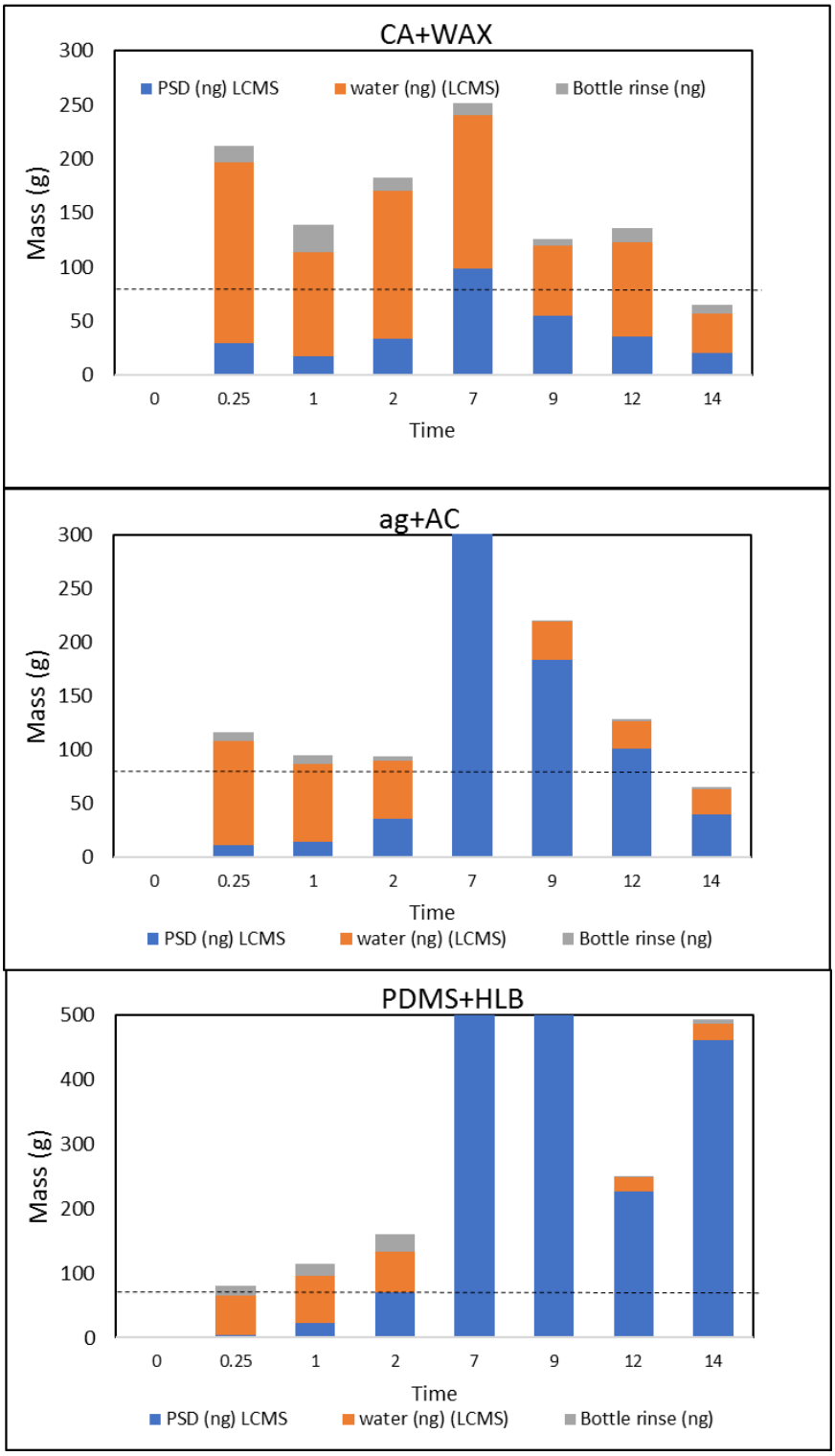
CA+WAX
PSD (ng) LCMS
water (ng) (LCMS)
Bottle rinse (ng)
Mass (g)
Time
ag+AC
PDMS+HLB

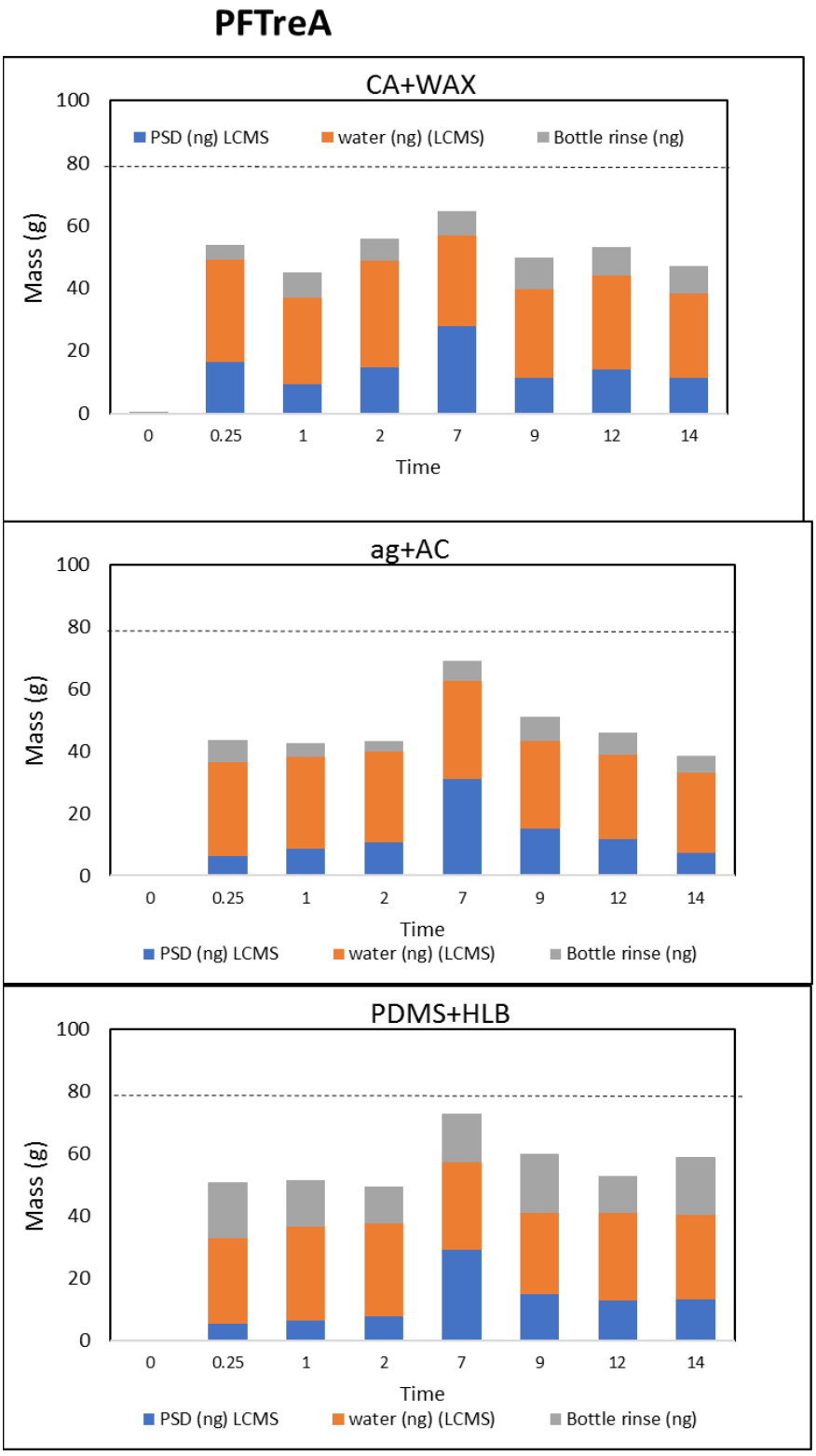

Figure A7. The mass balance results for the uptake kinetic studies for PFBA, PFOA, PFOS, FtS 8:2, NMeFOSSA, and PFTreA.

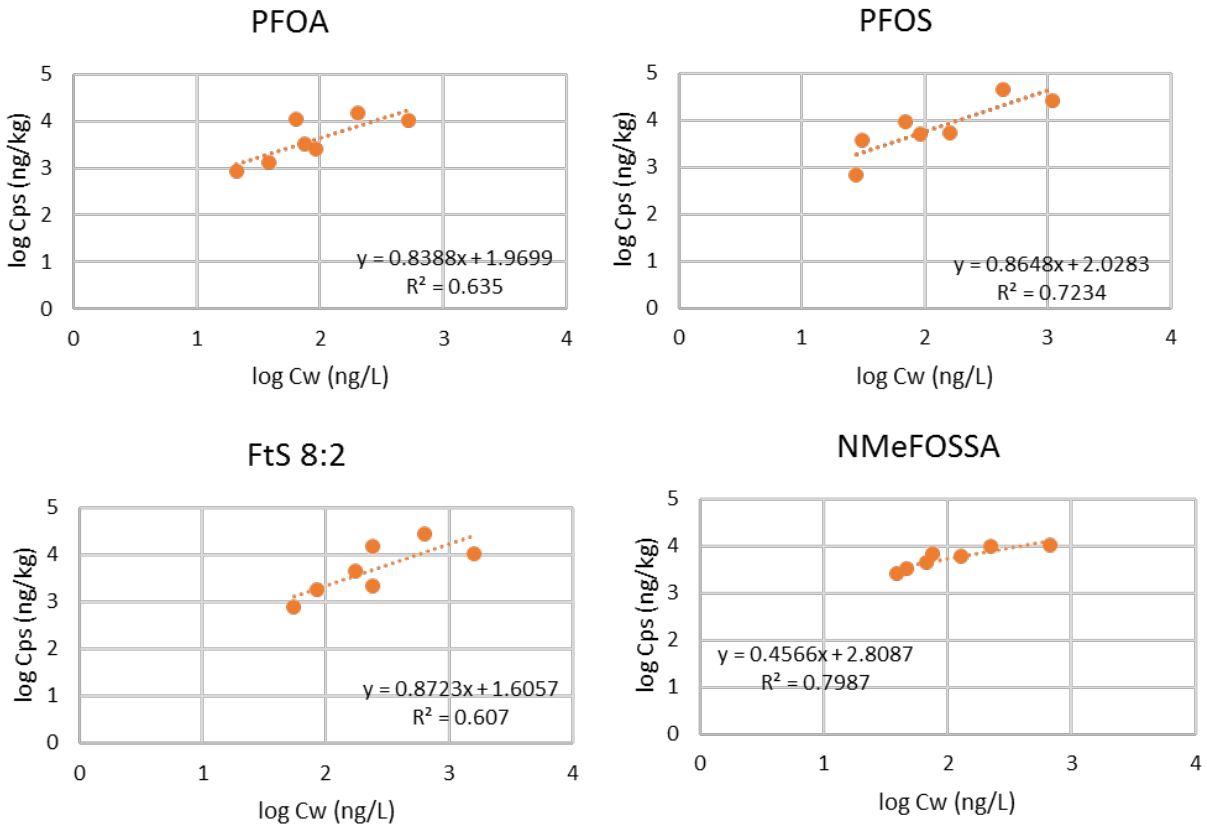

Figure A8. Linear regressions of log C_{ps} vs log C_w in the isotherm study for PFOA, PFOS, FtS 8:2, and NMeFOSSA using AG+AC films.

Data associated with figures in the report

Data for Table 5-3 Agarose mass ratio before and after different mixing conditions and extraction solvent.

Experiment number	Methanol	Meth (5 mL)+ Ace (5 mL)	Acetone	DI Water (10 mL)
	(10 mL)		(10 mL)	
Rolling table 16 hours	#1	#2	#3	#10
Rolling table 16 hours + vertex 5 min	#4	#5	#6	#11
Rolling table 16 hours + sonic 3 min	#7	#8	#9	#12

Polymer Dry Mass (mg)	Before Extraction	After Extraction	Remained Ratio
#1	27.1	25.9	0.96
#2	25.5	25.1	0.98
#3	30.7	29.6	0.96
#4	20.7	20.5	0.99
#5	25.1	24.2	0.96
#6	23.2	22.8	0.98
#7	27.6	26.8	0.97
#8	26.3	25.7	0.98
#9	28.6	25.4	0.89
#10		22.1	

#11	37.2	32.7	0.88
#12	30.3	26.5	0.87

Data for Figure 5.6 Wet mass and dry mass ratios for AC embedded agarose films (ag:AC 2:1) and base agarose gels with size of 1”x1”x1000 μm.

mass (g)	#	pan mass	pan + wet mass	pan + dry mass	wet mass ag	dry mass ag	dry mass%	water content	average	Standard deviation
ag:AC (2:1)	1	1.0544	1.8488	1.09595	0.7944	0.04155	5.2%	94.8%		
	2	1.0436	1.88645	1.08665	0.84285	0.04305	5.1%	94.9%		
	3	1.0385	1.97375	1.09115	0.93525	0.05265	5.6%	94.4%		
	4	1.0557	1.9389	1.1055	0.8832	0.0498	5.6%	94.4%		
	5	1.034	1.718	1.073	0.684	0.039	5.7%	94.3%		
	6	1.0554	1.79265	1.0917	0.73725	0.0363	4.9%	95.1%	5.4%	0.33%
ag base	7	1.0485	1.8843	1.0777	0.8358	0.0292	3.5%	96.5%		
	8	1.0576	1.8955	1.0871	0.8379	0.0295	3.5%	96.5%		
	9	1.0602	1.7786	1.0857	0.7184	0.0255	3.5%	96.5%		
	10	1.0436	1.6749	1.0661	0.6313	0.0225	3.6%	96.4%		
	11	1.0426	1.9805	1.0748	0.9379	0.0322	3.4%	96.6%		
blank	12	1.0523	1.0523	1.0523	0	0			3.5%	0.05%

Data for Figure 5.7 Surrogate recoveries of perfluoro-n-[1,2-13C2]hexanoic acid (13C2-PFHxA), perfluoro-n-[1,2-13C2]decanoic acid (13C2-PFDA) and N-deuterioethylperfluoro-1-octanesulfonamidoacetic acid (d5-NEtFOSAA) for the thirteen synthesized PFAS passive samplers.

Passive sampler Surrogate Recovery	13C2-PFHxA	13C2-PFDA	d5-NEtFOSAA
CA base	100.65%	91.18%	100.89%
CA + HLB	123.26%	116.00%	113.16%
CA + WAX	118.26%	120.28%	115.90%
CA + HSA	103.42%	92.05%	99.33%
CA + AC	95.17%	113.45%	103.51%
ag base	84.78%	91.85%	99.66%
ag + HLB	83.90%	91.98%	96.15%
ag + WAX	56.24%	66.24%	74.31%
ag + HSA	93.63%	96.80%	102.49%
ag + AC	97.80%	110.09%	113.63%
PDMS base	83.79%	85.84%	88.78%
PDMS + HLB	95.11%	103.57%	104.42%
PDMS + AC	52.26%	57.59%	71.56%

Data for Figure 5.8 PFAS mass extracted from passive samplers, water and bottle rinse solutions for first batch of 13 synthesized polymers, and the single point isotherm results at spiking level 800ng/L for four PFAS compounds: PFOA, PFOS, FtS 8:2, and NMeFOSSA (Mass balance).

Mass (ng)	CA base	CA + HLB	CA + WAX	CA + HSA	CA + AC	ag base	ag + HLB	ag + WAX	ag + HSA	ag + AC	PDMS base	PDMS + HLB	PDMS + AC
PFOA													
Sampler	5.3	5.8	15.0	4.7	9.7	5.6	4.4	14.5	10.9	44.3	3.8	2.5	2.0
Water	76.3	90.1	76.1	82.1	88.4	99.2	92.5	74.3	41.4	83.4	89.4	70.2	11.5
Bottle rinse	11.5	5.1	3.5	3.2	9.3	6.7	9.5	8.2	4.6	9.8	8.4	7.7	8.4
PFOS													
Sampler	18.7	17.3	30.3	14.8	10.7	17.4	17.2	18.0	16.5	23.6	3.2	13.5	3.3
Water	53.3	67.6	59.4	68.4	54.4	63.6	56.0	45.9	32.6	79.3	69.6	60.9	7.0
Bottle rinse	7.0	16.7	14.7	13.1	20.5	19.5	19.3	19.0	18.9	19.7	21.0	26.1	17.2
FtS 8:2													
Sampler	-	1.1	6.1	0.9	0.3	0.3	1.5	2.5	0.3	34.7	0.6	0.3	0.1
Water	53.5	60.8	78.8	95.1	79.8	62.6	61.6	48.6	32.9	76.6	79.2	86.3	15.7
Bottle rinse	15.7	12.7	9.9	3.3	13.7	18.3	18.0	15.3	12.8	5.7	7.5	8.9	7.7
NMeFOSSA													
Sampler	0.7	14.5	11.4	1.3	25.7	0.0	1.5	1.9	0.0	27.8	37.7	47.0	4.1
Water	36.4	49.6	108.3	70.3	86.9	56.2	62.3	38.0	27.6	14.0	12.5	18.4	16.0
Bottle rinse	16.0	17.6	18.3	9.1	9.4	44.3	29.6	24.7	20.5	16.4	3.4	4.6	4.1

Data for Figure 5.8 PFAS mass extracted from passive samplers, water and bottle rinse solutions for first batch of 13 synthesized polymers, and the single point isotherm results at spiking level 800ng/L for four PFAS compounds: PFOA, PFOS, FtS 8:2, and NMeFOSSA (log Kd values).

log Kd (L/kg)	CA base	CA + HLB	CA + WAX	CA + HSA	CA + AC	ag base	ag + HLB	ag + WAX	ag + HSA	ag + AC	PDMS base	PDMS + HLB	PDMS + AC
PFOA	1.9	1.9	2.5	2.0	2.1	3.3	2.5	2.4	3.3	3.1	1.6	1.5	2.2
PFOS	2.6	2.5	2.9	2.6	2.3	4.0	3.4	2.7	3.5	2.8	1.6	2.3	2.6
FtS 8:2	-	1.4	2.0	1.2	0.6	2.3	2.2	1.8	1.8	3.0	0.8	0.5	0.6
NMeFOSSA	1.4	2.6	2.2	1.6	2.5	-	2.3	1.8	-	3.7	3.4	3.4	2.4

Data for Figure 5.9 PFAS mass extracted from passive samplers, water and bottle rinse solutions for second batch of 14 synthesized polymers, and the single point isotherm results at spiking level 800ng/L for four PFAS compounds: PFOA, PFOS, FtS 8:2, and NMeFOSSA (Mass balance).

Mass (ng)	CA base	CA + HLB	CA + WAX	CA + HSA	CA + AC	ag base	ag + HLB	ag + WAX	ag + HSA	ag + AC	PDMS base	PDMS + HLB	PDMS + AC	CA+direct HSA
PFOA														
Sampler	9.4	8.9	14.3	7.1	9.9	7.4	4.6	15.6	9.8	42.4	2.8	5.5	5.8	0.5
Water	147.3	77.2	100.2	158.2	151.4	160.0	98.1	94.2	73.3	42.7	147.8	146.0	149.8	48.6
Bottle rinse	12.0	8.1	5.7	4.2	10.4	6.9	8.4	8.0	9.4	8.2	8.1	9.0	7.6	4.5
PFOS														
Sampler	24.9	20.2	32.3	16.8	19.3	23.8	22.5	20.4	22.2	48.9	16.2	19.0	16.0	1.4
Water	113.7	53.1	64.7	118.1	97.3	110.3	65.8	63.3	47.6	33.2	113.9	88.1	96.0	48.4
Bottle rinse	26.2	23.9	20.2	18.0	24.3	25.3	27.4	24.4	26.1	28.4	26.7	29.4	23.2	12.6
FtS 8:2														
Sampler	0.0	0.0	7.3	0.0	0.0	0.0	0.0	0.0	0.0	20.6	0.0	0.0	0.0	1.8
Water	88.5	50.5	55.8	115.5	90.6	102.9	59.9	58.9	45.9	29.0	95.1	82.5	90.7	40.1

Bottle rinse	14.1	9.3	6.3	0.8	10.3	15.8	15.0	11.4	9.8	7.8	7.7	10.5	7.0	10.6
NMeFOSSA														
Sampler	0.0	14.6	13.6	0.0	26.0	0.0	2.5	0.0	0.0	27.9	50.9	58.8	15.7	3.3
Water	93.9	36.6	49.6	107.3	70.2	86.2	56.1	62.1	38.0	27.7	14.2	12.5	19.0	57.2
Bottle rinse	21.1	17.9	18.5	10.7	16.7	24.6	29.9	24.9	20.9	16.7	5.5	6.6	12.4	15.3

Data for Figure 5.9 PFAS mass extracted from passive samplers, water and bottle rinse solutions for second batch of 14 synthesized polymers, and the single point isotherm results at spiking level 800ng/L for four PFAS compounds: PFOA, PFOS, FtS 8:2, and NMeFOSSA (log Kd values).

log Kd (L/kg)	CA base	CA + HLB	CA + WAX	CA + HSA	CA + AC	ag base	ag + HLB	ag + WAX	ag + HSA	ag + AC	PDMS base	PDMS + HLB	PDMS + AC	CA+direct HSA
PFOA	1.74	1.97	2.13	1.73	1.75	0.89	1.68	1.98	1.39	2.98	1.10	1.16	1.35	1.60
PFOS	2.27	2.49	2.67	2.23	2.24	1.55	2.54	2.27	1.93	3.15	1.97	1.92	1.98	2.02
FtS 8:2	-	-	2.09	-	-	-	-	-	-	2.84	-	-	-	2.22
NMeFOSSA	-	2.51	2.41	-	2.51	-	1.66	-	-	2.99	3.38	3.26	2.68	2.33

Data for Figure 6.4 Front/Back cartridge recovery% for various PFAS and Surrogates (SS)

Compound	Front cartridge	Back cartridge
13C2 PFHxA (SS)	99.6	0.2
13C2 PFDA (SS)	73.6	0.3
d5-NEtFOSA (SS)	54.0	8.0
PFBA	114.2	7.8
PFBS	112.7	25.9
PFOA	105.9	2.6
PFOS	116.1	28.8
FTS 8:2	96.0	3.7
NMeFOSE	74.0	6.4
PFTreA	89.2	24.1

Data for Figure 6.5 Fractional recovery percentage of target PFAS and Surrogates (SS) within five elusions.

	1st elution	2nd elution	3rd elution	4th elution	5th elution	Bottle
13C2 PFHxA (SS)	81.30	0.12	0.00	0.06	0.04	0.20
13C2 PFDA (SS)	77.86	0.04	0.18	0.00	0.00	0.54
d5-NEtFOSA (SS)	48.93	0.00	0.00	0.00	0.00	5.17
PFBA	78.76	2.20	0.52	0.99	1.52	0.70
PFBS	81.00	9.74	3.48	3.56	2.93	2.76
PFOA	85.11	0.37	0.30	0.42	0.68	1.66
PFOS	77.99	23.77	2.38	2.23	6.63	2.89
FTS 8:2	84.86	0.00	0.00	1.19	0.00	0.00
NMeFOSE	72.25	1.37	0.00	0.00	0.89	8.27
PFTeDA	38.34	4.50	5.55	1.82	3.17	13.70

Experimental Data for Figure 6.6 Experimental Cps vs Cw and the fitted models (Linear model, Langmuir model, Freundlich model, mix model for PFOA, PFOS, FtS 8:2, and NMeFOSSA.

PFOA		PFOS		FtS 8:2		NMeFOSSA	
Cw ng/L	Cs ng/kg	Cw ng/L	Cs ng/kg	Cw ng/L	Cs ng/kg	Cw ng/L	Cs ng/kg
524	28131	1093	54364	1579	40101	674	49161
204	26298	435	46690	628	40359	224	20633
93	9702	160	18050	241	18088	128	16799
64	15075	69	27993	172	19462	67	15888
75	14445	92	18318	242	22163	76	13835
38	5893	28	2899	85	12097	46	12518
21	7131	31	2585	55	10896	38	11270

Model fitted data (Partial) for Figure 6.2 Experimental Cps vs Cw and the fitted models (Linear model, Langmuir model, Freundlich model, mix model for PFOA. (The modeled data was obtained by the software Origin 2022).

PFOA	Linear fit	Langmuir fit	Freundlich fit	Freundlich-Langmuir fit
Cw ng/L	Cs ng/kg	Cs ng/kg	Cs ng/kg	Cs ng/kg
21	10011	5166	7553	5166
77	12358	13724	13237	13724
133	14705	18615	16767	18615
189	17052	21780	19521	21780
245	19399	23995	21841	23995
301	21745	25633	23877	25633
356	24092	27070	25988	27070
412	26439	27892	27381	27892
468	28786	28704	28930	28704
524	31133	29377	30378	29377

Model fitted data (Partial) for Figure 6.6 Experimental Cps vs Cw and the fitted models (Linear model, Langmuir model, Freundlich model, mix model for PFOS. (The modeled data was obtained by the software Origin 2022).

PFOS Cw ng/L	Linear fit Cs ng/kg	Langmuir fit Cs ng/kg	Freundlich fit Cs ng/kg	Freundlich-Langmuir fit Cs ng/kg
28	13631	6839	10293	6664
146	18843	25158	22559	25254
264	24054	35014	29862	35229
383	29266	41171	35568	41387
501	34478	45383	40399	45553
619	39690	48446	44658	48554
738	44901	50773	48506	50817
856	50113	52601	52040	52582
974	55325	54076	55325	53996
1093	60537	55290	58406	55155

Model fitted data (Partial) for Figure 6.6 Experimental Cps vs Cw and the fitted models (Linear model, Langmuir model, Freundlich model, mix model for FtS 8:2. (The modeled data was obtained by the software Origin 2022).

FtS 8:2 Cw ng/L	Linear fit Cs ng/kg	Langmuir fit Cs ng/kg	Freundlich fit Cs ng/kg	Freundlich-Langmuir fit Cs ng/kg
55	16197	8194	12312	8286
224	19417	22217	21021	22199
393	22636	29180	26033	29120
563	25855	33343	29826	33281
732	29074	36112	32962	36061
901	32294	38086	35675	38053
1071	35513	39566	38087	39550
1240	38732	40715	40272	40717
1409	41951	41635	42280	41653
1579	45171	42386	44143	42420

Model fitted data (Partial) for Figure 6.6 Experimental Cps vs Cw and the fitted models (Linear model, Langmuir model, Freundlich model, mix model for NMeFOSSA. (The modeled data was obtained by the software Origin 2022)

NMeFOSSA Cw ng/L	Linear fit Cs ng/kg	Langmuir fit Cs ng/kg	Freundlich fit Cs ng/kg	Freundlich-Langmuir fit Cs ng/kg
38	11880	6993	9452	9446
109	15965	16832	17009	17008
180	20051	24072	22533	22535
250	24136	29622	27158	27161
321	28221	34013	31238	31242
392	32307	37573	34941	34944
462	36392	40518	38361	38363
533	40477	42994	41559	41560
604	44563	45106	44577	44575
674	48648	46927	47444	47439

Experimental data for Figure 6.7 Experimental Cps vs Cw and the fitted models (Linear, Langmuir, Freundlich, and Sips models for PFAS using CA+WAX films, clockwise: PFBA, FtS 8:2, PFTreA, NMeFOSSA.

PFBA		FtS 8:2		PFTreA		NMeFOSSA	
Cw ng/L	Cs ng/kg	Cw ng/L	Cs ng/kg	Cw ng/L	Cs ng/kg	Cw ng/L	Cs ng/kg
95	2854	129	8204	60	11156	85	9407
187	2560	241	10019	64	12179	165	10750
248	6276	341	22988	160	16751	157	29382
362	9594	499	77867	105	37859	232	59108
661	7948	408	64021	182	63233	296	85347
2097	37600	1152	147637	610	76326	946	163229

Experimental data for Figure 6.8 Experimental Cps vs Cw and the fitted models (Linear, Langmuir, Freundlich, and Sips models for PFAS using CA+HSA films, clockwise: PFBA, FtS 8:2, PFTreA, NMeFOSSA.

PFBA		FtS 8:2		PFTreA		NMeFOSSA	
Cw ng/L	Cs ng/kg	Cw ng/L	Cs ng/kg	Cw ng/L	Cs ng/kg	Cw ng/L	Cs ng/kg
138	3035	106	19773	77	63461	104	28199
165	3146	137	9159	59	33236	162	11185
196	4266	196	28695	79	135921	157	66154
365	6407	412	39287	140	136103	372	50198
519	4880	602	60460	292	335280	538	122560
904	8275	1002	80098	345	459860	1067	133422
2739	14218	2258	153486	509	1184778	2373	333056

Experimental data for Figure 6.8 Experimental Cps vs Cw and the fitted models (Linear, Langmuir, Freundlich, and Sips models for PFAS using PDMS+HLB films, clockwise: PFBA, FtS 8:2, PFTreA, NMeFOSSA.

PFBA		FtS 8:2		PFTreA		NMeFOSSA	
Cw ng/L	Cs ng/kg	Cw ng/L	Cs ng/kg	Cw ng/L	Cs ng/kg	Cw ng/L	Cs ng/kg
390	4443	134	198	110	10274	20	12148
647	10186	274	840	174	29952	72	26397
580	10440	396	4389	206	18844	117	25302
1061	9651	628	4045	303	32173	191	66078
1635	12520	1179	4681	483	29835	245	98896

Data for Figure 7.1 Uptake Kinetics of PFBA, PFOA, PFOS, FtS 8:2, NMeFOSSA, and PFTreA in three type of lab synthesized passive samplers: AC embedded agarose, HLB embedded PDMS, and WAX embedded cellulose acetate films.

PFOA			**PFOS**			**FtS 8:2**		
CE+WAX	PDMS+HLB	Ag+AC	CE+WAX	PDMS+HLB	Ag+AC	CE+WAX	PDMS+HLB	Ag+AC
0.00	0.00	0.00	0.00	0.00	0.00	0	0.00	0.00
1.73	0.73	1.09	2.46	1.32	1.07	2.12	0.26	0.85
2.63	1.08	1.44	2.93	1.36	1.54	2.60	0.64	1.47
2.25	1.18	2.01	2.94	1.65	2.19	2.41	1.04	2.20
2.79	1.03	3.13	3.19	1.57	3.13	2.92	1.45	3.18
2.66	0.77	2.98	3.17	1.70	3.08	2.70	1.37	3.16
2.25	1.04	2.52	2.98	1.57	2.85	2.78	0.71	2.88
2.46	0.67	2.72	3.07	0.48	2.92	2.85	0.42	3.05
NMeFOSSA			**PFTreA**			**PFBA**		
CE+WAX	PDMS+HLB	Ag+AC	CE+WAX	PDMS+HLB	Ag+AC	CE+WAX	PDMS+HLB	Ag+AC
0	0.00	0.00	0.00	0.00	0.00	0.00	0.00	0.00
2.80	1.70	0.94	3.25	1.98	1.43	3.11	2.13	1.75
3.04	2.01	1.58	3.33	2.20	1.43	3.65	2.29	1.88
3.27	2.54	2.23	3.52	2.29	1.59	3.43	2.26	2.23
3.61	3.54	3.64	3.76	2.74	2.10	3.54	2.56	2.84
3.49	3.45	3.54	3.16	2.47	1.91	3.21	2.41	2.73
3.41	3.33	3.16	3.47	2.36	1.80	3.35	2.34	2.36
3.53	2.95	3.39	3.41	2.15	1.82	3.31	2.19	2.35

Desorption data for Figure 7.2 LogK_d values calculated for 7 days' desorption compared with uptake Kinetics of PFAS in AC embedded agarose and WAX embedded cellulose acetate films.

Desorption log Kd (L/kg)	PFBA	PFOA	PFOS	FtS 8:2	NMeFOSSA	PFTreA
CA+WAX	2.43	3.26	3.61	3.58	3.58	3.13
Ag+AC	2.44	3.38	2.83	2.86	3.25	2.25

Data for Table 7-2 Desorption ratio (C/C_0)% for PFBS, FtS 8:2, NMeFOSSA, and PFTreA in ag+AC and CA+WAX films

C(ng/g)	PFBS	FtS 8:2	NMeFOSSA	PFTreA
Ag+AC	61.2	66.4	59.0	9.8
CA+WAX	151.2	226.1	146.2	51.3
C_0(ng/g)	PFBA	FtS 8:2	NMeFOSSA	PFTreA
Ag+AC	701	574	2567	65
CA+WAX	16737	839	5839	1660

Data for Figure 7.3 Mass balance results for Activated carbon embedded agarose film with various casting formulation (thickness and AC ratio) in the first batch. Clockwise PFAS complex: PFBA, PFBS, PFOS

	Polymer Types	ag:AC 3:3 1000uM	ag:AC 3:3 484uM	ag:AC 3:2 1000uM	ag:AC 3:2 484uM	ag:AC 3:1 1000uM	ag:AC 3:1 484uM	NoAC 1000uM	NoAC 484uM
	water (ng)	37.8	54.9	39.2	41.8	-	-	50.1	92.3
PFBA	PS (ng)	24.0	11.9	21.0	-	9.5	-	3.5	12.0
	water (ng)	20.9	16.7	20.9	17.8	24.3	-	19.1	18.9
PFBS	PS (ng)	8.0	4.2	4.8	3.7	3.4	2.7	2.3	3.4
PFOA	water (ng)	91.0	-	46.2	-	39.6	-	-	61.8
	PS (ng)	69.9	34.2	52.3	33.7	32.2	29.1	7.1	15.7

Data for Figure 7.4 Calculated Kd values for activated carbon embedded agarose film with various casting formulation (thickness and AC ratio) in the first batch

	Polymer Types	ag:AC 3:3 1000uM	ag:AC 3:3 484uM	ag:AC 3:2 1000uM	ag:AC 3:2 484uM	ag:AC 3:1 1000uM	ag:AC 3:1 484uM	NoAC 1000uM	NoAC 484uM
PFBA	logKd (L/kg)	2.47	2.25	2.47	-	-	-	1.76	1.78
PFBS	logKd (L/kg)	2.25	2.31	2.10	2.31	1.99	-	1.98	1.92
PFOA	logKd (L/kg)	2.55	-	2.80	-	2.75	-	-	2.07

Data for Figure 7.5 Mass balance results for Activated carbon embedded agarose film with various casting formulation (thickness, and AC ratio) in the second batch. Clockwise PFAS complex: PFOS, PFOA, FtS 8:2

	Polymer Types	ag:AC 3:3 1000uM	ag:AC 3:3 484uM	ag:AC 3:2 1000uM	ag:AC 3:2 484uM	ag:AC 3:1 1000uM	ag:AC 3:1 484uM	NoAC 1000uM	NoAC 484uM
PFOA	Bottle rinse (ng)	47.6	10.6	45.7	48.2	42.8	40.3	41.1	47.7
	Water (ng)	7.3	12.1	6.9	8.6	8.9	4.6	4.7	6.0
	PS (ng)	35.0	57.8	55.3	41.0	14.1	19.6	42.1	67.1
	Total mass (ng)	90.0	80.5	68.7	72.3	105.0	90.0	114.2	94.5
PFOS	Bottle rinse (ng)	20.2	13.0	16.1	17.8	10.0	11.0	10.3	13.0

	Water (ng)	3.8	3.8	3.4	7.2	5.8	2.6	5.5	5.9
	PS (ng)	77.3	72.5	84.1	72.3	61.1	70.5	73.7	78.2
	Total mass (ng)	101.2	89.3	83.1	90.9	97.6	90.5	94.4	92.2
FtS 8:2	Bottle rinse (ng)	5.3	4.0	7.8	7.6	0.0	0.0	2.8	6.6
	Water (ng)	2.4	6.9	2.5	4.2	4.1	1.1	3.2	5.4
	PS (ng)	61.7	75.5	61.0	64.9	42.4	48.2	68.1	79.8
	Total mass (ng)	69.4	86.4	54.4	56.8	63.5	69.1	88.1	77.9

Data for Figure 7.6 Calculated Kd values for activated carbon embedded agarose film with various casting formulation (thickness and AC ratio) in the second batch

	Polymer Types	ag:AC 3:3 1000uM	ag:AC 3:3 484uM	ag:AC 3:2 1000uM	ag:AC 3:2 484uM	ag:AC 3:1 1000uM	ag:AC 3:1 484uM	NoAC 1000uM	NoAC 484uM
PFOA	logKd (L/kg)	3.86	3.80	3.64	3.98	4.10	4.01	4.13	4.05
PFOS	logKd (L/kg)	4.45	4.40	4.33	4.71	4.58	4.34	4.20	4.28
FtS 8:2	logKd (L/kg)	4.58	4.16	4.17	4.94	4.58	4.52	4.25	4.44